

A COMPARATIVE HEAT TRANSFER EXAMINATION OF INDIGENOUS NATURAL
FIBERS FOR BUILDING INSULATION USING A DYNAMIC WALL SIMULATOR

By

Arun Palaniswamy Kuppusamy

Submitted to the graduate degree program in Architectural Engineering and the
Graduate Faculty of the University of Kansas in partial fulfillment of the requirements for
the degree of Master of Science.

Mario A. Medina, Ph.D., P.E., Chairperson

Brian Lines, Ph.D., FMP., Member

Jae D. Chang, Ph.D., Member

Date Defended:

The Thesis Committee for Arun Palaniswamy Kuppusamy
certifies that this is the approved version of the following thesis:

A COMPARATIVE HEAT TRANSFER EXAMINATION OF INDIGENOUS NATURAL
FIBERS FOR BUILDING INSULATION USING A DYNAMIC WALL SIMULATOR

Mario A. Medina, Ph.D., P.E., Chairperson

Brian Lines, Ph.D., FMP., Member

Jae D. Chang, Ph.D., Member

Date approved:

ABSTRACT

The objective of this thesis was to evaluate natural indigenous fibers as potential, cost-effective, alternatives for building insulation. The natural fibers used were Timothy grass, wheat straw, and coconut fiber. A well-calibrated dynamic wall simulator was used for the experimental evaluation under both transient and steady-state heat transfer processes. The experiments centered on comparing the thermal performance of the indigenous natural fibers to a well-known and widely-used building insulation product, namely extruded polystyrene (XPS). The indigenous natural fibers were evaluated at densities of 30, 45, and 65 kg/m³. R-values were calculated for the natural fibers based on the experiments and mathematical expressions of R-value as a function of fiber material density were developed. The experimental results showed that wheat straw at a density of 65 kg/m³ performed within 6% of the XPS insulation. Extrapolations via the mathematical expressions indicated that Timothy grass would perform identically to the XPS insulation if the grass were used at a density of 68.3 kg/m³. The cost, however, would be about 32 times less than the XPS insulation.

ACKNOWLEDGEMENTS

I am very grateful to my dearest parents, brother, and friends, whose unconditional love and support, made me what I am today. I would like to express my deepest gratitude to my advisor and committee chair Dr. Mario A. Medina for his valuable advice and guidance, for giving me hope and courage during my difficult times, and for the opportunity to pursue my thesis research under him. I would like to sincerely appreciate and thank William Bennett in the CETE department, who was a very kind and understanding boss and offered to fund my tuition.

I would like to thank Dr. Lee Ok Kyoung and Gautham Somana, who taught me how to set up and use the dynamic wall simulator and the principles behind it. I also would like to thank Kun Xie and Matthew L. Mcfarlane, who helped me during the experimental phase. I also would like to thank the lab technician, David G. Woody, who helped me disassemble, assemble and alter the dynamic wall simulator.

I would like to express my sincere appreciation to Dr. Brian Lines and Dr. Jae D. Chang for accepting to be the members of my thesis committee and for their valuable time and ideas to enhance my thesis. I would like to thank all the professors that I took classes with, for their valuable time and wisdom. I would like to thank all the great people in the University of Kansas, who helped me in one way or another, to achieve my goal. Last but not least, I would like to thank the God almighty for showering me with blessings, with what I was able to achieve my goals.

TABLE OF CONTENTS

Abstract	iii
Acknowledgements	iv
Table of Contents	v
List of Figures	ix
List of Tables	xiii
List of Symbols	xiv
Chapter I. Introduction	1
Straw	4
Biofuels	5
Biomass	5
Bedding	5
Animal Feed	6
Construction Materials	6
Other Uses	6
Hay	7
Mulch	9
Compost	9
Garden Bed	9
Coconut Fiber	10
Retting	11

Defibering	11
Geotextiles	12
Coir Ply	12
Planting Medium	13
Other Uses of Coconut Fiber	13
Extruded Polystyrene	13
Chapter II. Literature Review	16
Chapter III. Experimental Set-up	28
Dynamic Wall Simulator	28
Thermocouples	35
Heat Flux Meters	37
Data Logger	38
Chapter IV. Wall Heat Transfer	39
One-Dimensional Transient Heat Conduction	41
Steady Heat Conduction in Plane Walls	42
Thermal Mass	44
Chapter V. Results, Analyses and Discussions	45
Dynamic Wall Simulator Calibration	45
Exterior Surface Temperatures	46
Layer Temperatures	49
Interior Surface Temperatures	52
Air Temperatures	54

Heat Fluxes	57
Thermal Performance Evaluation of the Indigenous Materials	60
Case 1	61
Exterior Surface Temperatures	62
Interior Surface Temperatures	65
Layer Temperatures	70
Heat Fluxes	74
Case 2	78
Exterior Surface Temperatures	78
Interior Surface Temperatures	82
Layer Temperatures	85
Heat Fluxes	89
Case 3	93
Exterior Surface Temperatures	93
Interior Surface Temperatures	97
Layer Temperatures	100
Heat Fluxes	104
Steady State Heat Transfer Conditions	109
Case 1	110
Timothy Grass	110
Wheat Straw	111
Coconut Fiber	111

Case 2	112
Timothy Grass	112
Wheat Straw	112
Coconut Fiber	113
Case 3	113
Timothy Grass	113
Wheat Straw	114
Coconut Fiber	114
Economic Analysis	115
Chapter VI. Conclusions and Recommendations	119
Recommendations	121
References	122

LIST OF FIGURES

Figure 1.1	Straw Bales in an Open-field	4
Figure 1.2	Timothy Grass	8
Figure 1.3	USDA Plant Hardiness Zone Map	8
Figure 1.4	Parts of a Coconut Fruit	11
Figure 1.5	Coir Ply Board	13
Figure 3.1	Dynamic Wall Simulator	28
Figure 3.2	Structural Frame of Simulator	29
Figure 3.3	Wall Panel Cavity	30
Figure 3.4	Light Bulbs Cluster	31
Figure 3.5	Dimmers	32
Figure 3.6	Circulation Fan	32
Figure 3.7	Securing Clamps	33
Figure 3.8	Air Gap Separators	33
Figure 3.9	Cavity Filled with Straw	34
Figure 3.10	Removable Cavity Panel	34
Figure 3.11	Removable Cavity Panel with Coconut Fiber	35
Figure 3.12	Thermocouples Covered with Aluminum Foil	36
Figure 3.13	Location of Thermocouples	36
Figure 3.14	Heat Flux Meter Covered with Aluminum Foil	37
Figure 3.15	HFM Locations	37

Figure 3.16	Data Logger	38
Figure 4.1	Schematic Representation of Heat Transfer	40
Figure 4.2	Temperature Gradient of a Multi-Layer Wall	43
Figure 5.1	East Wall Exterior Surface Temperatures During Calibration	46
Figure 5.2	South Wall Exterior Surface Temperatures During Calibration	47
Figure 5.3	West Wall Exterior Surface Temperatures During Calibration	48
Figure 5.4	North Wall Exterior Surface Temperatures During Calibration	48
Figure 5.5	Cross-Section of Wall Panel	49
Figure 5.6	East Wall Layer Temperatures During Calibration	50
Figure 5.7	South Wall Layer Temperatures During Calibration	50
Figure 5.8	West Wall Layer Temperatures During Calibration	51
Figure 5.9	North Wall Layer Temperatures During Calibration	51
Figure 5.10	East Wall Interior Surface Temperatures During Calibration	52
Figure 5.11	South Wall Interior Surface Temperatures During Calibration	53
Figure 5.12	West Wall Interior Surface Temperatures During Calibration	53
Figure 5.13	North Wall Interior Surface Temperatures During Calibration	54
Figure 5.14	Top Exterior Air Temperatures	55
Figure 5.15	Bottom Exterior Air Temperatures	55
Figure 5.16	Top Interior Air Temperatures	56
Figure 5.17	Bottom Interior Air Temperatures	56
Figure 5.18	East Wall Heat Fluxes During Calibration	58
Figure 5.19	South Wall Heat Fluxes During Calibration	58

Figure 5.20	West Wall Heat Fluxes During Calibration	59
Figure 5.21	North Wall Heat Fluxes During Calibration	59
Figure 5.22	Cross Section of Retrofit Wall Panel	61
Figure 5.23	South Wall Exterior Surface Temperatures at 30 kg/m ³	62
Figure 5.24	West Wall Exterior Surface Temperatures at 30 kg/m ³	63
Figure 5.25	North Wall Exterior Surface Temperatures at 30 kg/m ³	64
Figure 5.26	South Wall Interior Surface Temperatures at 30 kg/m ³	66
Figure 5.27	West Wall Interior Surface Temperatures at 30 kg/m ³	67
Figure 5.28	North Wall Interior Surface Temperatures at 30 kg/m ³	69
Figure 5.29	South Wall Layer Temperatures at 30 kg/m ³	70
Figure 5.30	West Wall Layer Temperatures at 30 kg/m ³	71
Figure 5.31	North Wall Layer Temperatures at 30 kg/m ³	72
Figure 5.32	South Wall Heat Fluxes at 30 kg/m ³	74
Figure 5.33	West Wall Heat Fluxes at 30 kg/m ³	75
Figure 5.34	North Wall Heat Fluxes at 30 kg/m ³	77
Figure 5.35	South Wall Exterior Surface Temperatures at 45 kg/m ³	79
Figure 5.36	West Wall Exterior Surface Temperatures at 45 kg/m ³	80
Figure 5.37	North Wall Exterior Surface Temperatures at 45 kg/m ³	81
Figure 5.38	South Wall Interior Surface Temperatures at 45 kg/m ³	82
Figure 5.39	West Wall Interior Surface Temperatures at 45 kg/m ³	83
Figure 5.40	North Wall Interior Surface Temperatures at 45 kg/m ³	84
Figure 5.41	South Wall Layer Temperatures at 45 kg/m ³	86

Figure 5.42	West Wall Layer Temperatures at 45 kg/m ³	87
Figure 5.43	North Wall Layer Temperatures at 45 kg/m ³	88
Figure 5.44	South Wall Heat Fluxes at 45 kg/m ³	90
Figure 5.45	West Wall Heat Fluxes at 45 kg/m ³	91
Figure 5.46	North Wall Heat Fluxes at 45 kg/m ³	92
Figure 5.47	South Wall Exterior Surface Temperatures at 65 kg/m ³	94
Figure 5.48	West Wall Exterior Surface Temperatures at 65 kg/m ³	95
Figure 5.49	North Wall Exterior Surface Temperatures at 65 kg/m ³	96
Figure 5.50	South Wall Interior Surface Temperatures at 65 kg/m ³	97
Figure 5.51	West Wall Interior Surface Temperatures at 65 kg/m ³	98
Figure 5.52	North Wall Interior Surface Temperatures at 65 kg/m ³	99
Figure 5.53	South Wall Layer Temperatures at 65 kg/m ³	100
Figure 5.54	West Wall Layer Temperatures at 65 kg/m ³	101
Figure 5.55	North Wall Layer Temperatures at 65 kg/m ³	102
Figure 5.56	South Wall Heat Fluxes at 65 kg/m ³	104
Figure 5.57	West Wall Heat Fluxes at 65 kg/m ³	105
Figure 5.58	North Wall Heat Fluxes at 65 kg/m ³	107
Figure 5.59	Comparison of Percentage Difference in Average Heat Flow	109
Figure 5.60	Section of Wall Panel	110
Figure 5.61	R-Value Curve of Timothy Grass	115
Figure 5.62	R-Value Curve of Wheat Straw	116
Figure 5.63	R-Value Curve of Coconut Fiber	117

LIST OF TABLES

Table 1.1	Heat Loss Through Building Enclosure Elements	2
Table 5.1	Comparison of Peak Temperatures and Peak Temperature Differences at 30 kg/m ³	73
Table 5.2	Comparison of Peak Temperatures and Peak Temperature Differences at 45 kg/m ³	89
Table 5.3	Comparison of Peak Temperatures and Peak Temperature Differences at 65 kg/m ³	103
Table 5.4	Comparison of Average Heat Flow Values	108

LIST OF SYMBOLS

Q	=	Total heat flow (W)
q	=	Heat Flux (W/m^2)
T_o	=	Exterior surface temperature of the wall ($^{\circ}C$)
T_i	=	Interior surface temperature of the wall ($^{\circ}C$)
ΔT	=	Temperature difference between the exterior and interior surfaces ($^{\circ}C$)
R	=	Thermal resistance offered by the material ($m^2 \text{ }^{\circ}C/W$)
ρ	=	Density of the material (kg/m^3)

CHAPTER I

INTRODUCTION

Building insulation is an integral part of building construction because it plays an important role in controlling energy fluxes. In buildings, insulation has been used since early human civilizations. For example, ancient Egyptians used asbestos for insulating their houses and other household articles. Ancient Greeks and Romans invented wall cavities for the purpose of insulating. They built two layers of stone walls with a cavity in between, which trapped air inside. This trapped air served as a natural insulator, which kept the heat produced in fireplaces inside the dwelling. During the medieval ages, pieces of cloth were used to insulate buildings. In colder northern climatic regions, straw and clay were stuffed together in walls to insulate the buildings. The use of cavities within walls was re-introduced and widely used in European and American buildings during the 19th century. Asbestos was used, in part, as building insulation until the 1970's after which its use in buildings was banned, as it was found to cause asbestosis (Cann, 2013).

In 1932, Dale Kleist accidentally invented fiberglass, when he was attempting to create a vacuum-tight seal between two glass blocks. During his research, a high-pressure jet of air produced fine fibers of glass from a stream of molten glass. Later, insulation containing fiberglass was manufactured, which has dominated the building insulation industry to date although it was found that fiberglass also causes some health hazards such as skin irritation and damage to lungs if fine particles of fiber glass are

inhaled. Cellulose is another important type of insulating material widely used in buildings. Most of the cellulose insulation used nowadays consists of recycled newsprint and cardboards, which are chemically treated with non-toxic borate compounds and made into fibrous form (Fisette, 2005). Polyurethane foam, which is available as sheets as well as spray-in forms, became popular in the 1980's. Increase in energy prices during the 1970's and 1980's prompted government policies and building standard requirements to become more stringent in terms of building insulation. This led to the development of numerous synthetic building insulation materials and methods. As a result, research and development activities led to the development of efficient insulation materials, which have contributed in reducing building energy use and costs and in turn in making buildings more energy efficient.

If a building is properly insulated, up to 50% of energy loss through the building enclosure elements can be saved when compared to an uninsulated building (Banfi, 2008). Areas of heat transfer through the building enclosure and the possible energy losses are given in the table below.

Table 1.1 Heat losses through building enclosure elements (Energetika, 2012)

Areas of Heat Transfer	Possible Energy Loss
Windows and outside doors	30% to 50%
External walls	20% to 40%
Ceilings and roofs	15% to 20%
Floors	5% to 10%

As a result of increased awareness on energy savings and strict building codes,

synthetic insulation materials are widely used in buildings. Some of the most commonly used synthetic materials include:

- Fiberglass insulation
- Mineral wool insulation
- Plastic fiber insulation
- Polystyrene insulation
- Polyisocyanurate insulation
- Polyurethane insulation
- Cementitious foam insulation
- Phenolic foam insulation

These materials are fabricated and most can cause health hazards while also not being eco-friendly. There are wide varieties of natural, even indigenous, fibers that can be used as building insulation, which would not cause any health problems, are cost effective and eco-friendly.

In this research, three indigenous natural fibers, namely straw, hay and coconut fiber were tested against extruded polystyrene foam (XPS) insulation for their insulation performance under controlled conditions using a dynamic wall simulator. The purpose of this research was to study the insulation performance of the natural fibers, which are available in abundance and at very low costs.

Straw

Straw is a by-product of harvesting grains such as rice, wheat, rye, barley, oats, etc., Surplus quantity of straw is produced and is mainly used as livestock feed and bedding. Approximately 2,000 million tons of cereal straw is produced annually throughout the world (Jackson, 1977). Disposal of straw has always been a problem to the farmers. In some countries, farmers burn the straw to dispose of it. This causes air pollution and serious threats to living organism, soil, and water (Brady, 1996).

Figure 1.1 shows one agricultural use of straw in a developed country.



Figure 1.1 Straw Bales in an Open-field (Photo courtesy of Many Hands Builders)

Because of increased awareness on sustainability and care for the environment,

straw is being used for various purposes, which are explained below.

Biofuels

Straw is used in the production of bio-butanol. Bio-butanol can be used as an alternative fuel when blended with gasoline. Straw is fermented using anaerobic conversion of the carbohydrates by strains of *Clostridium* bacteria (EBTP-SABS). This involves hydrolysis of straw in a fed-batch reactor, in which *Clostridium beijerinckii* P260 bacterial strain is added simultaneously with sugar solution (Qureshi, et al., 2007).

Biomass

Straw is also used in large-scale biomass power plants (Zeng, et al., 2007). It is becoming widely used in EU countries. Straw is used either as straw bale or as densified straw pellets. Straw is densified into pellets through a process called torrefaction. Torrefaction is the process in which straw is ground into powder and is heated to 200-300°C in the absence of oxygen and compacted. During torrefaction, straw loses most of its moisture and other volatile components that reduces the heating value. Torrefied straw pellets are easy to transport, requires less space for storage, it is hydrophobic and has high combustion properties. For now, torrefied straw pellets are mixed with coal and fired in power plants (van del Stelt, 2011).

Bedding

Straw is widely used in making mattresses in many parts of the world. This

bedding is called palliasse. Straw is also used as bedding for cattle and horses because of its better thermal properties.

Animal Feed

Straw is partially used as an animal feed. It is helpful for the animals to maintain body heat in cold climatic conditions. In many parts of the world including India, China and some African countries, straw is used as a main feed for cattle (Jackson, 1977). A result of its low crude protein content and low digestibility, straw is treated with chemicals such as ammonia and used as a partial feed for cattle during winter in USA and some Latin American countries (Salem and Smith, 2008).

Construction Materials

Straw is also used in construction. For example, it is used to bind clay and concrete. In olden days, people used to mix clay and straw to make building blocks, called cobs. Straw bale is also used to make straw bale construction, where walls of the buildings are made with straw bales, because of their excellent insulation properties (Ashoura et. al., 2011).

Other Uses

Straw is also used for other various applications such as the manufacturing of hats, thatching, packaging, paper, horse collars, ropes, basketry, horticulture, decoration and erosion control to a certain extent.

The type of straw used for this research was wheat straw, which is widely available in Kansas (Nelson, 2002). The scientific name of wheat is *Triticum aestivum*. It is an annual grass that grows up to 1.5 meters tall in some species. Each plant will have 1 to 5 strands of stem called culms. The culms are hollow and have hairless or hairy nodes. Each culm has around six leaves, which may have varying lengths between 20 and 35 cm (KRBG, 2016).

Hay

Hay consists of grasses from different types of plants such as ryegrass, Timothy grass, fescue, orchard grass, etc.; Hay is cultivated mainly as a fodder for cattle. The grasses are either dried in the field or cut down, dried, baled and are stored for use in winter. Aged hay, which have been stored for a very long period cannot be used to feed cattle. It becomes an issue for the farmers to dispose of the spoiled hay. A statistical report estimates that in 2014, around 140 million tons of hay was produced in the United States (USDA, 2016). The type of hay used in this research was Timothy grass hay (Fig. 1.2). Its scientific name is *Phleum pratense*.



Figure 1.2 Timothy Grass (Photo courtesy of Mary Jelks, M.D.)

Timothy grass is commonly grown in United States Department of Agriculture (USDA) zones 2 through 8. USDA zones are classified based on average annual minimum winter temperature. These are called plant hardiness zones. Plant growers can determine which plants can be planted and grown at a particular location by the standard. Figure 1.3 shows the USDA plant hardiness zone map

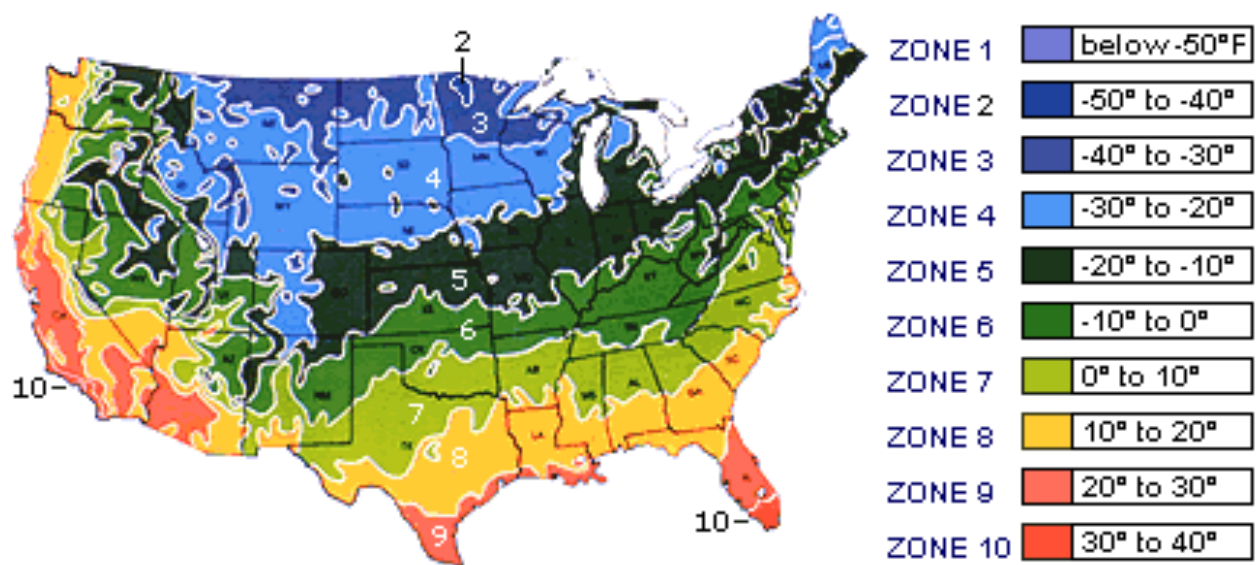


Figure 1.3 USDA Plant Hardiness Zone Map (USDA)

Timothy grass grows well in high altitudes and cooler climatic regions (USDA NRCS Plant Guide, 2016). It is a perennial grass and is mainly fed for horses and so, it is called as 'horse hay.' It has shallow root and poor drought resistance. Various varieties include Clair, Mohawk and Timfor. Apart from being used as fodder, hay is also used in the following fields.

Mulch

Hay can be used to cover the soil under plants. They suppress the weed, retain moisture, prevent slashes from rainfall and protect the plants from some soil borne diseases such as blight. It also protects the plants from cold winds and freezing temperatures (Neill and Lee, 2001).

Compost

Chopped hay can be mixed with green matter such as fruit and vegetable peel, grass clipping and other kitchen wastes and composted. This can be ploughed into the farming fields, which can be a very good source of nitrogen for the crops.

Garden Bed

Spoiled hay bales can be used to make garden beds similar to straw bales. The bales have to be conditioned before using as beds. They are kept in moist condition for few days and are covered with few inches of soil. Over this, seeds or plants are planted and watered, which would slowly decompose and provide nutrients to the plants.

Coconut Fiber

Coconut fiber is obtained from the outer covering of the coconut fruit and is the thickest and most resistant of all natural fibers. The scientific name of coconut plant is *Cocos nucifera* (DebMandal and Mandal, 2011). Coconut trees are mainly found in the tropical areas of the world such as south Asia, Africa, Latin America and states of USA such as Florida and Hawaii. They are believed to be native to Malay Archipelago or the South Pacific. The coconut palm starts producing fruits after 6 to 10 years of germination and reaches its full potential in 15 to 20 years. Each tree produces around 50 to 200 fruits per year, depending upon the breed and produces fruits approximately until 80 years of age. Coconut fruit has four parts such as outer leathery skin, middle fibrous coir, inner hard shell and the innermost fleshy copra (Broschat, 2014). These are shown in Figure 1.4.

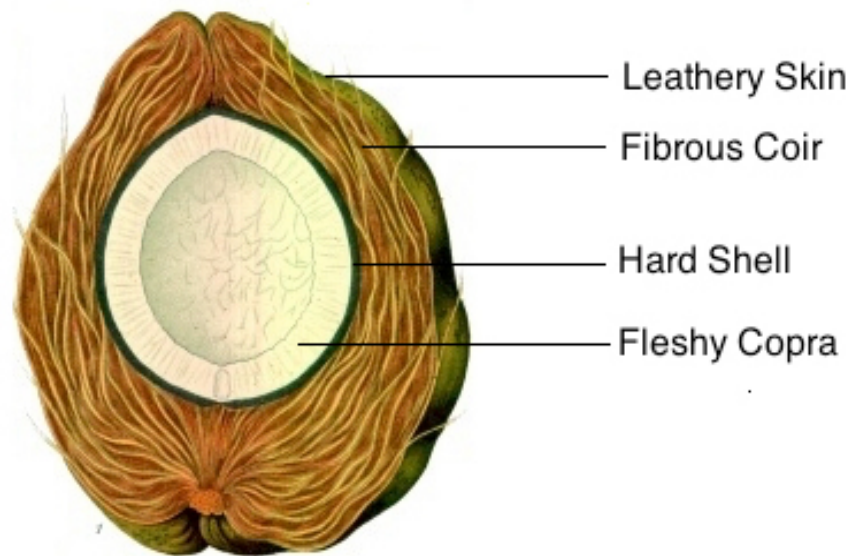


Figure 1.4 Parts of a Coconut Fruit (Image processed by Shoepke)

The fibrous coir is extracted and the final product is made into coconut fiber through following processes.

Retting

It is the process in which the coconut fruit is soaked in either fresh or salt water for a certain period. Microbes act on the fibers to make them soft and easy to work on. Retting uses mechanical crushing machines, which extract the fibrous layer and the skin from the inner nut (FAO, 2016).

Defibering

Defibering uses machines with flat beater arms in which the retted fiber is beaten

and in this process, the fiber, sponge-like pith and the leathery skin are separated. Then the fiber is collected and dried either mechanically or using solar energy. The fiber is then compacted and rolled or made into bales and stored for further use. The following are the areas where coconut fiber is used (FAO, 2016).

Geotextiles

Geotextiles made from coconut fibers are used in sustainable vegetation and erosion control as the coconut fiber has extremely high strength and low decomposition rate when compared to other natural fibers. They are durable, absorb water, resist sunlight and are biodegradable. They are used as insulation in cold storages, food industry, etc (FAO, 2016).

Coir Ply:

Coir ply is a substitute for plywood. Coir is processed with some adhesives and phenols and are made into boards or sheets of required strengths and thicknesses. They are very successful in countries like India. A picture of Coir Ply is shown in Figure 1.5.



Figure 1.5 Coir Ply Board (Photo courtesy of TNKKSS)

Planting Medium

Ground coconut husk along with fibers is used as a planting medium, because of its high nutritional value and water retention properties. It is widely used as planting medium for orchids and mushrooms.

Other Uses of Coconut Fiber

Coconut fibers are also used in the manufacture of ropes, floor mats, carpets, scrubber brush, apparels, bedding for farm animals and in the manufacture of mattresses.

Extruded Polystyrene (XPS)

Extruded polystyrene is a polymer made by a process which involves the following steps (Emil, 1982):

- Polymerization of styrene
- Extrusion
 - o Heating
 - o Mixing
 - o Injection of blowing agent
- Extrusion of foam sheet
- Storage of XPS sheet

Polystyrene polymer is heated and extruded through a set of extruder screws. During this process, a blowing agent is injected into the polystyrene material which is in a molten state. Before 1980s, HCFC (Hydro Chloro Fluoro Carbon) gases were used as blowing agents which are harmful to the ozone layer. Now-a-days, most of the manufacturers use carbon dioxide as a blowing agent, which is a green gas which has very high global warming potential (Shine, 2005). Then the sheet is extruded into a mold of desired thicknesses and dimensions.

Various grades of XPS sheet insulation are available from different manufacturers. The type of XPS sheet used in this research was Foamular insulation sheathing manufactured by Owens Corning. Each sheet was of 12.7 mm thickness and had a dimension of 1.2 m x 2.4 m. To be used in the dynamic wall simulator, the sheet was cut for 1.1 m x 0.46 m dimensions. The R value of each sheet was $0.528 \text{ }^{\circ}\text{C m}^2/\text{W}$. XPS sheets for commercial use are reinforced with film facers on both sides for added damage resistance, moisture retention, corrosion and rot. XPS sheets meet ASHRAE

90.1 standards and fire protection codes. Some of the advantages of using these sheets include:

- Can be used with other blanket type insulations for higher R-value
- Ease of handling, cutting and installing
- Resistance to mildew, moisture, corrosion, rot
- Meet building codes and standards

CHAPTER II

LITERATURE REVIEW

Ma et al. (2010) estimated the reduction in energy consumption when straw-based building insulation materials (SBBIM) are used in buildings as well as the reduction of CO₂ emission that can be avoided by reduced burning of straw. The energy consumption, CO₂ emission and economic terms of SBBIM and expandable polystyrene (EPS) were compared. They found that, when straw is used as building insulation, it could save up to 51 MJ.kg⁻¹, which is much higher than the energy it releases when burned (7.1 ~ 16.7 MJ.kg⁻¹). As per their research, if 100,000 rural households in China were to use the SBBIM, the CO₂ emissions could be reduced by about 16 million tons in a period of 10 years. They also found that the SBBIM performed similar to EPS in terms of thermal insulation, consumed less energy to make, and emitted less CO₂ than EPS in production, and was less expensive than the EPS insulation. Based on their experimental results, they suggested extrapolating the technology using straw as building insulation material for use in the rural areas of North China.

Ashoura et al. (2010), conducted an experiment to measure the thermal conductivity of some natural plaster materials such as soil, sand and straw. To reinforce the plaster, they used straw. They used three types of fibers such as wood shavings, wheat straw, and barley straw. Based on their experimental results, they concluded that the thermal conductivity decreased when the straw fiber content was increased and the thermal conductivity decreased when the sand content was increased. The straw fibers

played a very important role on the change of thermal conductivity than the sand. They also found that, barley straw reinforced plaster had the highest thermal insulation value.

Goodhew and Griffiths (2005) conducted an experiment on un-fired clay bricks, a straw clay mixture and straw bales to measure their thermal conductivity, U-value and diffusivity. They used thermal probe technique and iterative methods for data analysis. They also studied how the thermal properties of those materials changed with time. Based on their experimental data, they found that the cavity walls made of un-fired clay bricks that used paper, straw or wool cavity as insulation material, had thermal conductance of $0.35 \text{ W/m}^2 \text{ K}$ or lower, which satisfied the then United Kingdom Building Regulations. They extrapolated possible methods to improve the insulation performance of existing earth walls by adding a layer of sustainable insulation containing timber frames and the tested materials in this experiment, at the inside surface of the wall, which also satisfied the UK building regulations.

Toguyenia et al. (2012) investigated insulated roofing materials and walls made of composite clay–straw mixture, and insulated materials made of red wood, white wood, and insulated panels. They studied their influence on air conditioning loads of houses located in dry tropical climates such as Burkina Faso. Their experimental setup consisted of an apparatus based on hot plate method. Using this apparatus, they studied the thermophysical properties of the insulating materials and the clay-straw composite. They found that the results obtained by their research were similar to the results found in the literature. They used the climatic data of Ouagadougou to model and simulate a house using TRNSYS. The house was a one story residential building

with two bedrooms, a bathroom and a living room. It was assumed that the building walls were made of clay or clay-coated straw with mortar coating inside and outside. Based on the simulation, they found that the clay–straw mixture reduced the air conditioning load by about 8% when compared to the uninsulated clay wall houses. Their study also indicated the influence of roof insulation on the air conditioning load. Their results showed that, a 1.5 cm thick insulation made of red wood reduced the energy use for cooling by about 6.2% while the insulation panel made of natural fiber and lime-cement mixture saved about 12.1% of energy used to run the air conditioning.

Garas et al. (2009) studied the production, use, and disposal of straw in Egypt. They also studied the different methods of straw bale construction across the globe. According to their study, in Egypt, about four million tons of rice-straw is produced annually. They found that the majority of this residual straw is disposed by burning it in the field. The burning of large quantities of straw causes high levels of air pollution which is known as black cloud and causes chronic lung diseases in the population. The main objective of their research was to find the most economical and environment friendly method to construct straw bale buildings by comparing various methods of straw bale constructions that were constructed throughout the world. They conducted an economical comparison between a load bearing wall unit built with locally produced rice straw bales and a traditional load bearing wall unit built with cement bricks. Based on their results, they concluded that using straw bale construction could save about 40% of construction cost and also save a considerable amount of energy and insulation costs.

Khedaria et al. (2004) conducted a research to develop a particle board made of durian peel and coconut fiber and to find the optimum ratio to enhance the thermal insulation of a particle board. The two main parameters that were investigated were weight of the durian peel and coconut fiber to measure the ratio and the density of the particle board. They manufactured particle boards using common board manufacturing techniques. They observed a considerable difference in properties of the particle board with different mixing ratios as well as density. Based on their results, they concluded that the optimum ratio of the durian peel and coconut fiber was 10:90 by weight, respectively, and the optimum board density was 856 kg/m^3 . For the optimum ratio and density of the particle board, they found the values of the following properties as follows: thermal conductivity was 0.1342 W/m K , modulus of rupture (MOR) was 440.46 kgf/cm^2 , modulus of elasticity (MOE) was $21,867 \text{ kgf/cm}^2$, 10.49% thickness swelling, and 6.22% moisture content. They found that the particle boards made by mixing durian peel and coconut fiber had better properties when compared to the boards made with individual durian peel or coconut fiber, except the modulus of elasticity (MOE), which was decreased. They also concluded that the particle board made with durian peel and coconut fiber board had very low thermal conductivity, which can be used as insulation in roofs and walls of the buildings. They also suggested that the particle board can be used to manufacture furniture, thus aiding in agriculture waste management.

Manohar et al. (2006) investigated the use of natural fibers, such as coconut fiber and sugarcane fiber, as building insulation. They were intended to prove that the use of biodegradable natural fibers as building insulation could help in solving the problems

associated with disposal of hazardous man-made insulation materials. They investigated the apparent thermal conductivity (k) of biodegradable coconut fiber and sugarcane fiber in accordance with ASTM C 518. They tested various density ranges from 40 kg/m^3 to 90 kg/m^3 for coconut fiber and 70 kg/m^3 to 120 kg/m^3 for sugarcane fiber. Their test temperature ranged from $13.2 \text{ }^\circ\text{C}$ to $21.8 \text{ }^\circ\text{C}$ for coconut fiber and $18 \text{ }^\circ\text{C}$ to $32 \text{ }^\circ\text{C}$ for sugarcane fiber. They used the experimental data to determine empirical equations for different k values which varied with density and temperature for both coconut and sugarcane fiber. They compared the k value of coconut fiber and sugarcane fiber at $24 \text{ }^\circ\text{C}$ with seven different conventional insulations, whose values were obtained from published results. Their results indicated that the k value of both coconut fiber and sugarcane fiber were similar to the range that satisfied the building insulation standards. Their results also showed that the variation of k -values with different densities and temperatures for both coconut fiber and sugarcane fiber were similar to the results obtained by using loose-fill thermal insulations.

Andoha et al. (2010) investigated the performance of coconut fiber if used as insulation in solar water heaters. The reason for this study was that the majority of the population in Africa could not afford solar water heaters because of their high prices. Therefore, the study focused on solar water heaters that used coconut fibers as insulation. Coconut trees are widely available in tropical countries. They compared the thermal performances of solar collector that used coconut fiber as insulation and a conventional solar collector that used glass wool as insulation with similar design, fabrication and under the same conditions. They also compared the solar collector that

used coconut fiber insulation with eight randomly selected designs that used different insulation materials. Based on their study, they found that the solar collector that used coconut fiber were 25% less expensive than the collector that used glass wool insulation. Their results showed that the thermal performance of the collector that used coconut fiber insulation was acceptable when compared to the conventional solar collectors. For example, the outlet hot water temperature of the coconut fiber collector was more than 80 °C. Internal hot water temperature rise was more than 40 °C. It was found that the thermal efficiencies of conventional solar collectors were less than 50% while the solar collectors with coconut fiber insulation had a thermal efficiency of 51%. Based on their results, they concluded that the solar collectors with coconut fiber insulation were economical in countries where coconut coir is widely available because of their low cost and better performance.

Yaakob et al. (2011) investigated the use of coconut fiber and natural rubber mixture as thermal insulation in Malaysia. Coconut fiber and rubber latex are available in abundance in Malaysia and have acceptable thermal characteristics. The coconut fibers were finely chopped and mixed with rubber latex to produce the insulation material. They tested twelve different ratios of latex-coconut fiber mix, which were manufactured using cold press technologies. The tested ratios of latex ranged from 5% to 60% by weight. Their result showed that the latex with 30% by weight and 70% coconut fiber by weight absorbed 95% of heat in the heat test whose performance was better than the product made using synthetic rubbers. Hence, they concluded that the

product with 30% of latex by weight and 70% of coconut fiber is the best ratio to be used as an insulator.

Rodriguez et al. (2011) studied the thermal characteristics of coconut fiber when used with concrete slabs in the construction industry. They extracted the husk of coconut fruit and manufactured the specimen at 115.54 MPa. They solved the heat diffusion equation with experimental temperatures as boundary conditions and found the thermal conductivity (k) to be 0.048 W/m K. They solved Fourier's law using the heat flux and temperature values obtained from their experiments and found the k -value to be 0.0499 W/m K. They used the k -value of 0.048 W/m K for numerical analysis. They found the density to be 174 kg/m³ and heat capacity to be 2600 J/kg K. They carried out further numerical work to modulate temperature in concrete slabs. Based on the results, they found that if the coconut fiber were used on the external surface of the concrete, the room temperature would fall within the comfort range. They widely varied the density, thermal conductivity and heat capacity of coconut fiber to determine the sensitivity of temperature with respect to those changes. Based on the experiments, they concluded that the heat could be considered sensible only for thermal conductivity variations.

Abdou and Budaiwi (2005) stressed the importance and effectiveness of thermal insulation in buildings and explained how they could help lower the energy costs. Thermal conductivity (k) of a material depends on its density, porosity, moisture content, and mean temperature difference which determines the thermal insulation performance of that material. As per ASTM standards, the k -value of a material is calculated at 24°C.

However, when a material is used as an insulation for buildings, it undergoes variable temperatures, in which the performance of that material varies. The aim of their research was to determine the k-value of the materials commonly used in building enclosures, under varying temperatures. They used automated heat flow meters to produce variable temperatures and measured the k-values of seven different materials such as fiberglass, rock wool, wood wool, mineral wool, polystyrene, polyethylene and polyurethane. They obtained some of the k-values from the research performed by Budaiwi et al. (2002) where they measured the values under induced cooling loads. They undertook comprehensive measurements, compared and analyzed the values obtained from various materials under different temperatures. They claimed that their experimental results would provide better understanding of the k-values of materials under variable temperatures that would help builders select better performing building insulation materials.

Ucara and Balob (2010) conducted a research to determine the optimum thickness of insulation material that had to be used for external walls. They selected four cities located in four different climatic zones in Turkey. They calculated the energy savings and payback for four different insulation materials and five different types of energy such as natural gas, liquefied petroleum gas (LPG), and electricity. The insulation materials that they used were extruded polystyrene, expanded polystyrene, nil siding, and rock wool. They followed the P1–P2 method to calculate the net energy savings in this research. P1-P2 method is one of the methods of calculating the life-cycle cost of a system in engineering economics. P1 represents the ratio of life-cycle

fuel cost to the first year fuel cost. P2 represents the ratio of life-cycle expenditures incurred because of the investment. Based on their experimental results, they claimed that about \$4.2/m² to \$9.5/m² of energy cost savings could be achieved, which depended on the city and the type of insulation material used. Their results confirmed that using natural gas as heating source in the city of Mersin had the best payback period of 2.25 years whereas, using LPG as a heating source in the city of Bitlis had the lowest energy savings.

Vo and Paquet (2004) compared the insulation performance of extruded polystyrene (XPS) foams that were manufactured using different halogenated blowing agents. Extruded polystyrene that used residual blowing agents and aged up to 26 years were tested. They calculated, mathematically, the thermal conductivity of the material in the gas phase. To predict the long-term thermal resistance of extruded polystyrene foams accurately, they used the calculated thermal conductivity values using an in-house known as the Dow model. The Dow model was developed by the Dow chemical company, USA, to predict the long term thermal resistance of extruded polystyrene foams. XPS blown with different gases such as CFC-12, HCFC-142b, HCFC-22, HFC-134a, HFC-152a, and CO₂ were used. Materials stored in laboratory conditions as well as the ones gathered from field studies, such as cellars and roof, were tested. They found that the measured values and the predicted thermal conductivity values. Based on their results, they confirmed that the XPS foam blown with gases such as HFC-134a or HFC-142b were well suited to be used for long term thermal insulation applications. They also found that the thermal performance of XPS

foam blown with gases such as HCFC-22 and HFC-152a reached similar levels to the thermal performance of XPS foam blown with CO₂ after a short period of aging.

Al-Ajlan (2006) conducted a research on insulation materials commonly used in Saudi Arabia and that are made by local manufacturers, and described various measuring techniques to evaluate the thermal properties of those insulating materials. R-value of the material determines the resistance offered to transfer of heat, which could be determined by the thermal conductivity (k) and hence the k-value was regarded as the most important thermal property. It was also found that thermal properties such as specific heat capacity (c) and density (ρ), were helpful to assess the heat transfer characteristics of the materials under transient conditions. The thermal properties could accurately be measured using the transient plate source (TPS) technique (Log, 2004) under transient conditions. This is also known as hot plate method. The thermal properties of the insulation materials at room temperature were measured as well as at variable high temperatures when these insulations were used in buildings that were air-conditioned. In addition, the thermal conductivity of the materials under various densities were measured. Based on experimental results under controlled variable temperature settings, it was concluded that the thermal conductivity increased with increase in temperature and decreased with increase in density of the material for the density range used for the experiment.

Frydrych et al. (2002) made a study on yarn made of natural and man-made cellulose fibers which are commonly used in textile industries. The properties of the finished goods mainly depend on the type of raw material and the fabric type. Through

this research, the thermal properties (i.e., thermal conductivity, absorption, and thermal resistance) of fabrics composed of Tencel and cotton were comparatively analyzed. For test purposes, six types of fabrics made of cotton yarn and nine types of fabrics made of Tencel yarn were used. All fabrics had warp and weft yarns of nominal linear density of 20 tex. Three kinds of weaves such as plain, combined and twill with nominal warp and weft densities of 320/dm were studied. An alambeta (Yildiz, 2007) was used to perform the measurements on the finished fabrics. The influence on the thermal properties of fabrics made of Tencel and cotton based on the type of weave was studied. Based on these experimental results, it was concluded that the fabrics made of Tencel yarn had lower thermal conductivity, higher thermal diffusion and higher thermal resistance when compared to the fabrics made of cotton yarns.

Kymalainen and Sjoberg (2008) evaluated the suitability of bast fibers of flax and hemp which can be used as thermal insulation. Thermal insulation made of bast fibers of flax and hemp have a very small share in the market. Through this assessment, the authors discussed about the functions, thermal properties, such as thermal resistance and the requirement of these fibers. The thermal conductivity and the effect of other parameters on thermal properties, raw materials cost and environmental aspects of using these fibers were all discussed.

Korjenic et al. (2011) conducted a research to find the suitable physical and mechanical properties of natural fibers such as jute, flax and hemp so that these can be compared with commercial synthetic building insulation materials such as polystyrene (EPS). Energy efficiency in buildings was evaluated based on the heating energy

demand and ecological properties of the building material. Sustainability in building design and the need for green building strategies are needed. Therefore, the use of natural fibers as thermal insulation has been explored to conserve energy and to make use of natural materials, which are green building strategies. Using natural fibers could ameliorate the need for disposal of synthetic insulation materials, which may be harmful to the environment. However, natural materials are more sensitive to moisture, decompose on exposure to differential temperatures and moisture, and are attacked by microorganisms. All of these aspects make fibers have shorter lifetime than synthetic materials. Hence, the evaluation of the degradation rate of built-in materials and their actual in situ hygrothermal properties based on their moisture content, and volume changes is important. The main focus of their investigation was the impact of changes in moisture content in relation to the rate of change of other properties. Based on these test results, it was concluded that the correct combination of natural materials could be compared with conventional materials.

CHAPTER III

EXPERIMENTAL SET-UP

Dynamic Wall Simulator

A dynamic wall simulator was used in this research. The simulator was a cube with six sides (Figure 3.1). Each side had a removable wall panel of length and breadth of 1.2 meters each.



Figure 3.1 Dynamic Wall Simulator

The structural frame of the simulator was made of 6.35 millimeters thick structural steel angle (Figure 3.2). The frame was supported by four steel angled legs and was raised from the floor by 0.6 meters. The corners were hinged to install and uninstall the wall frames easily whenever necessary.



Figure 3.2 Structural Frame of Simulator

The wall panels were built in such a way as to imitate the actual walls in residential buildings. Each wall panel was divided into two compartments. The wall panels consisted of wooden boards at the back and sides, gypsum board (dry wall) on the outer side and a cavity of 0.1 meter deep in the inside (Figure 3.3). The outer gypsum board could be removed, if needed, for the insulation to be installed or removed.



Figure 3.3 Wall Panel Cavity

Six 200 W incandescent bulbs were used as a heat source for this simulator. The bulbs were attached to a bulb cluster and the cluster was suspended at the center of the simulator inside using thin steel wires (Figure 3.4). The heat output was controlled with

dimmers and timers (Figure 3.5). The heat output was calibrated and the timers were set to simulate the temperature changes very similar to those occurring in buildings located under full weather conditions. The four bulbs at the sides of the cluster had a separate timer for control and the top and the bottom bulbs in the cluster had a different timer for control.

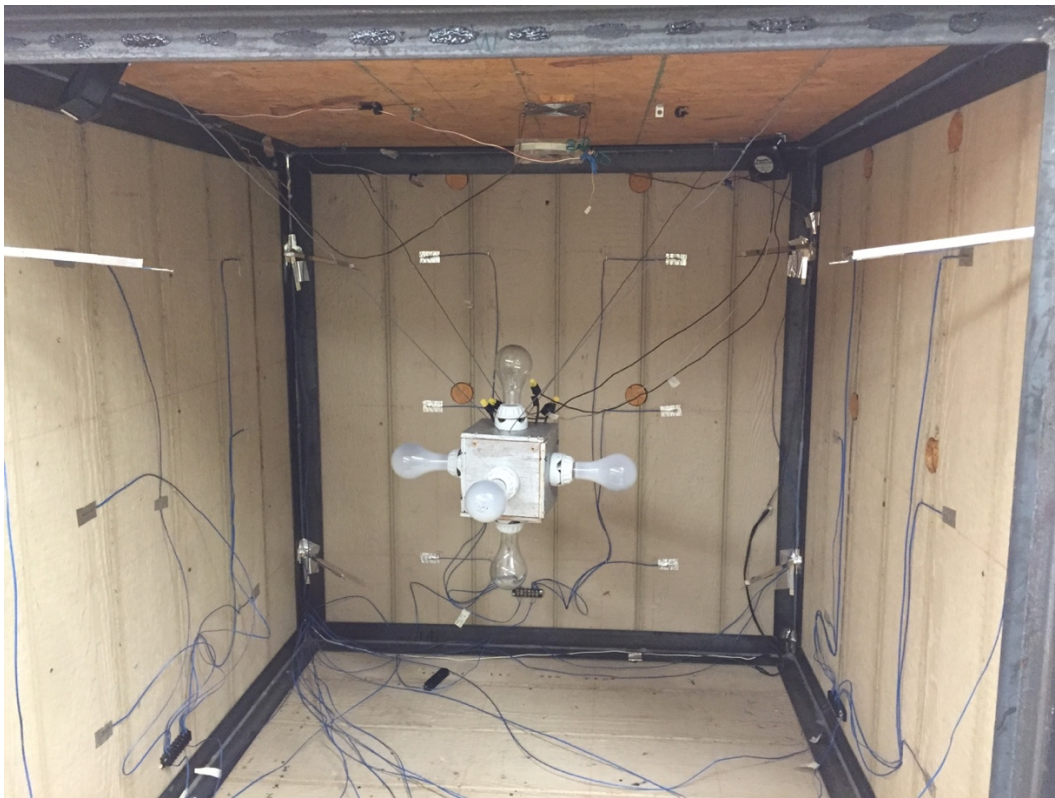


Figure 3.4 Light Bulbs Cluster

Two small fans were placed at diagonally opposite top corners within the simulator (Figure 3.6). These fans facilitated the air circulation inside the simulator. A relatively larger fan was placed at the top center on the inside of the simulator. This fan was controlled by a timer and was used for cooling the simulator during the night

setting. These fans were connected to a power source using 18 to 24 V power adapters. The timers operated in such a way as to imitate the day and night cycles experienced by walls exposed to full weather conditions.

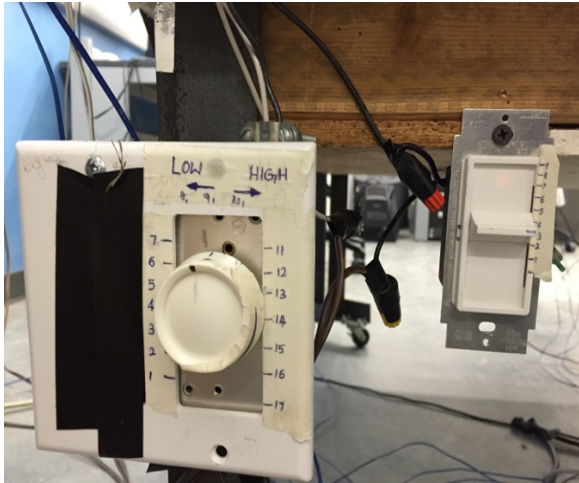


Figure 3.5 Dimmers



Figure 3.6 Circulation Fan

The wall panels were installed to the simulator frame using angle clamps (Figure 3.7). Four extruded polystyrene foam sheets (XPS) of 12.7 mm in thickness were cut to fit inside each compartment and placed inside the cavity of each wall panel. This was referred to as the calibration condition. An air gap of about 38 mm thickness was maintained at the inner side of the wall cavity using air gap separators (Figure 3.8).

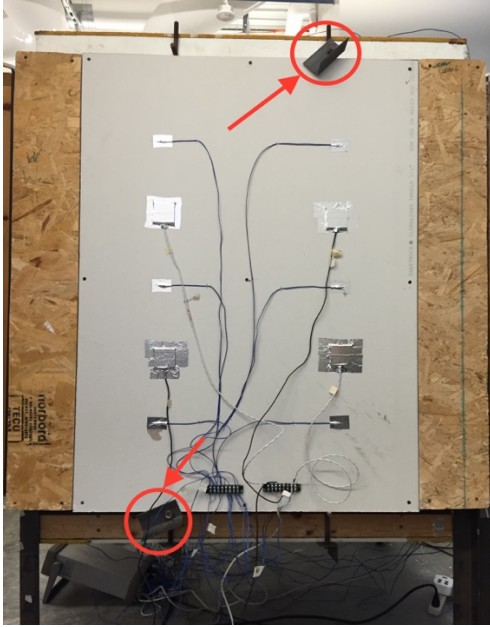


Figure 3.7 Securing Clamps



Figure 3.8 Air Gap Separators

A calibration was performed to ensure that all four walls received the same amount of heat from the heat sources. For this, extruded polystyrene foam sheets were installed in the cavities of all four panels.

During experimentation with different fibers such as straw, hay and coconut fiber, the situation became very difficult to place those materials into those cavities. Many number of trials were performed to determine the optimum method to place the materials inside the cavity. During the first trial, a 12.7 mm thick XPS sheet was placed inside and the material to be experimented was stacked inside the cavity. Since the material was fibrous, the material constantly slipped from the cavity. During the second trial, it was decided to alter the simulator setup by making the wooden plank at the top of the cavity removable. As a result, in this trial, the dry wall was installed and the

materials could be filled from the top and then the top wooden plank was closed. At first, this method seemed to be successful, but when the dry wall was removed to change the material, it was noticed that there was some settling in between the fibers and that the cavity was not uniformly filled with the materials (Figure 3.9). Therefore, this method also had to be abandoned. Finally, it was decided to redesign the removable panels. The removable panels were built using wooden sticks, cardboard pieces, and bird mesh glued together to keep them intact. The final removable cavity panel is shown in the Figure 3.10.



Figure 3.9 Cavity Filled with Straw

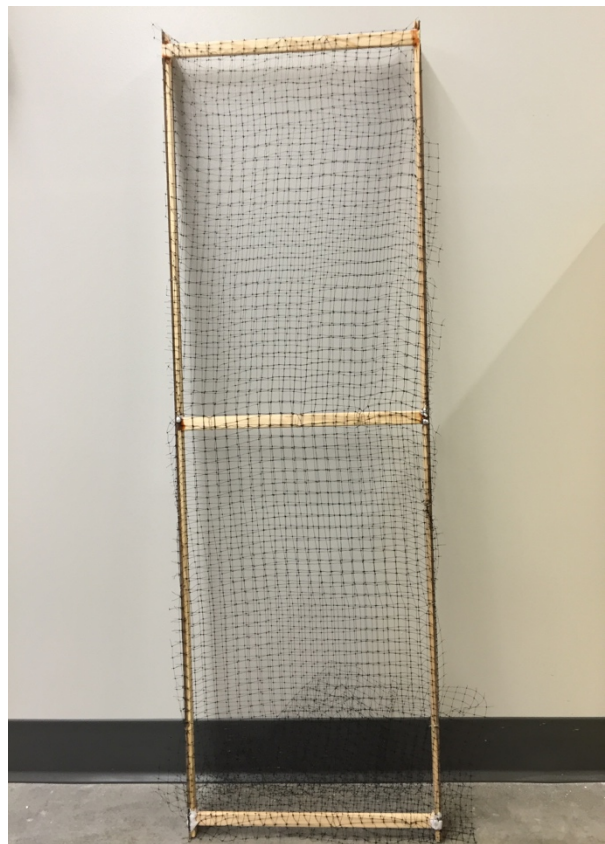


Figure 3.10 Removable Cavity Panel

The removable cavity panel was laid on the floor horizontally and the materials were spread evenly. This design helped in keeping the fibers in position without settling. Then the panels were placed inside the cavities of the wall panels. The evenly spread materials was kept inside the cavities of the wall panels using these last design made of removable cavity panels, which is shown in Figure 3.11.



Figure 3.11 Removable Cavity Panel with Coconut Fiber

Thermocouples

Thermocouples (TCs) are used to measure temperature. Type T thermocouples were used to measure both air and surface temperatures. The accuracy of temperature measurement of these TCs was $\pm 0.5^{\circ}\text{C}$. Each wall panel was outfitted with nine TCs on

the exterior side, nine TCs on the interior side and nine TCs in the interior layer of the XPS sheet to measure one internal layer temperature. The TCs were spaced in such a way that they were at the center of each compartment. In addition, the TCs were connected in parallel. In this fashion the average temperature values at each surface was measured. About eight TCs were installed at the exterior top and bottom corners at about 0.2 m from the simulator to measure interior air temperature. Similarly, eight TCs were installed at the exterior top and bottom corners at about 0.2 m from the simulator to measure the exterior air temperature. All the TCs were covered with aluminum foil to reduce radiation effects.



Figure 3.12 Thermocouples Covered with Aluminum Foil

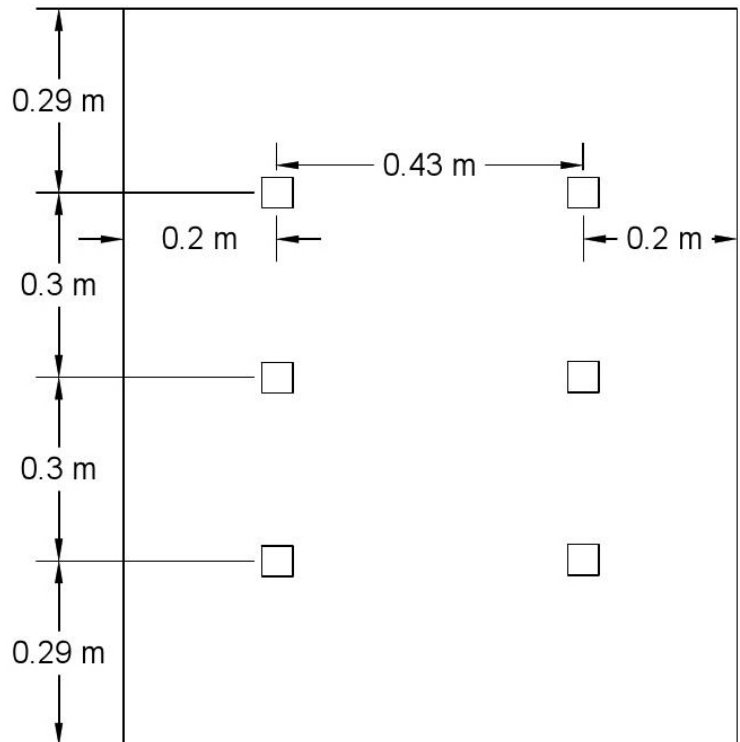


Figure 3.13 Location of Thermocouples

Heat Flux Meters

Heat flux meters (HFMs) were used to measure the heat flux through the wall panels. Over a range of repeated measurements, the HFMs had a deviation of up to 2% in readings. Four heat flux meters were installed on the outer side (dry wall) of each wall panel using pressure screws as shown in Figure 3.14. It was ensured that there was no air space between the surface of dry wall and the HFMs. The heat flux meters were also covered with aluminum foil to reduce the effects of radiation. Each heat flux meter was individually connected to the data logger. Figure 3.15 shows the location of the HFMs.



Figure 3.14 Heat Flux Meter Covered with Aluminum Foil

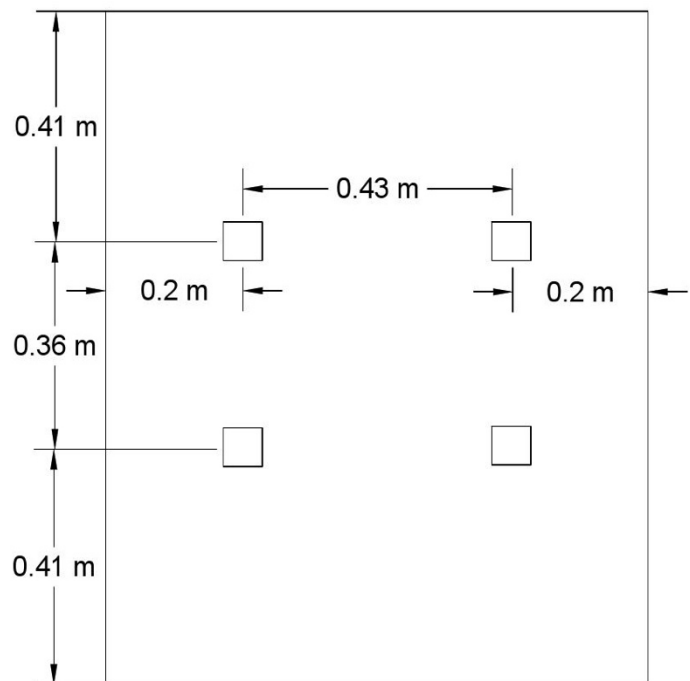


Figure 3.15 HFM Locations

Data Logger

The data logger was an Agilent model 34970A (Figure 3.16) connected to a computer. The data logger had three slots to connect multiplex boards (MUX) of twenty channels each. TCs and HFMs were connected to these channel slots and the temperature and heat flux values were fed into the computer system as °C and mV, respectively. Later, the heat flux values were converted into W/m^2 values manually using MS Excel.



Figure 3.16 Data Logger

CHAPTER IV

WALL HEAT TRANSFER

To fully estimate the energy use in buildings, it is important to understand the heat transfer mechanisms in building walls. In general, there are two processes of heat transfer namely:

- 1) Steady state heat transfer
- 2) Transient or un-steady state heat transfer

For example, if in a wall of a building the temperature on one surface were 25°C and the temperature at the other surface were 10°C , heat will always transfer from the region of higher temperature to the region of lower temperature. If these temperatures were to remain constant (i.e., 25°C and 10°C), then the heat transfer process in this case is steady-state heat transfer. If the temperature at any surface of the wall changes over a period of time, then the heat transfer process is transient heat transfer.

In a real world scenario, the heat transfer occurs in a three dimensional manner. However, in building walls, the heat transfer occurring in one dimension is much greater than in the other two, and therefore, one dimensional heat transfer equations can be used for calculating the heat transfer through the walls. In addition, in building walls heat transfer occurs in three modes, namely conduction, convection, and radiation. Figure 4.1 represents the heat transfer occurring in a building in which the interior temperature is higher than the exterior temperature (winter).

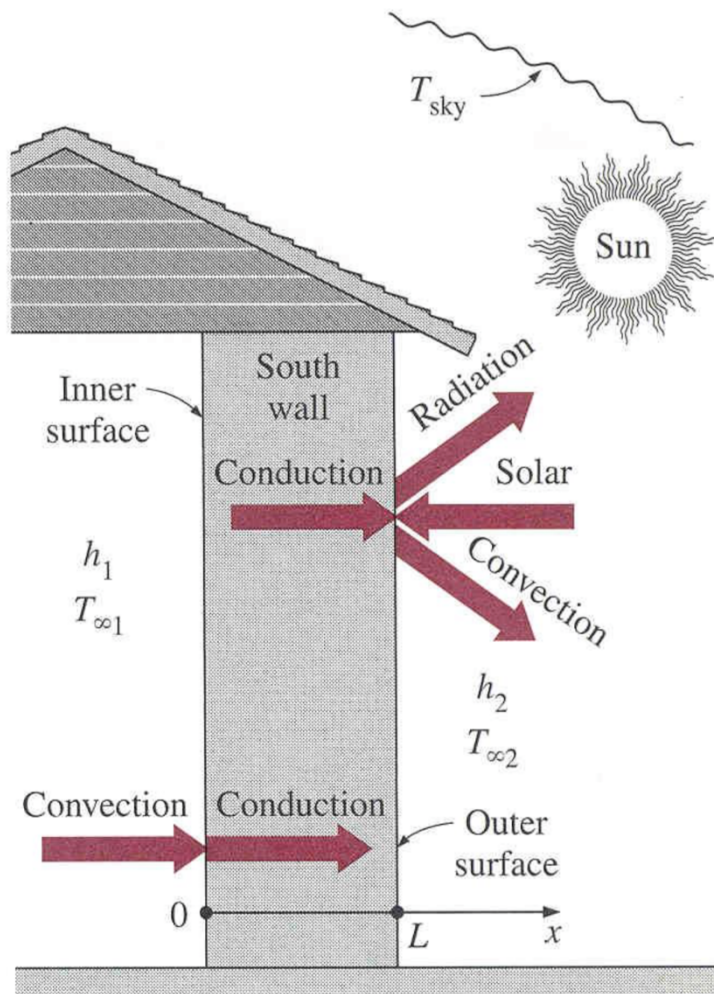


Figure 4.1 Schematic Representation of Heat Transfer (Cengel, 2015)

The research presented in this thesis was based on summer conditions in which the interior temperature of the building was lower than the exterior temperature. Hence, the direction of heat transfer was exactly opposite to the schematic representation shown above.

In this experiments, the temperature of the heat source inside the simulator was varied over time to imitate actual summer weather conditions. Consequently, it was a transient heat transfer process.

The purpose of this research was to evaluate the effectiveness of indigenous fibrous materials such as straw, hay and coconut fiber acting as insulation by comparing their performance to the performance of XPS sheets. The ultimate aim was to evaluate the R-values of these fibrous materials. The temperatures at both interior and exterior surfaces of the wall as well as the temperature at one inside layer within the wall were measured.

One-Dimensional Transient Heat Conduction

The exact solution of the one-dimensional transient heat conduction through a plane wall of thickness $2L$ is given by the Fourier's equation (Cengel, 2015),

$$\theta = \sum_{n=1}^{\infty} \frac{4 \sin \lambda_n}{2\lambda_n + \sin(2\lambda_n)} e^{-\lambda_n^2 \tau} \cos(\lambda_n x/L) \quad \text{--- Eq. (4.1)}$$

where,

$\theta = (T - T_{\infty}) / (T_i - T_{\infty})$ is the dimensionless temperature,

λ_n is the root of $\lambda_n \tan \lambda_n = Bi$,

$Bi = hL/k$ is the Biot number,

$F_0 = \tau = \alpha t/L^2$ is the Fourier number.

The solution can also be determined using numerical methods or finite difference formulations of the governing equation. The following steady state one-dimensional heat conduction equation was used to evaluate the R-values of the indigenous fibrous materials.

Steady Heat Conduction in Plane Walls

According to Fourier's law of heat conduction (Cengel, 2015),

$$\dot{Q}_{cond, wall} = -kA \frac{\Delta T}{\Delta x} \text{ (W)} \quad \text{--- Eq. (4. 2)}$$

where,

\dot{Q} is the rate of conduction heat transfer (W)

k is the thermal conductivity (W/m-°C)

A is the cross sectional area (m²)

$\Delta T/\Delta x$ is the temperature gradient (°C/m)

From this equation, the heat transfer rate per unit area (q) or the heat flux equation can be obtained as,

$$q = \frac{\Delta T}{R} \quad \text{--- Eq. (4.3)}$$

where,

$R = \frac{\Delta x}{k}$ is the thermal resistance (m² °C/W)

In the building industry, this is known as the R-Value of the material. During calibration, four XPS sheets of known R-value and thickness were used. The thickness of the wall panel and the temperatures at both surfaces of the wall panel were also measured. Using these values, the thermal resistance of the air gap was calculated. When the fibers were used as retrofits, all other values including heat flux values were known. Once all these values were plugged into the Fourier's equation, the R values of the indigenous insulation were obtained.

The temperature gradient of a typical multi-layered wall is shown in Figure 4.2.

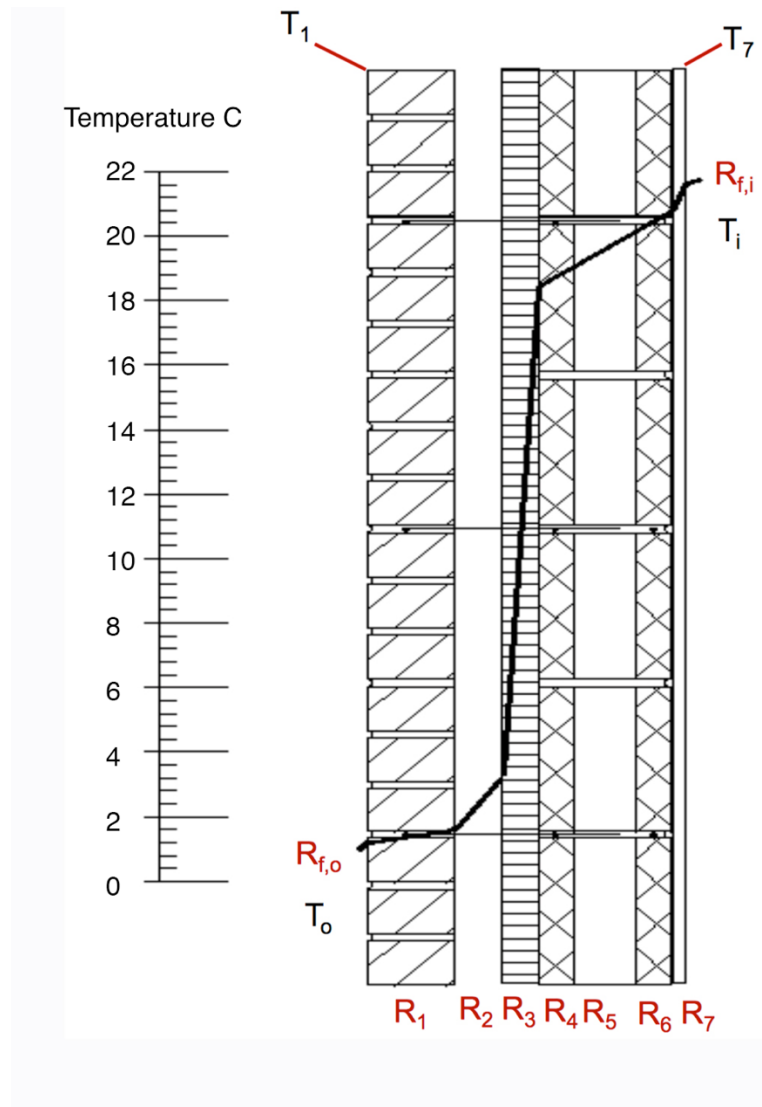


Figure 4.2 Temperature Gradient of a Multi-Layered Wall (Straube, 2005)

In the above figure, $R_{f,i}$ and $R_{f,o}$ denote the resistances of the air films at the interior and exterior surfaces of the wall, respectively. R_1 through R_7 are the thermal resistances offered by each layer. T_1 and T_7 are the exterior and interior surface temperatures, respectively. T_o and T_i are the exterior and interior air temperatures respectively. $R_{f,i}$ and $R_{f,o}$ were not used because the interior and exterior surface temperatures were known.

Thermal Mass

Materials used in buildings have the ability to store heat. The property associated with thermal mass is the thermal diffusivity. Based on the thermal mass, certain materials can dampen the sudden changes in the environment such as temperature. If materials with appropriate thermal mass were used in building structures such as walls, they can complement the building insulation. The thermal mass of a material depends on Specific heat capacity of the material c_p (J/kg. °C)

- Density of the material ρ (kg/m³)
- Thermal conductivity k (W/m. °C)

The thermal diffusivity (α) is given by,

$$\alpha = \frac{k}{\rho c_p} \quad \text{--- Eq. (4.4)}$$

A low value of thermal diffusivity of a material, means that the heat absorbed and stored by the material are greater.

CHAPTER V

RESULTS, ANALYSES AND DISCUSSIONS

Dynamic Wall Simulator Calibration

The dynamic wall simulator was calibrated by installing XPS sheets in all of the cavities. The left cavity of each wall panel was left as a control and the right cavity was used for the retrofits. The control side was filled with four XPS sheets each of 12.7 mm thickness, followed by a 38 mm thick air gap from the exterior towards the interior. Each XPS sheet had an R-value of $0.528 \text{ }^{\circ}\text{C m}^2/\text{W}$. During the calibration period, the retrofit side was also filled with XPS sheets in the same configuration as the control side. In this case, the retrofit was called pre-retrofit. As explained earlier, the top fan, four side light bulbs, and the top and bottom light bulbs had separate timers to control their functioning. The timer of the side light bulbs was programmed to be turned on at 6:00 AM and turned off at 6:00 PM. The timer for the top and bottom light bulbs was programmed to be turned on at 11:00 AM and turned off at 4:00 PM. The timer for the top fan was programmed to be turned on at 6:00 PM (as soon as the side light bulbs were turned off) and turned off at 6:00 AM just before the side light bulbs turned on. This configuration produced the equivalent temperature variation pattern of the actual surfaces exposed to full weather conditions (Jin, 2013). The simulation was performed continuously for 48 hours. The initial settings of the TCs, HFMs and the timers were adjusted after each set of readings until the calibration produced similar temperature and heat flux variations as the actual field data (Jin, 2013). The temperature of the room

where the dynamic wall simulator was placed, was conditioned using a HVAC system and the temperature was always maintained between 22°C and 25°C. For this research, since the room was maintained at room temperature, the readings from the exterior side of the simulator to the exterior side were considered as interior temperatures and heat fluxes. To imitate the original temperature profile of a wall under full weather conditions, the heat source was placed inside the simulator; therefore, internal simulator readings were considered as exterior temperatures and heat fluxes.

Exterior Surface Temperatures

The exterior wall temperature profiles of the wall panels are shown in Figure 5.1 through Figure 5.4.

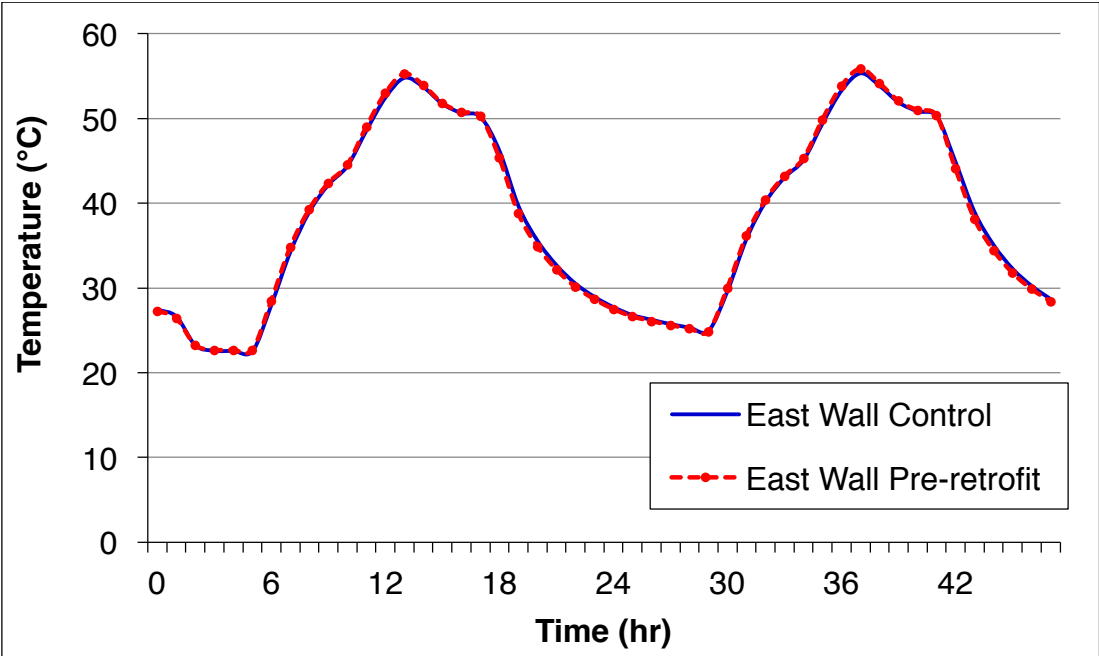


Figure 5.1 East Wall Exterior Surface Temperatures During Calibration

The 0th hour started exactly at 12:00 AM and under the above said conditions, the temperature started rising at 6:00 AM and gradually reached the peak at around 2:00 PM. Then the temperature was gradually reduced until the next day at 6:00 AM, at which time the temperature of the simulator was at its lowest value. From the temperature profiles of the exterior walls, it was noted that the peak temperature reached about 55°C and the lowest temperature was about 25°C, which was the room air temperature. The temperatures along both curves were almost identical. Therefore, a calibration process such as this would lead to acceptable results when comparing various insulation systems.

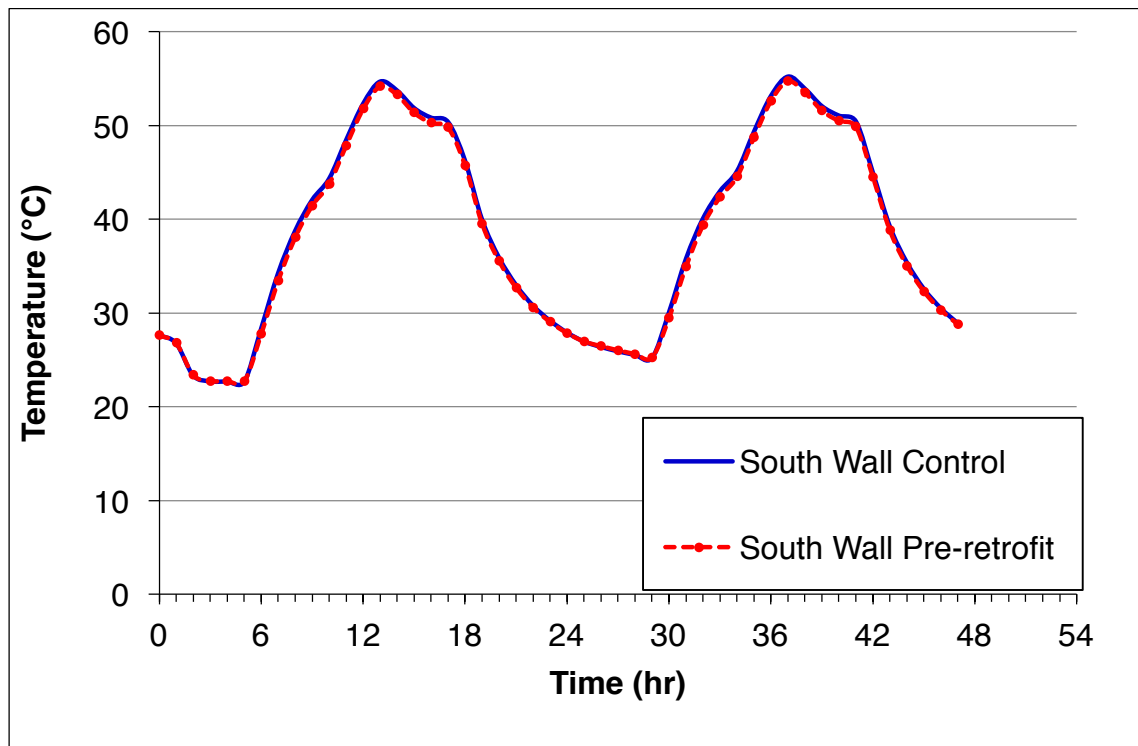


Figure 5.2 South Wall Exterior Surface Temperatures During Calibration

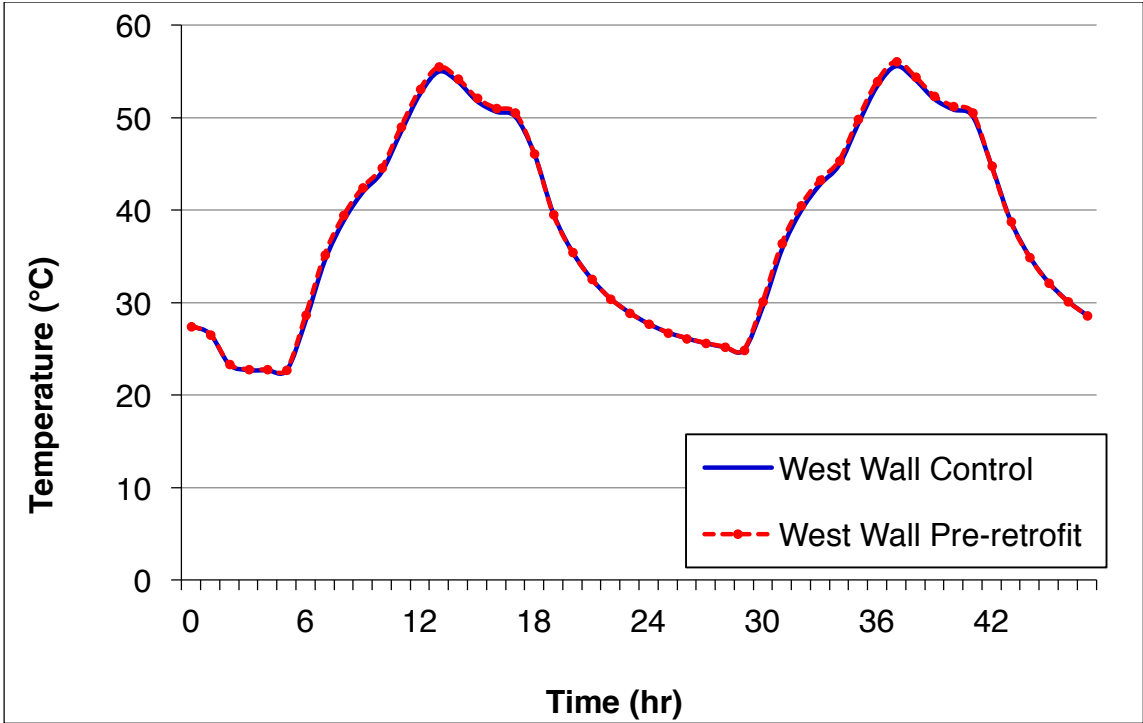


Figure 5.3 West Wall Exterior Surface Temperatures During Calibration

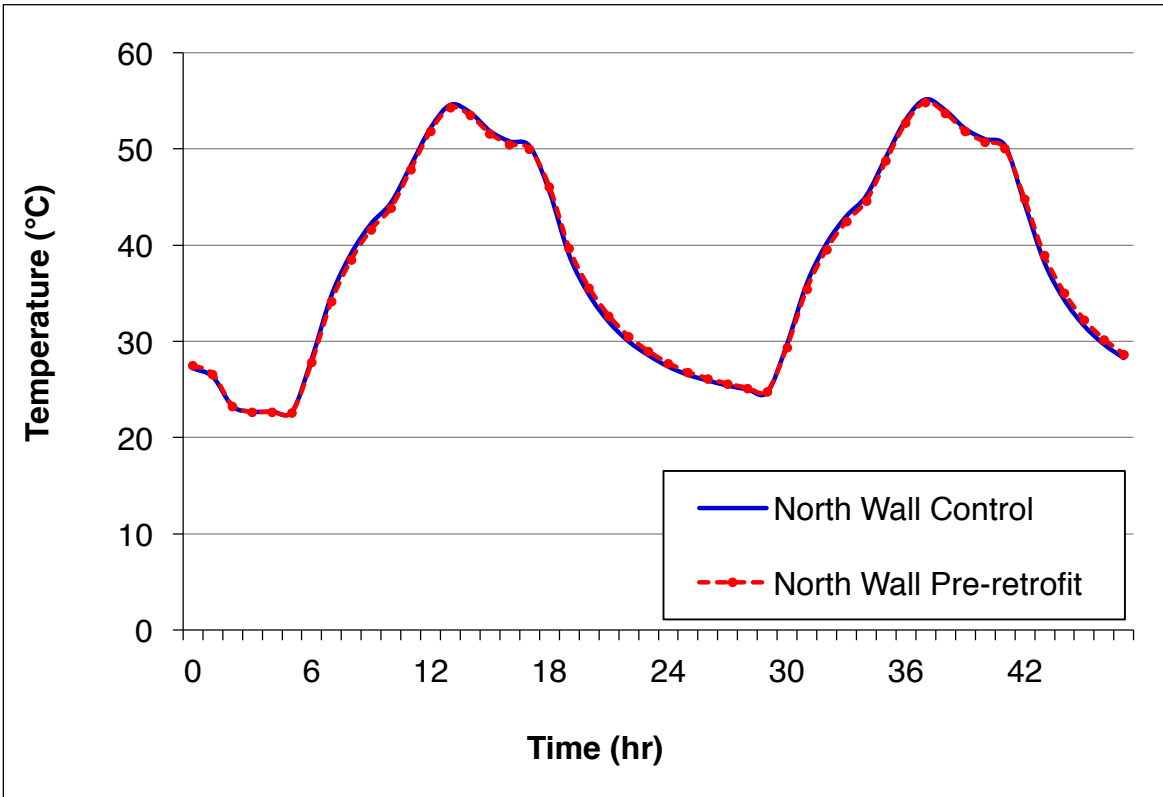


Figure 5.4 North Wall Exterior Surface Temperatures During Calibration

Layer Temperatures

Layer temperatures were measured using TCs attached to the fourth XPS sheet, which happened to be just next to the air gap in the interior side of the panel cavity. This is shown in Figure 5.5. These values were recorded to determine the effects, if any, produced by having an air gap, which in modern construction serves as both insulation and for wall drying purposes. The temperature variations at this layer over a period of time is shown in the Figure 5.6 through Figure 5.9. These graphs show that the peak temperature difference between the exterior surface and the layer was about 6°C , which was caused by the air gap.

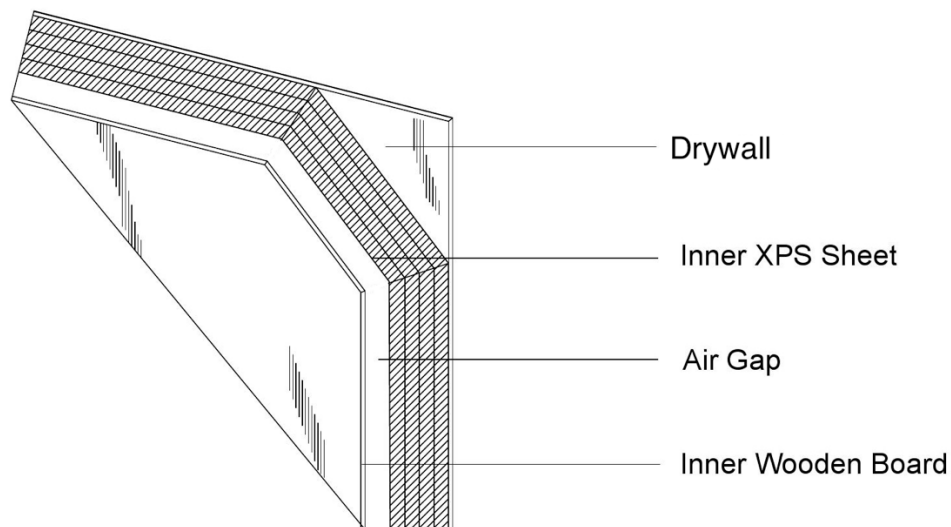


Figure 5.5 Cross-Section of Wall Panel

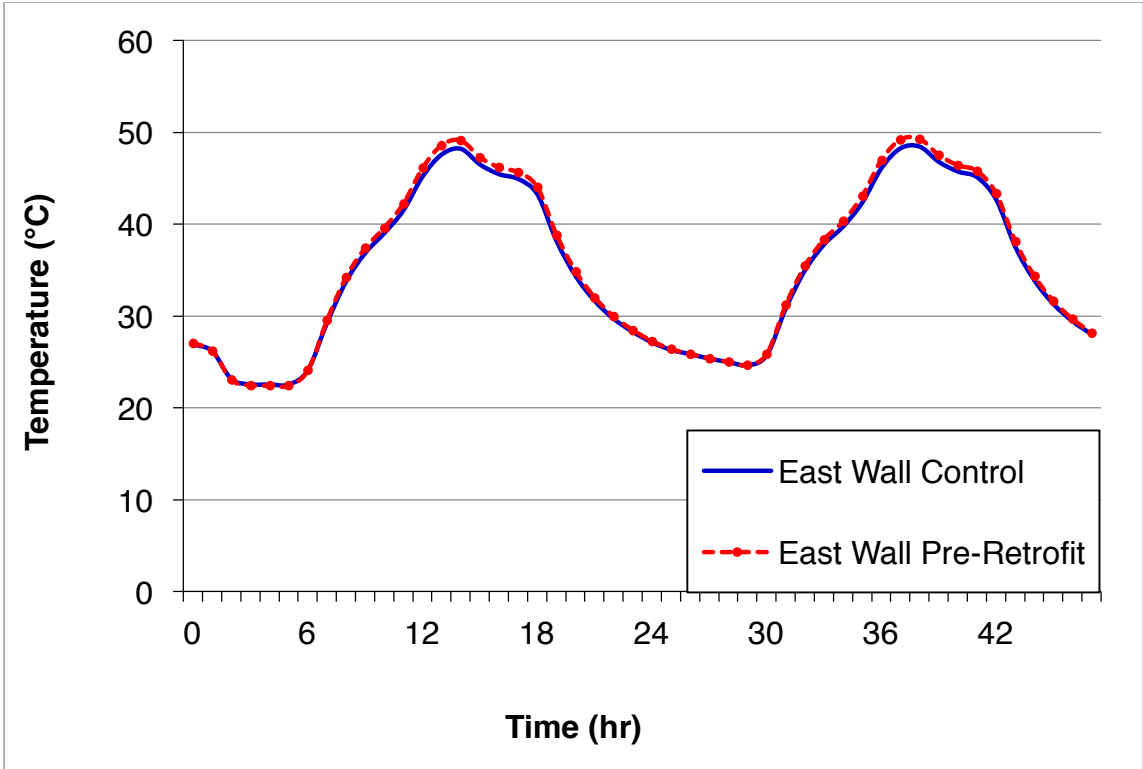


Figure 5.6 East Wall Layer Temperatures During Calibration

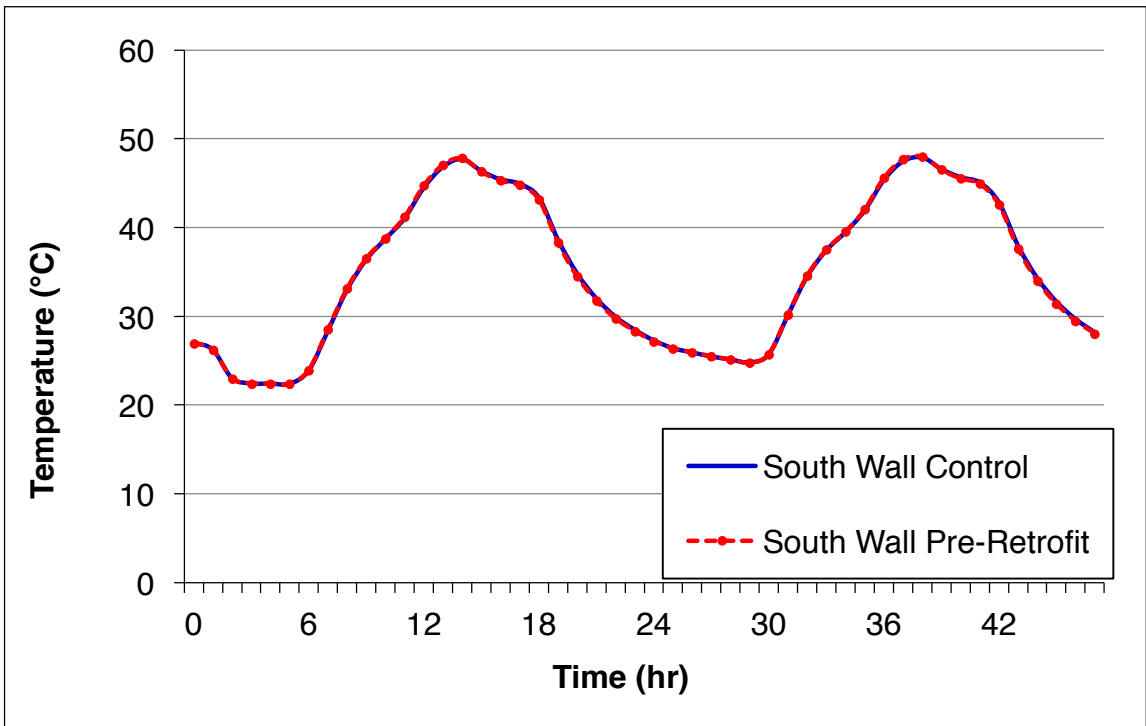


Figure 5.7 South Wall Layer Temperatures During Calibration

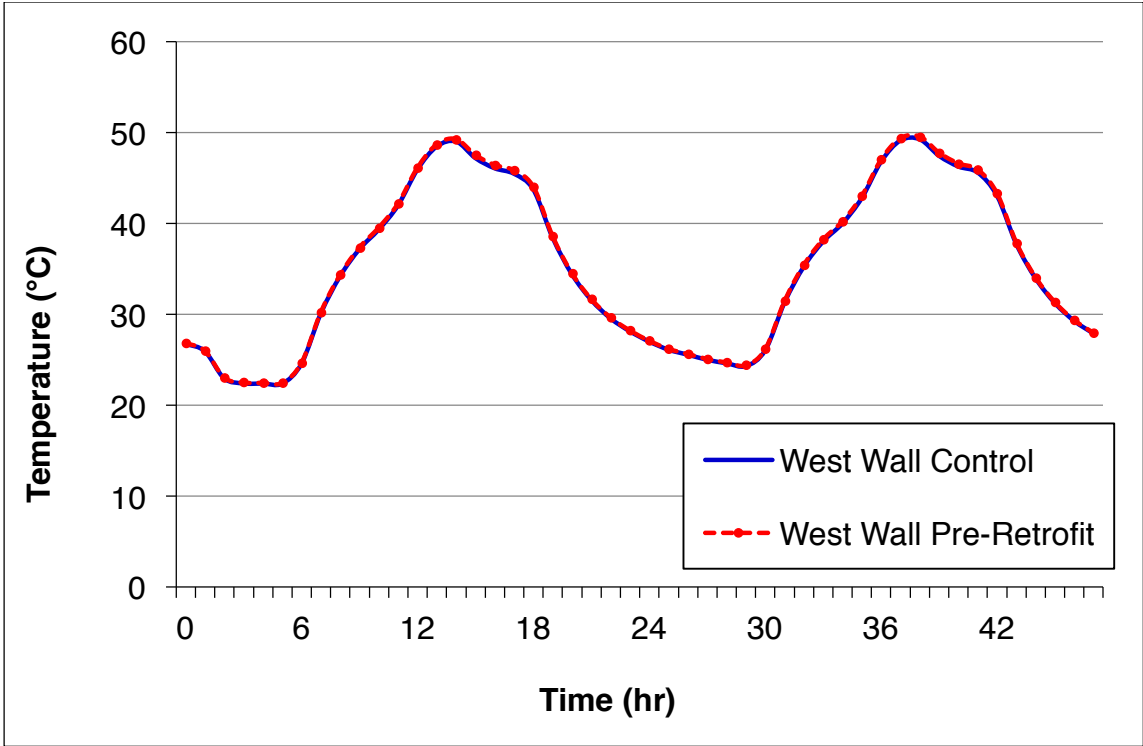


Figure 5.8 West Wall Layer Temperatures During Calibration

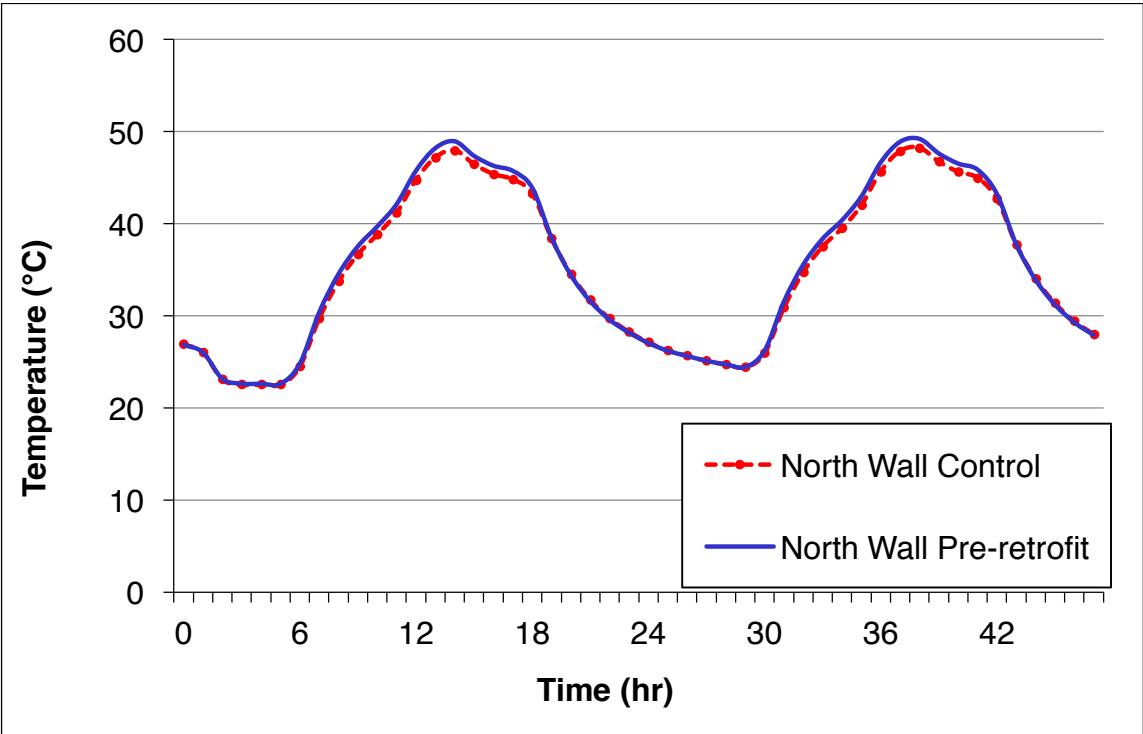


Figure 5.9 North Wall Layer Temperatures During Calibration

Interior Surface Temperatures

Interior surface temperatures were also measured to determine the effect of insulation on the heat transfer through the walls. Since the room where the simulator was placed was air conditioned, the difference between the lowest and the highest temperatures was about 3°C, which is very similar to what happens in actual buildings exposed to full weather conditions. This shows that the air conditioning in the room played a significant role in keeping the interior surface temperature at near constant values. The interior surface temperatures data are shown in Figure 5.10 through Figure 5.13.

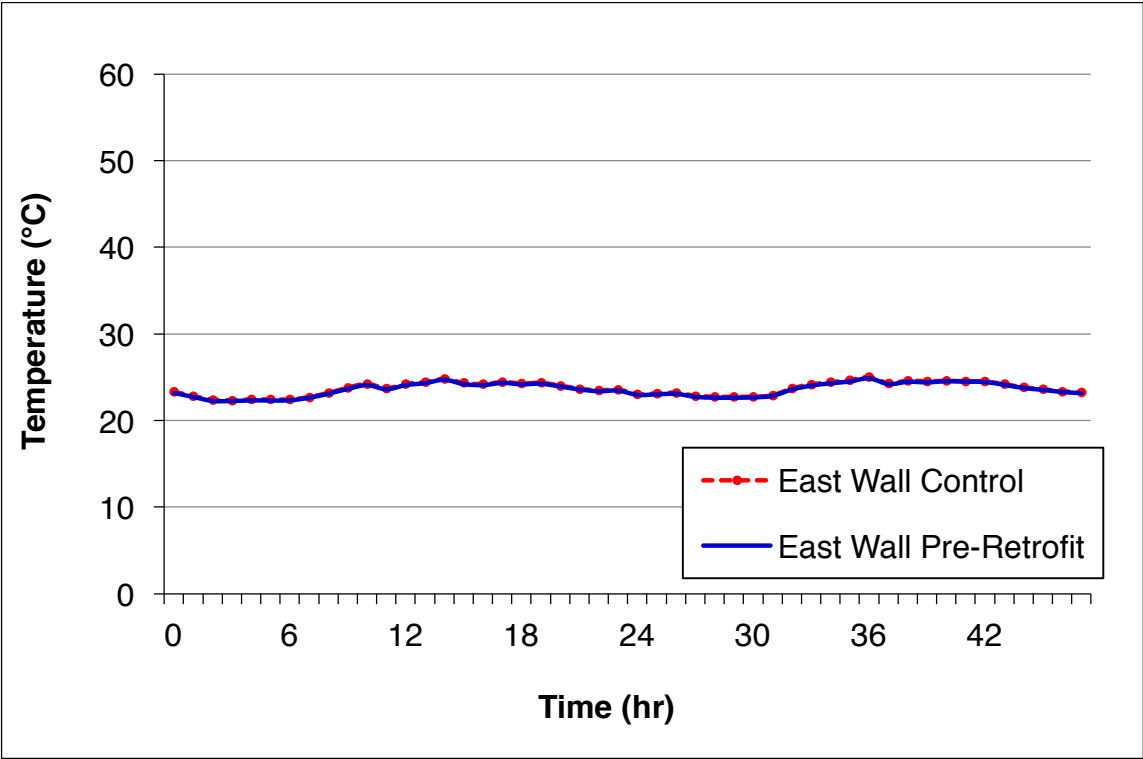


Figure 5.10 East Wall Interior Surface Temperatures During Calibration

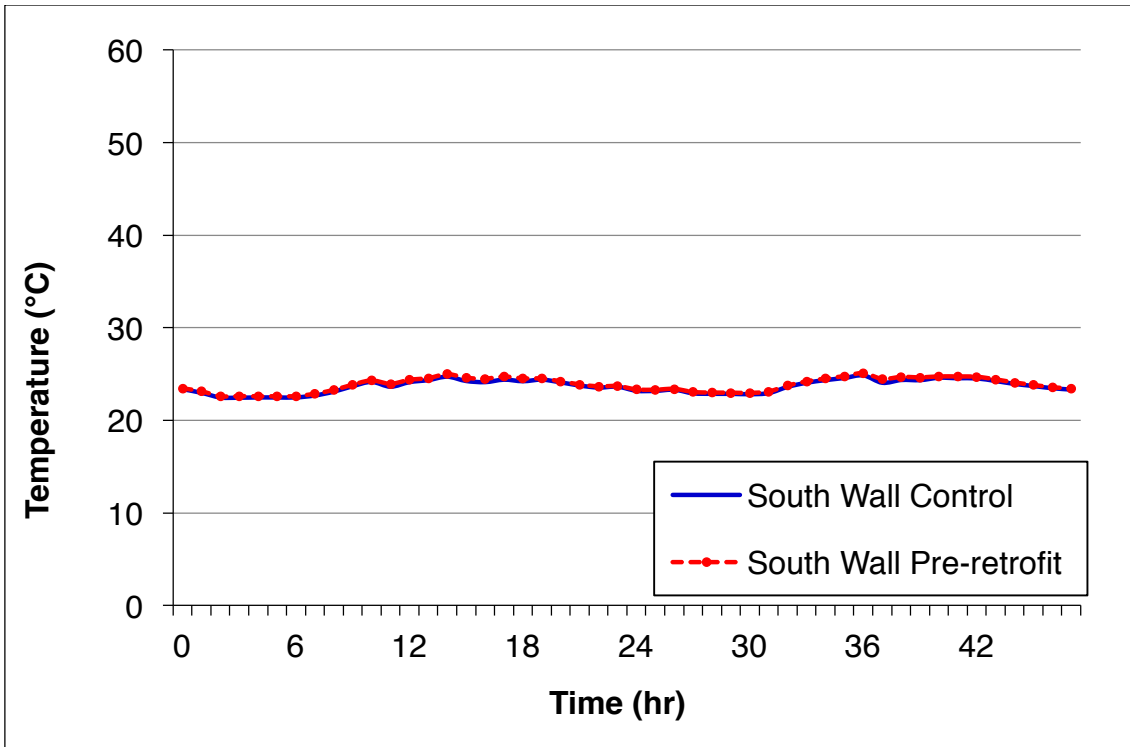


Figure 5.11 South Wall Interior Surface Temperatures During Calibration

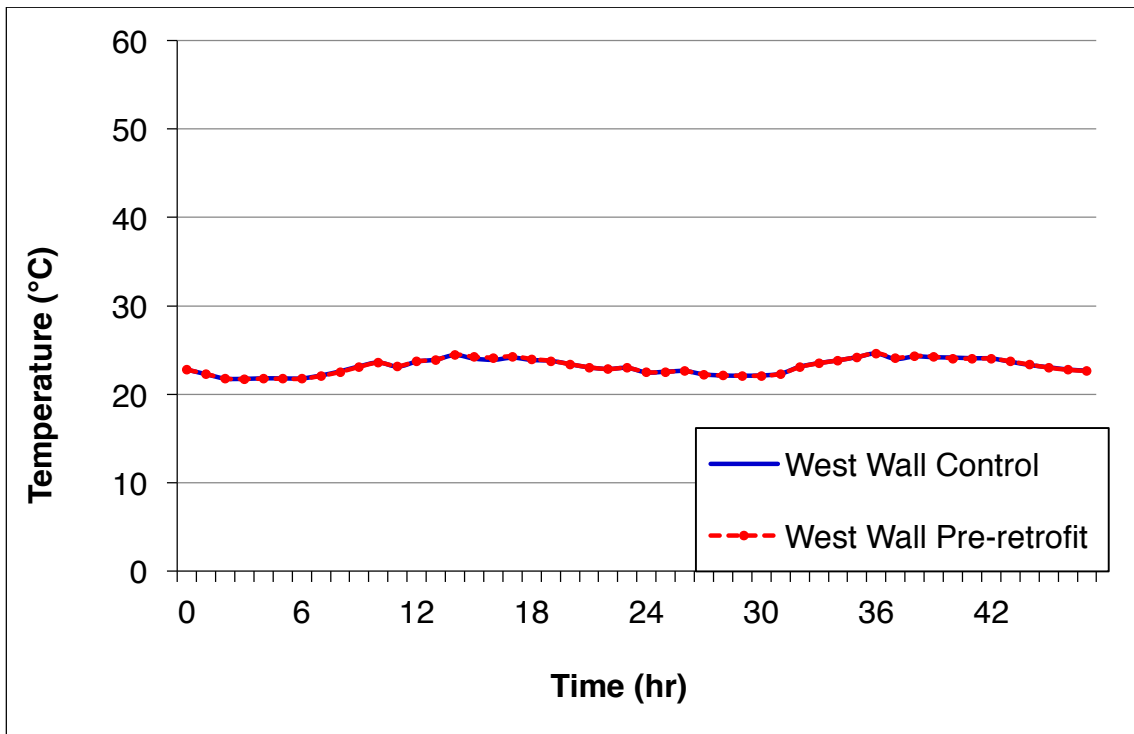


Figure 5.12 West Wall Interior Surface Temperatures During Calibration

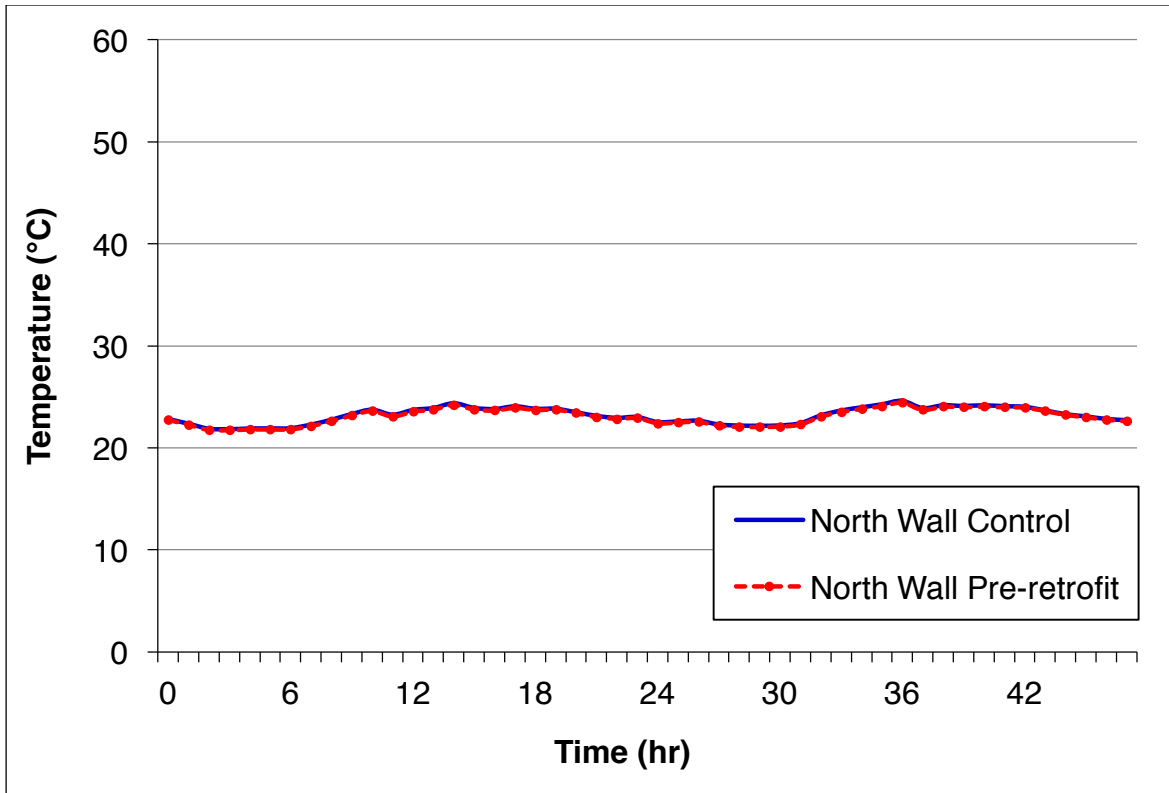


Figure 5.13 North Wall Interior Surface Temperatures During Calibration

All surface temperatures shown in Figures 5.1 – 5.4 and Figures 5.6 – 5.13 are indicative of a very well calibrated system. Basically, all temperatures which were compared in each of the graphs were nearly identical. This would allow for well-controlled comparisons between each of the indigenous fibers to XPS sheets.

Air Temperatures

The TCs were extended out from the interior and exterior surfaces to measure the interior and exterior air temperatures at the top and bottom of the dynamic wall simulator. Similarly, graphs were generated to study the trends in temperature changes with time. These are shown in Figure 5.14 through Figure 5.17.

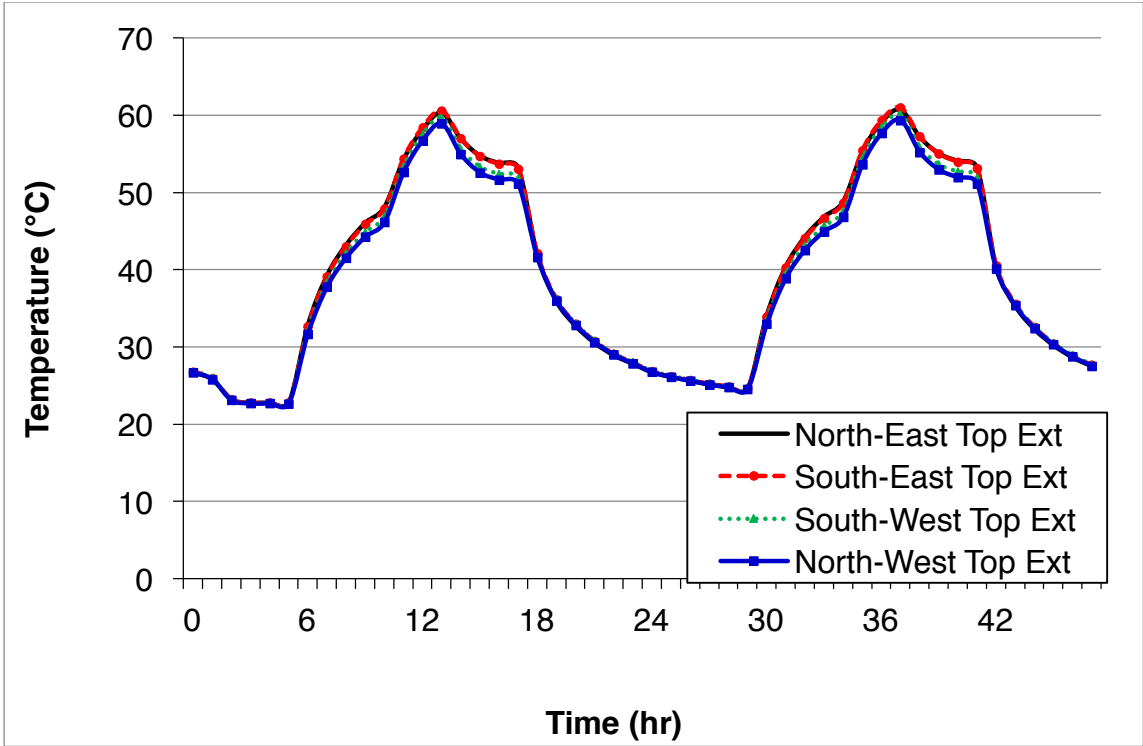


Figure 5.14 Top Exterior Air Temperatures

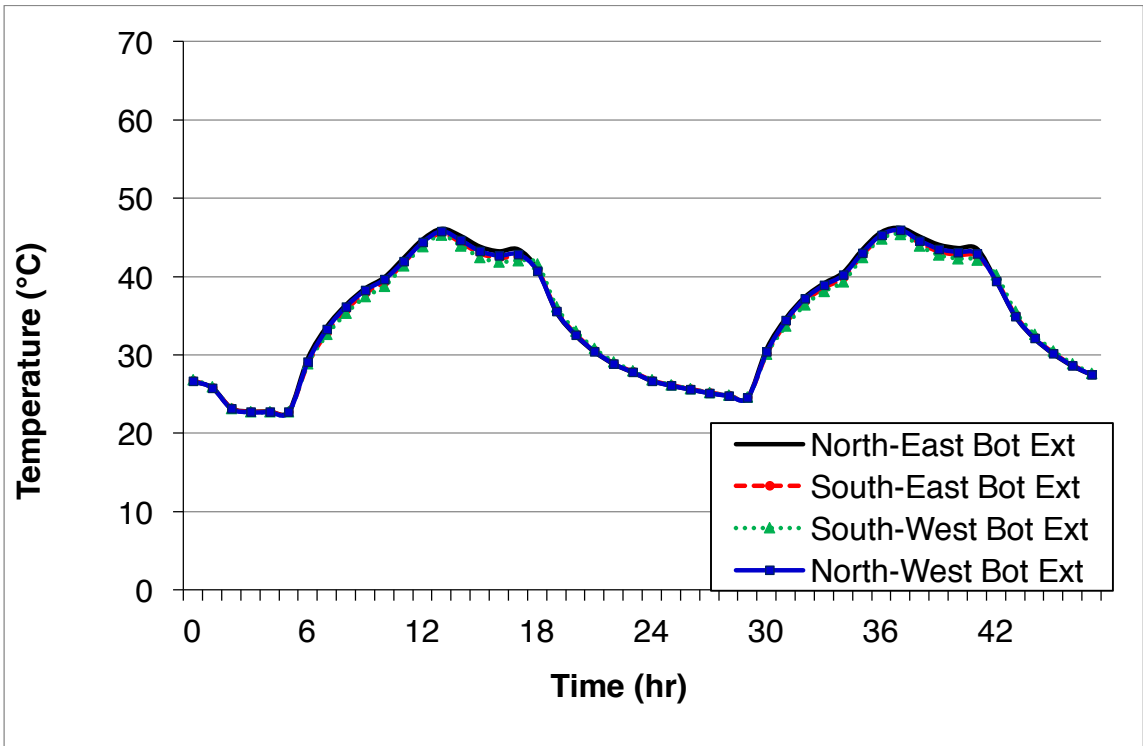


Figure 5.15 Bottom Exterior Air Temperatures

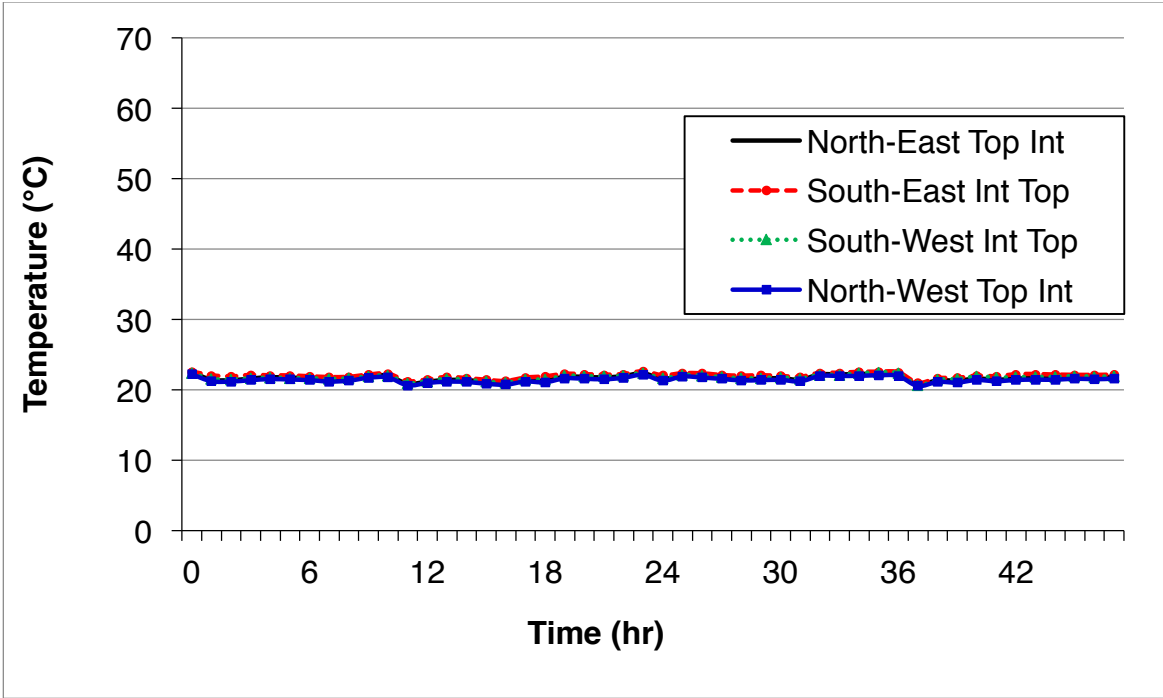


Figure 5.16 Top Interior Air Temperatures

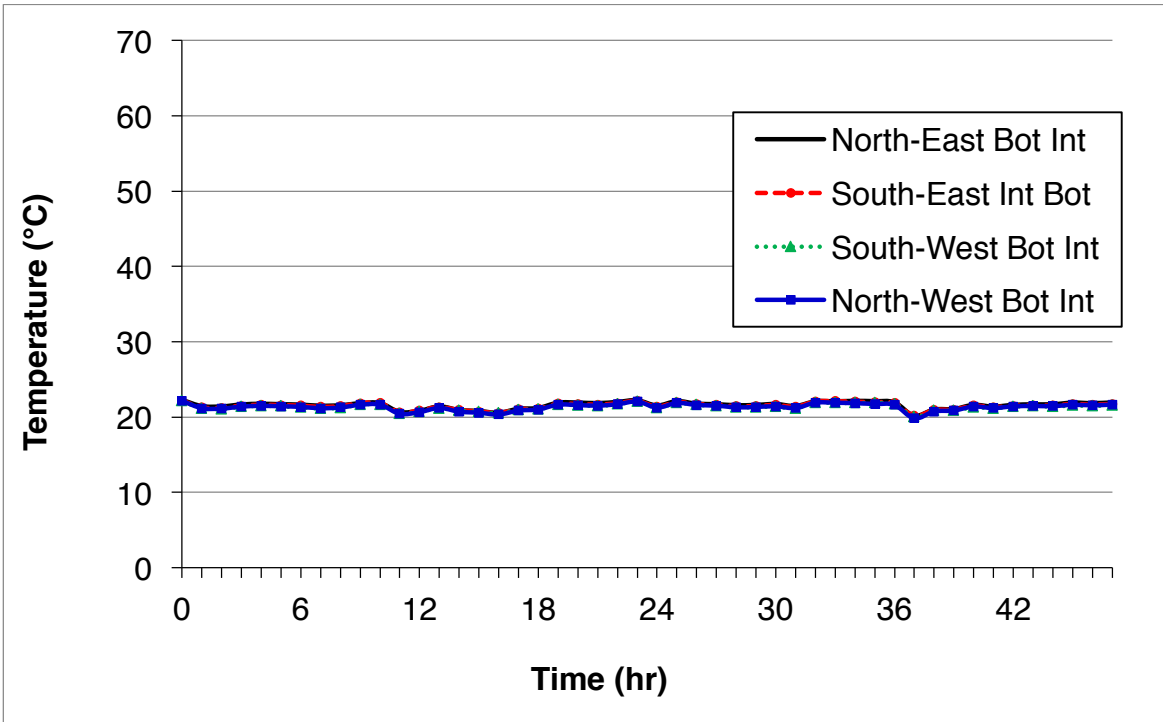


Figure 5.17 Bottom Interior Air Temperatures

The exterior air temperatures clearly showed the effect of the heat source, while the interior air temperatures were considerably affected by the HVAC system in the room where the simulator was placed. The exterior air temperatures ranged from about 22°C to 60°C. The interior air temperature was maintained fairly constant from about 22°C to 25°C throughout the experimental period.

Heat Fluxes

Heat fluxes through each wall were also measured using heat flux meters attached to the dry wall surface of the dynamic wall simulator. As stated above, this surface represented the interior surface of the system. Average heat fluxes from the control and retrofit sides were compared for each wall. For the calibration period, all segments of the walls labeled “control” and “retrofit” were filled with XPS sheets as explained before. Based on the results, the east wall reached a peak heat flux of about 12 W/m². The peak heat fluxes of south, west and north walls were 10 W/m², 9 W/m², 11 W/m², respectively. Graphs of heat fluxes over the calibration period are shown in Figure 5.18 through Figure 5.21.

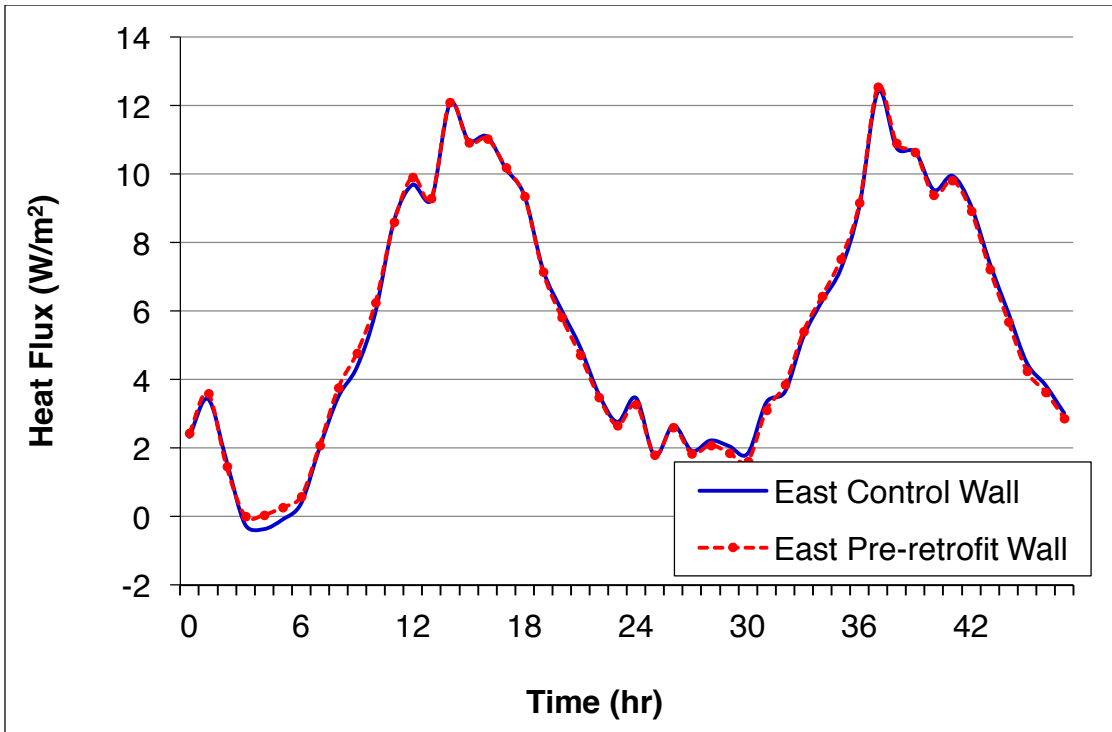


Figure 5.18 East Wall Heat Fluxes During Calibration

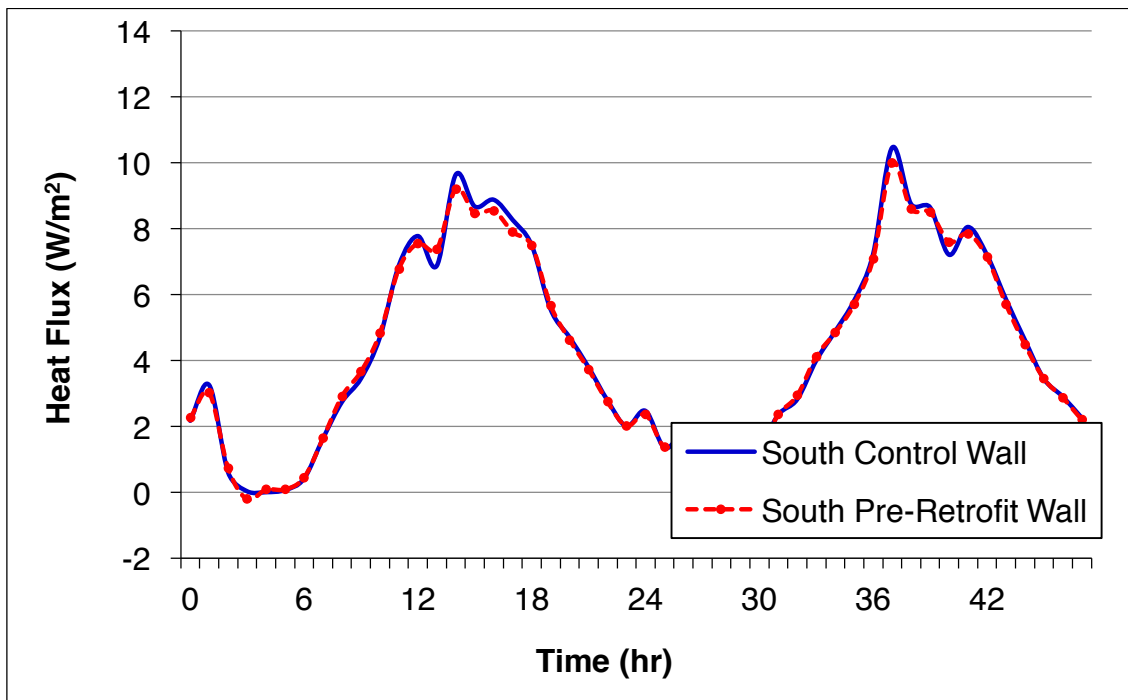


Figure 5.19 South Wall Heat Fluxes During Calibration

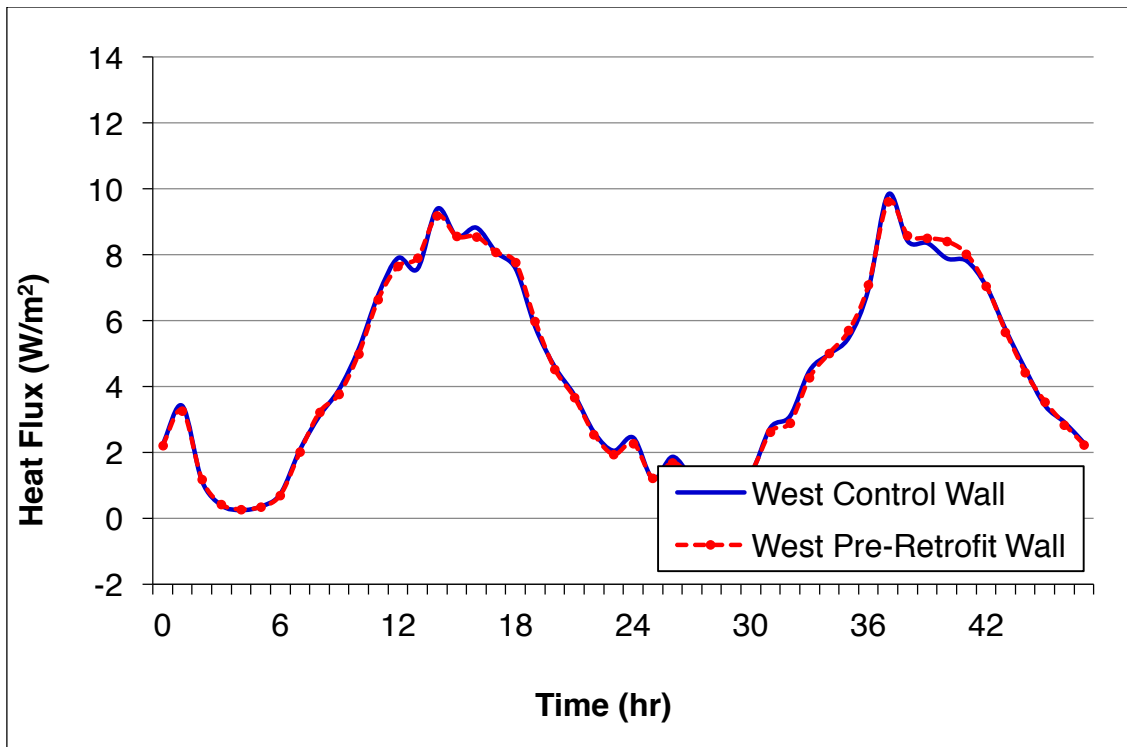


Figure 5.20 West Wall Heat Fluxes During Calibration

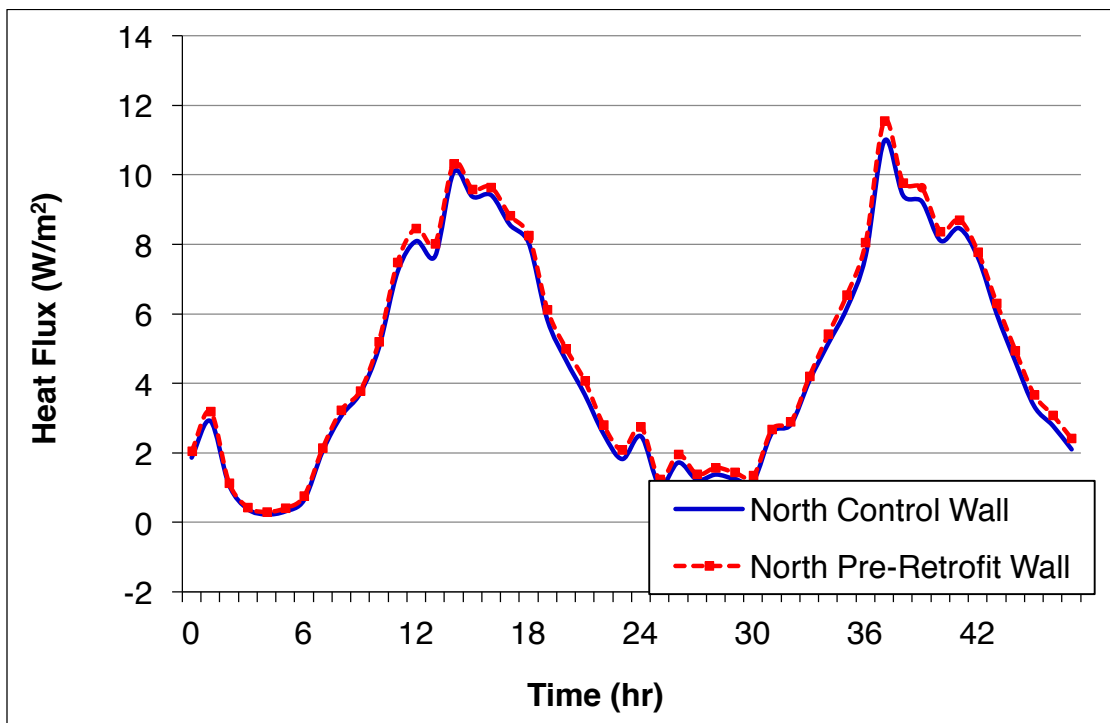


Figure 5.21 North Wall Heat Fluxes During Calibration

Similar to the temperature profiles, the heat flux values in all wall comparisons were nearly identical. In the following sections, any deviations in the magnitudes of the heat fluxes between control and retrofit segments of the walls could be solely attributed to the indigenous insulation.

Thermal Performance Evaluation of the Indigenous Materials

As stated before, each wall was subdivided into two spaces for different heat transfer paths (see Figure 3.11). Along one path, the heat transfer would go through XPS sheets (control) and along the other path the heat transfer would go through an indigenous material. In both paths, the heat would be transferred through identical dry wall and wood siding. The indigenous materials were tested at three different densities while the thickness and number of sheets of the XPS remained constant. The densities tested were:

- Case 1: Density of materials tested - 30 kg/m^3
- Case 2: Density of materials tested - 45 kg/m^3
- Case 3: Density of materials tested - 65 kg/m^3

These densities were calculated by measuring the masses of the materials and the volume of the wall panel cavities. The insulation material was then placed within the wall cavity. In addition, an air gap was created with a thickness that remained constant during calibration and testing of the indigenous insulation. A sheet of XPS with installed thermocouples was placed next to the air gap. These temperatures were referred to as “*layer temperatures*.” The replaceable panel described in the experimental setup was

placed and the cavity was sealed with a drywall sheet. The arrangement of the wall is shown in Figure 5.22.

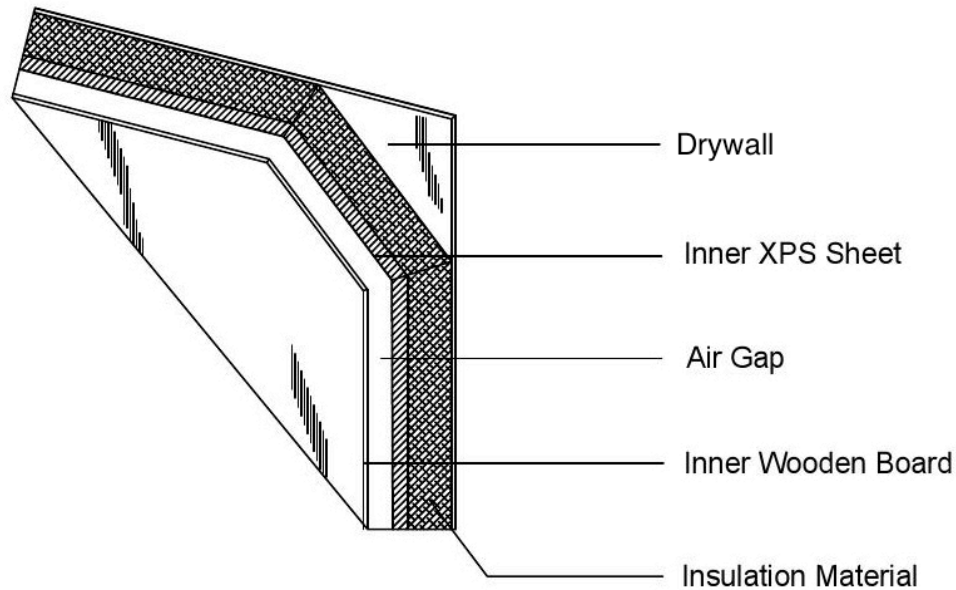


Figure 5.22 Cross Section of Retrofit Wall Panel

Case 1

As stated before, all the wall cavities were subdivided into two sections. One section in each wall cavity had XPS sheets that were used as control. The retrofit insulations used in the south, west, and north walls were Timothy grass, wheat straw, and coconut fiber, respectively. The density of all of the indigenous insulation was 30 kg/m^3 . A set of external surface conditions were imposed by the simulator to replicate actual wall temperatures similar to those observed when walls are under full weather conditions. Each experiment lasted 72 hours. The heat sources were adjusted to work exactly as they did during the calibration period. The data logger collected the data

every 10 seconds which were then converted into average hourly values. The values of the control path and retrofit path were compared using graphs.

Exterior Surface Temperatures

The exterior surface temperature profiles of the retrofit wall segment (segment with Timothy grass) and the control wall segment (segment with XPS sheets) were compared and are shown in Figure 5.23.

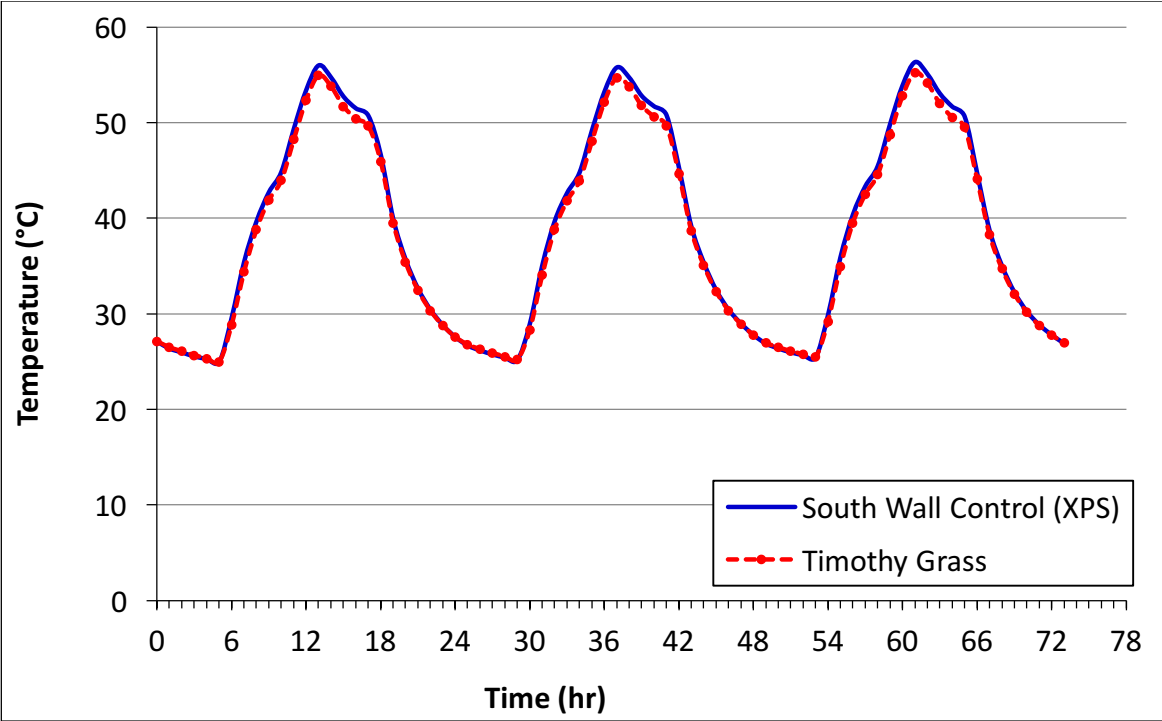


Figure 5.23 South Wall Exterior Surface Temperatures at 30 kg/m³

The temperature profiles show a maximum temperature difference of about 1°C at peak temperature. The temperature of the exterior wall surface with Timothy grass reached a peak temperature of 54.9°C and the exterior wall surface with XPS sheets

reached a peak temperature of 55.9°C. As the temperature values decreased, the curves gradually merged. From this observation, it was assumed that the Timothy grass facilitated slightly more heat transfer than the XPS sheets, increasing the conduction heat transfer and hence making the surface slightly cooler by the faster dissipation of heat. From this, it was assumed that the Timothy grass at 30 kg/m³ had a lower resistance to heat transfer when compared to the XPS sheets.

The exterior surface temperature comparison between the wall segment with wheat straw and the wall segment with XPS sheets is shown in Figure 5.24.

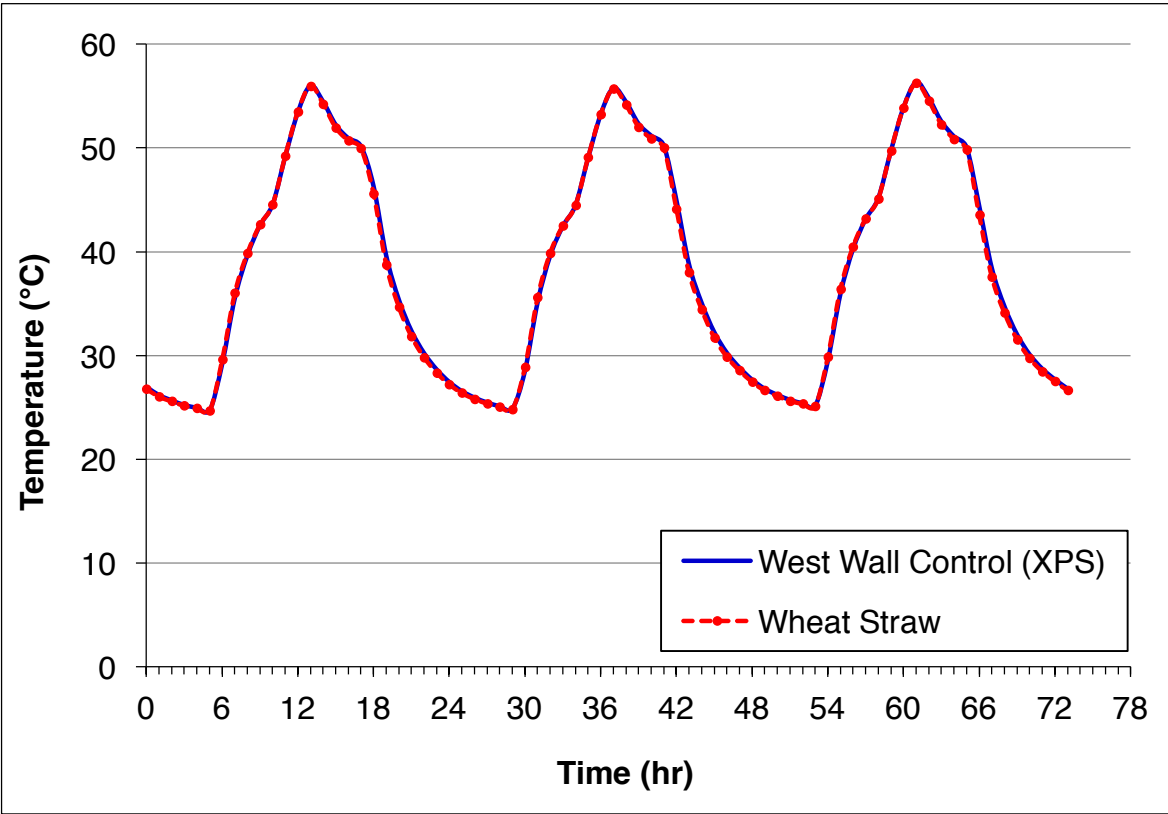


Figure 5.24 West Wall Exterior Surface Temperatures at 30 kg/m³

The exterior surface temperature profiles of both segments of the wall, one containing the XPS sheets and the other wheat straw were comparatively similar. The maximum temperature in both wall cavity surfaces reached a value of about 55.9°C during the hottest time of the day. From this observation, it was assumed that the wheat straw at 30 kg/m³ and the XPS sheets had similar resistance to heat transfer.

The exterior surface temperature comparison between the wall segment with coconut fiber and the wall segment with XPS sheets is shown in Figure 5.25.

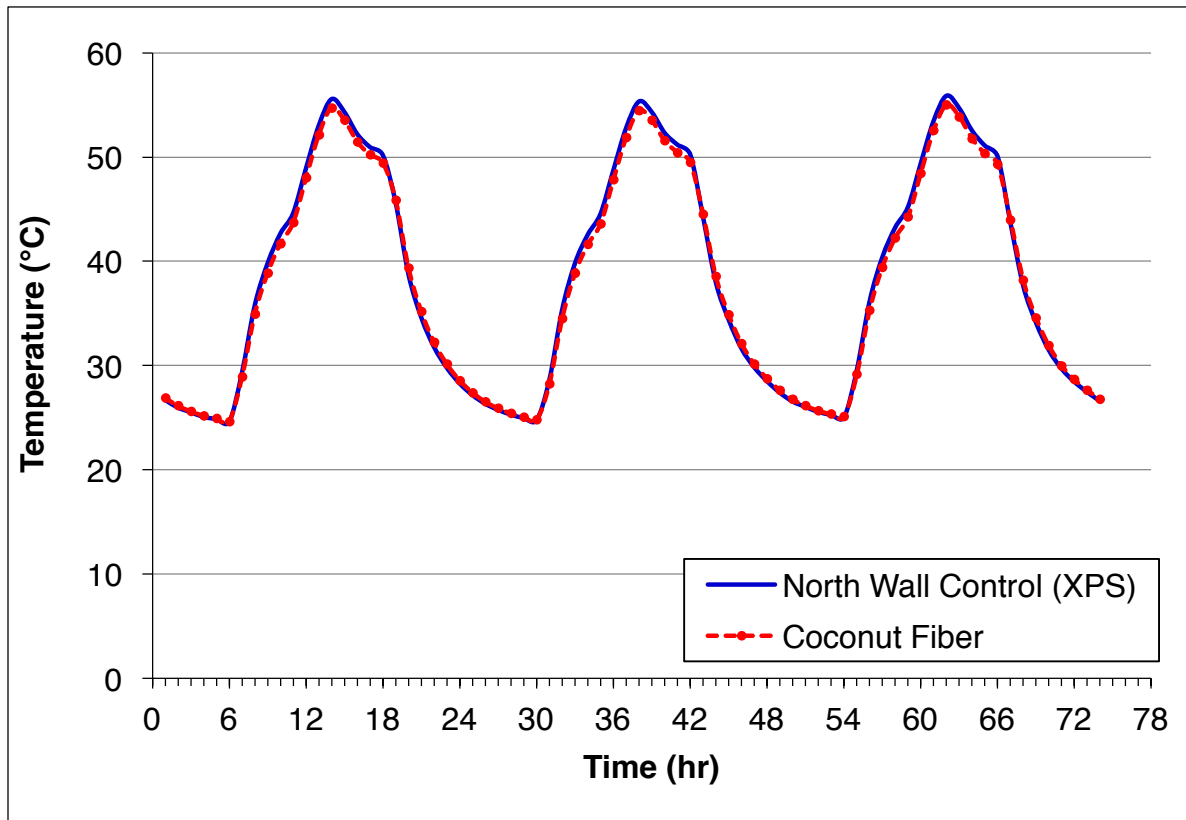


Figure 5.25 North Wall Exterior Surface Temperatures at 30 kg/m³

The temperature profiles show a maximum temperature difference of about 0.8°C at peak temperature. The temperature of the exterior wall surface with coconut fiber

reached a peak temperature of 54.7°C and the exterior wall surface with XPS sheets reached a peak temperature of 55.5°C. Similar to the other two natural fibers, as the temperatures decreased during the cooling mode, the temperature profiles gradually merged. From this observation, it was assumed that the coconut fiber facilitated slightly more heat transfer than the XPS sheets, increasing the conduction heat transfer and hence making the surface slightly cooler by faster dissipation of heat. From this, it was assumed that the coconut fiber at 30 kg/m³ had lower resistance to heat transfer when compared to the XPS sheets in this configuration.

Interior Surface Temperatures

The interior surface temperature profiles of the retrofit wall (the wall with Timothy grass as insulation) and the control wall (the wall with XPS sheets) were compared and are shown in Figure 5.26.

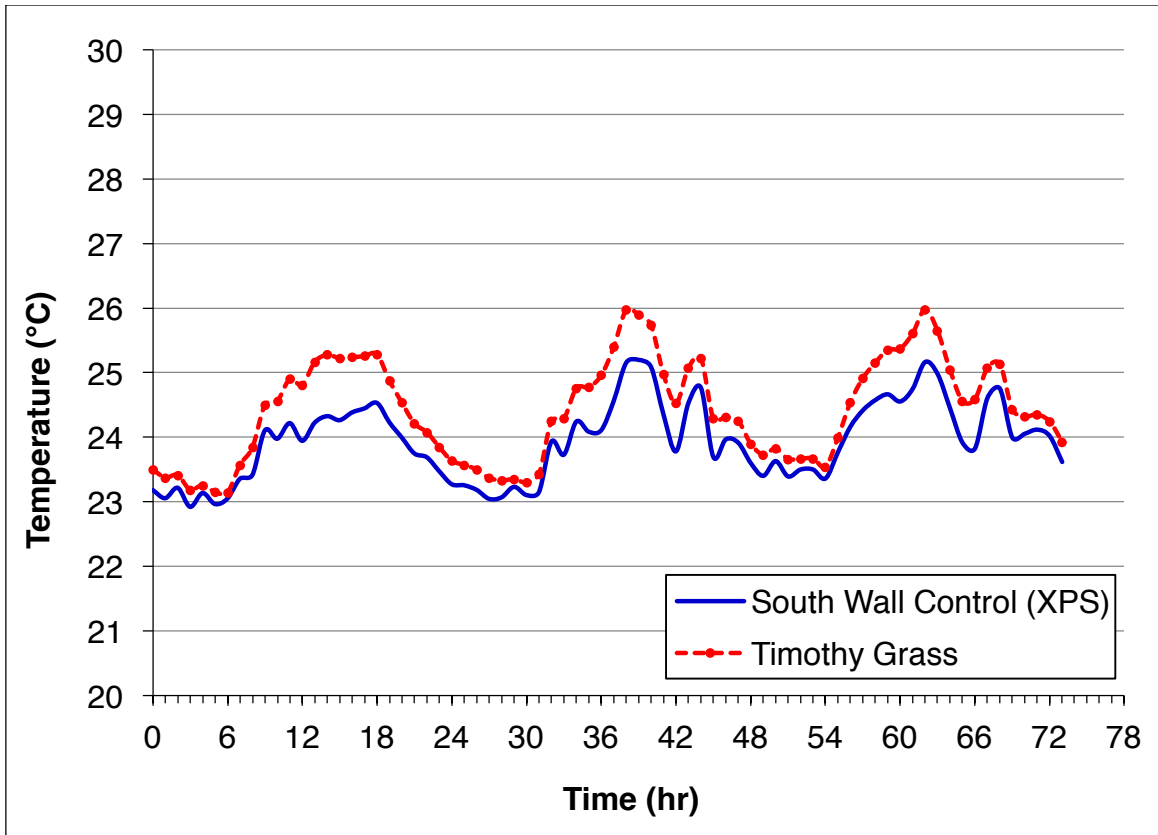


Figure 5.26 South Wall Interior Surface Temperatures at 30 kg/m³

As previously stated, the interior air temperature of the room where the simulator was placed was air conditioned. The temperature profiles of the wall cavities that had XPS sheets and Timothy grass showed that during the peak temperature of the day, the temperature difference between the interior surface with XPS sheets and the Timothy grass was about 0.9°C. The peak temperature of the interior wall surface with Timothy grass reached 26°C whereas the peak interior surface temperature of the wall with XPS sheets reached a maximum of 25.1°C. The average temperature of the interior wall surface with Timothy grass was 24.4°C whereas the average interior surface temperature of the wall with XPS sheets was 23.9°C. This could be interpreted as the

Timothy grass slightly facilitating more heat transfer when compared to the XPS sheets, adding another evidence to the previous assumption.

The interior surface temperature comparison between the segment of the wall containing wheat straw and the segment of the wall containing XPS sheets is given in Figure 5.27.

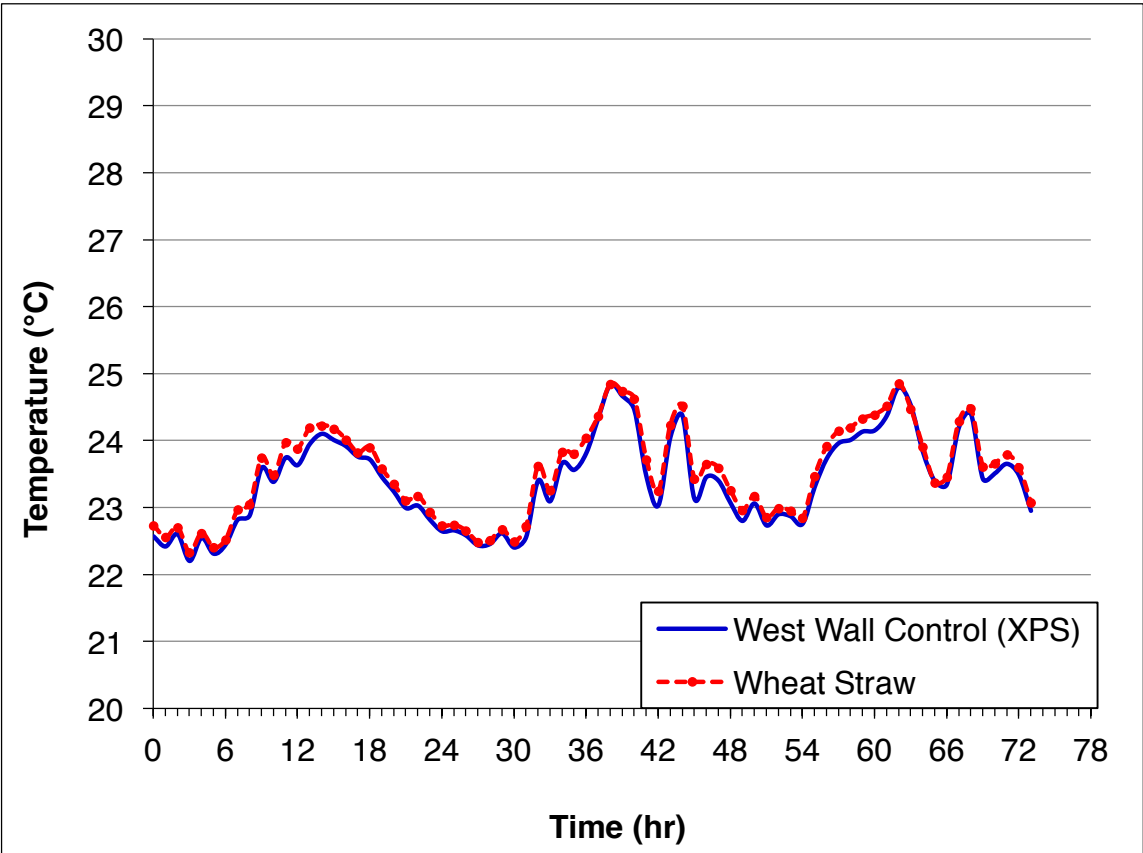


Figure 5.27 West Wall Interior Surface Temperatures at 30 kg/m³

The temperature difference between the wheat straw and XPS sheets during the peak time of the day in this case was about 0.2°C, which could be considered negligible. The peak interior surface temperature of the wall with wheat straw reached

24.8°C whereas the peak temperature of the interior wall surface with XPS sheets reached a maximum of 24.6°C. The average interior surface temperature of wall with wheat straw was 23.5°C whereas the average temperature of the interior wall surface with XPS sheets was 23.4°C. From the graph, it was noted that the fluctuation in temperature was smoother in the wall containing wheat straw, which suggested that the wheat straw insulation may have had slightly more thermal mass, therefore resisting sudden fluctuations in temperature. This shows that the heat transfer through wheat straw and the XPS sheets were almost similar in this case, adding another evidence to the previous assumption.

The interior surface temperature comparison between the wall segment containing coconut fiber and the wall segment containing XPS sheets is given in Figure 5.28.

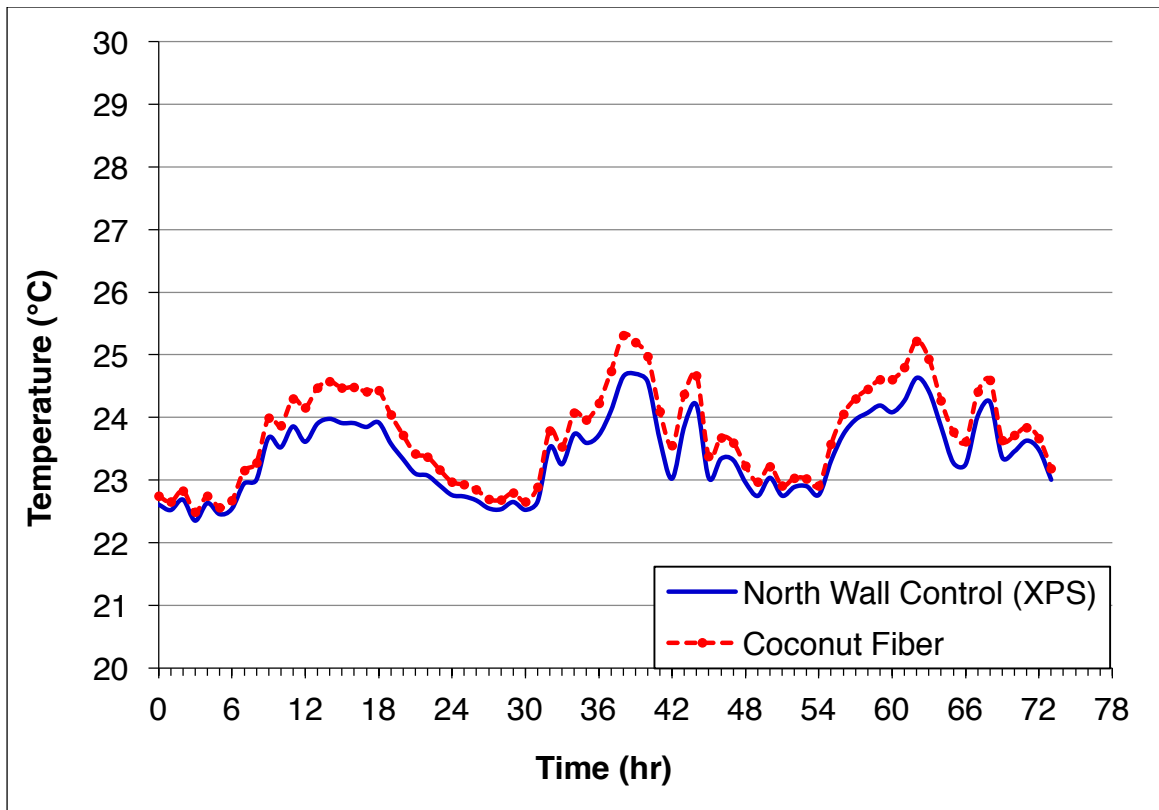


Figure 5.28 North Wall Interior Surface Temperatures at 30 kg/m³

The temperature profiles of the wall cavities that had coconut fiber and XPS sheets show that during the peak temperature of the day, the temperature difference between the interior surface of the wall segment with the coconut fiber and the one with XPS sheets was about 0.7°C. The peak interior surface temperature of the wall with coconut fiber reached 25.3°C whereas the peak temperature of the interior wall surface with XPS sheets reached a maximum of 24.6°C. The average interior surface temperature of the wall with coconut fiber was 23.7°C whereas the average temperature of the interior wall surface with XPS sheets was 23.4°C. This shows that the coconut fiber slightly facilitated more heat transfer when compared to the XPS sheets, adding another evidence to the previous assumption.

Layer Temperatures

The layer temperature profiles of the retrofit (Timothy grass) and control (XPS sheets) wall segments were compared and are shown in Figure 5.29.

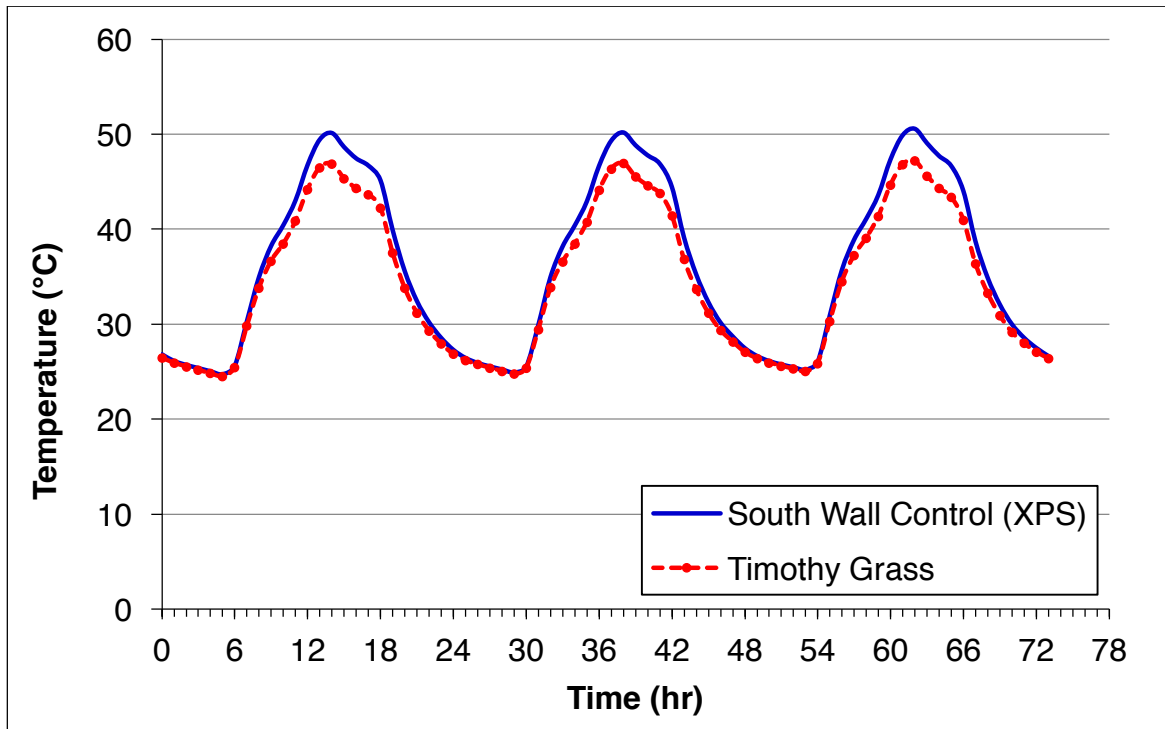


Figure 5.29 South Wall Layer Temperatures at 30 kg/m³

The temperature profiles show a maximum temperature difference of about 3.3°C at peak temperature. The layer temperature of the wall segment with Timothy grass reached a peak temperature of 47.2°C and the layer temperature of the wall segment with XPS sheets reached a peak temperature of 50.5°C. When the temperatures decreased during the cooling mode, the temperature profiles gradually merged. From this observation, it was assumed that the Timothy grass slightly facilitated more heat transfer than the XPS sheets, increasing the conduction heat transfer and hence

making the surface slightly cooler by dissipating heat faster. This added up an evidence that the Timothy grass at 30 kg/m^3 had lower resistance to heat transfer when compared to the XPS sheets in this configuration and facilitated faster heat dissipation.

The layer temperature profiles of the retrofit segment (wheat straw) and control segment (XPS sheets) were compared and are shown in Figure 5.30.

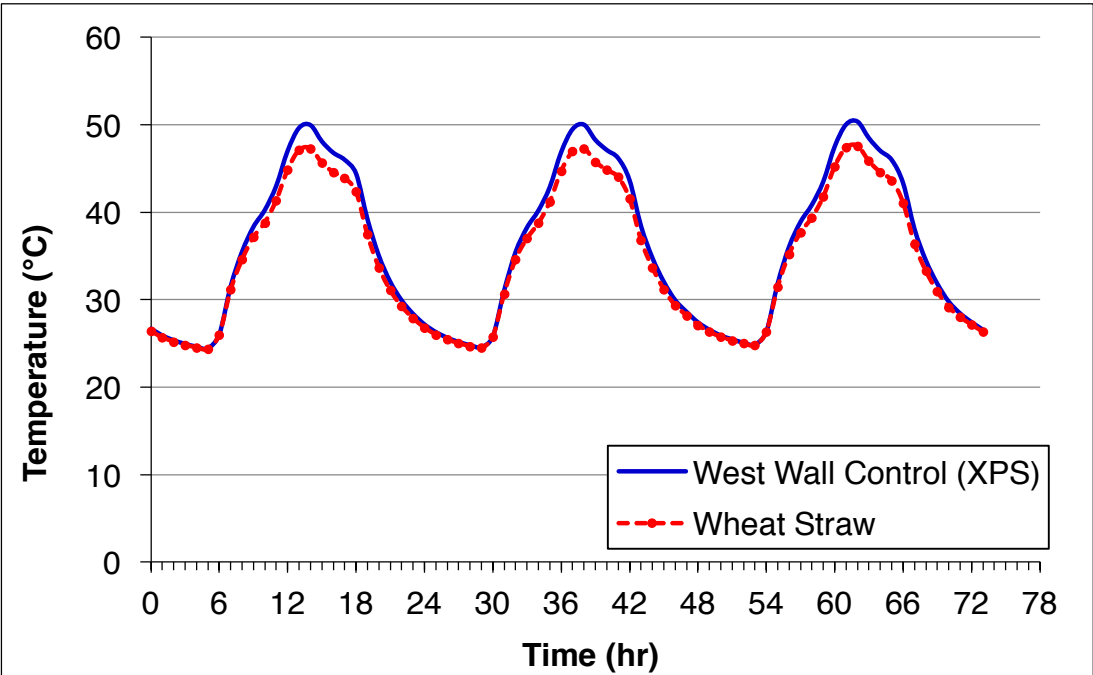


Figure 5.30 West Wall Layer Temperatures at 30 kg/m^3

Interestingly, the temperature profiles show a maximum temperature difference of about 2.6°C at peak temperature. The layer temperature of the retrofit segment (wheat straw) reached a peak temperature of 47.6°C while the layer temperature of the control segment (XPS sheets) reached a peak temperature of 50.2°C . When the temperatures decreased during the cooling mode, the temperature profiles gradually merged. From this observation, it was assumed that the wheat straw facilitated more

heat transfer than the XPS sheets, increasing the conduction heat transfer and hence making the surface slightly cooler by dissipating heat faster. It was noted that the temperature difference in this case was lower when compared to the peak temperature difference between the wall segment with XPS sheets and that with Timothy grass, which was 3.3°C.

The layer temperature profiles of the retrofit segment (coconut fiber) and control segment (XPS sheets) were compared and are shown in Figure 5.31.

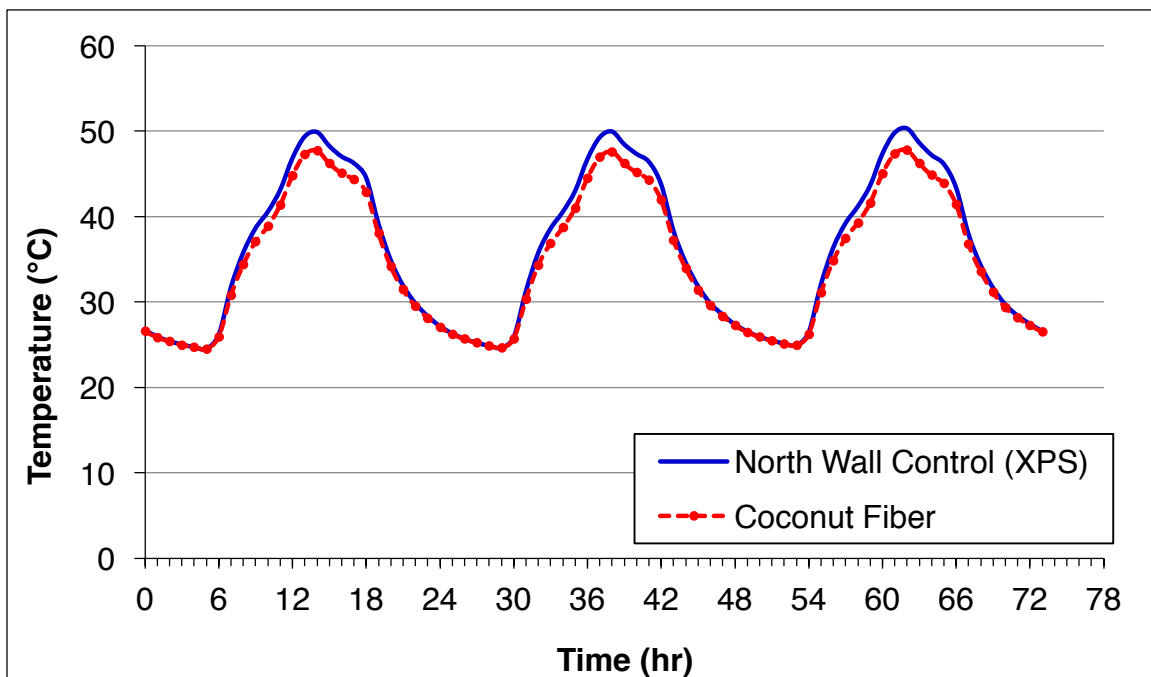


Figure 5.31 North Wall Layer Temperatures at 30 kg/m³

The temperature profiles show a maximum temperature difference of about 2.5°C at peak temperature. The temperature of the layer with coconut fiber reached a peak temperature of 47.7°C and the layer with XPS sheets reached a peak temperature of 50.2°C. When the temperatures were reduced during the cooling mode, the temperature

profiles gradually merged and reached the same temperatures. Interestingly, this profile was very similar to the temperature profile of wheat straw. From this observation, it was assumed that the coconut fiber facilitated more heat transfer than the XPS sheets, increasing the conduction heat transfer and hence making the surface slightly cooler by dissipating heat faster. One thing to be noted is that the temperature difference in this case was lower than the peak temperature difference between the XPS sheets and the Timothy grass, which was 3.3°C, and similar to the peak temperature difference between the XPS sheets and wheat straw.

The comparison of peak temperature values and the temperature differences are given in Table 5.1.

Table 5.1 Comparison of Peak Temperatures and Peak Temperature Differences at 30 kg/m³

Wall	Control / Retrofit	Peak Temperature (°C)	Temperature Difference (°C)
South Exterior Surface	XPS sheets	55.9	1
	Timothy grass	54.9	
West Exterior Surface	XPS sheets	55.9	0
	Wheat straw	55.9	
North Exterior Surface	XPS sheets	55.5	0.8
	Coconut fiber	54.7	
South Interior Surface	XPS sheets	25.1	-0.9
	Timothy grass	26	
West Interior Surface	XPS sheets	24.6	-0.2
	Wheat straw	24.8	
North Interior Surface	XPS sheets	24.6	-0.7
	Coconut fiber	25.3	
South Layer	XPS sheets	50.5	3.3
	Timothy grass	47.2	
West Layer	XPS sheets	50.2	2.6

	Wheat straw	47.6	
North Layer	XPS sheets	50.2	2.5
	Coconut fiber	47.7	

Heat Fluxes

Heat flux values were measured using heat flux meters. Figure 5.32 shows the comparison of heat fluxes between Timothy grass and XPS insulation.

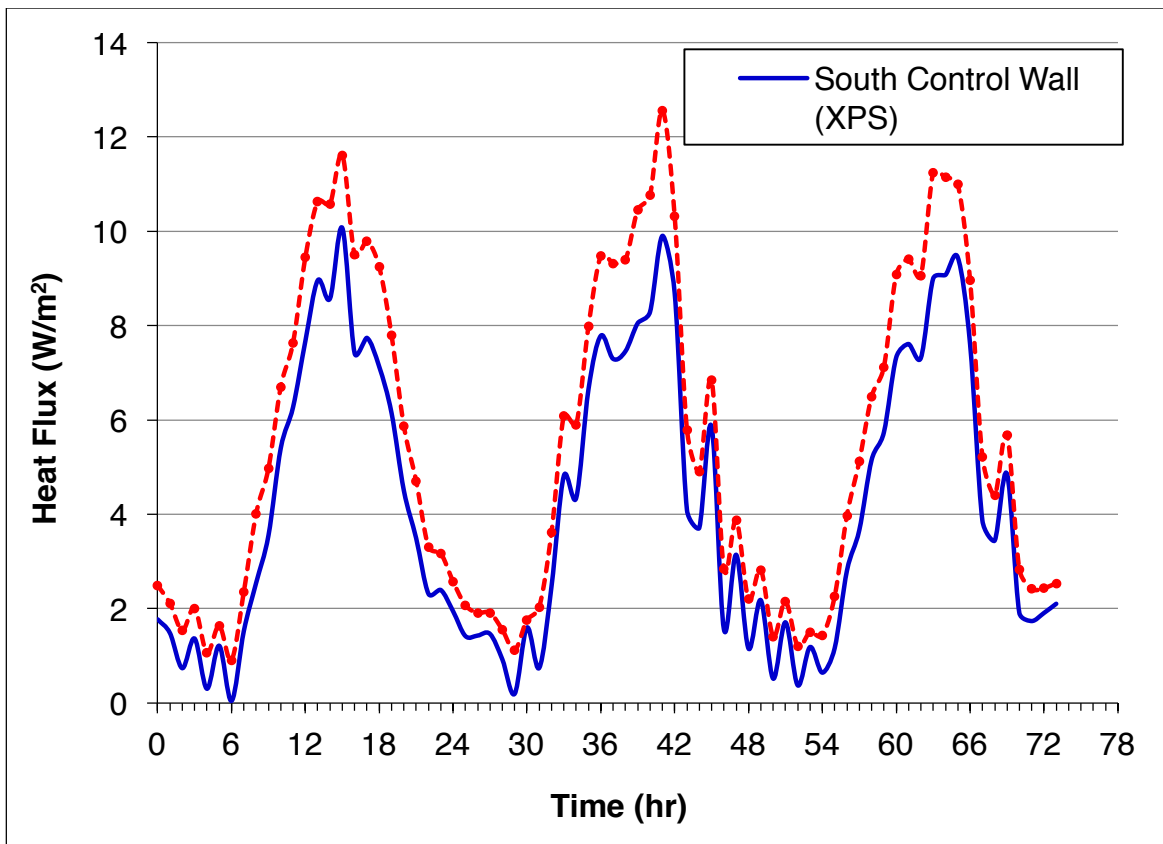


Figure 5.32 South Wall Heat Fluxes at 30 kg/m^3

The heat fluxes through the wall cavity with Timothy grass were consistently higher than the wall cavity with heat fluxes through the XPS insulation throughout the

testing cycle. The differences in heat fluxes were highest during the peak temperatures of the day. The highest peak heat flux through Timothy grass was about 12.5 W/m^2 and the highest peak heat flux through XPS insulation was about 10 W/m^2 . This translated to a difference of 25% in peak heat flux values. The average heat flow per m^2 -day through the Timothy grass was 133.8 Wh/m^2 -day and the average heat flow per m^2 -day through the XPS sheets was 103.2 Wh/m^2 -day, which was around 30% lower than for the XPS sheets. Therefore, it was proven that the XPS sheets outperformed the Timothy grass as a building insulation material when used in a density of 30 kg/m^3 .

Figure 5.33 shows the comparison of heat fluxes between wheat straw and XPS insulation.

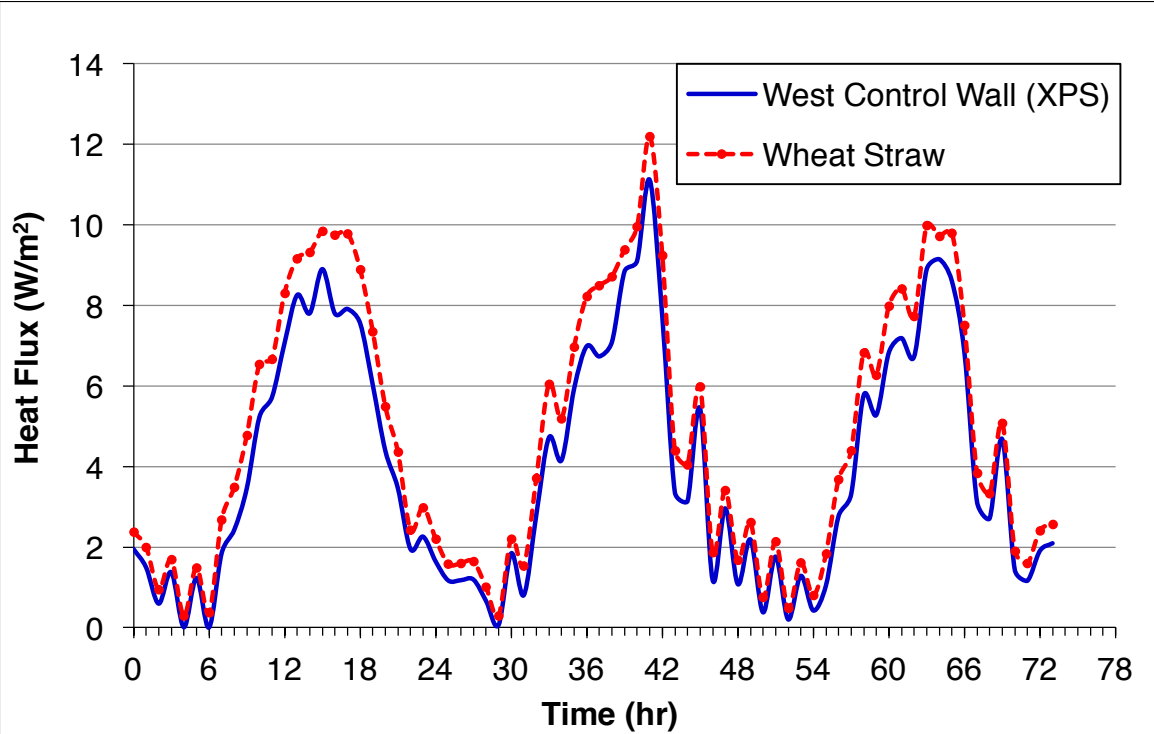


Figure 5.33 West Wall Heat Fluxes at 30 kg/m^3

The heat fluxes through the wall cavity with wheat straw were marginally higher than the heat fluxes through the wall cavity with XPS insulation throughout the testing cycle, except during the peak temperatures of the day. The differences in heat fluxes were highest during the peak temperatures of the day. The highest peak heat flux through wheat straw was about 12 W/m^2 and the highest peak heat flux through XPS insulation was about 11.2 W/m^2 . This translated to a difference of 7% in peak heat flux values. The average heat flow per m^2 -day through the wall cavity with wheat straw was 18.6 Wh/m^2 -day and the average heat flow per m^2 -day through the wall cavity with XPS sheets was 98.5 Wh/m^2 -day, which was around 20% lower. Therefore, it was proven that the XPS sheets outperformed the wheat straw as a building insulation material when used in a density of 30 kg/m^3 .

Figure 5.34 shows the comparison of heat fluxes between coconut fiber and XPS insulation.

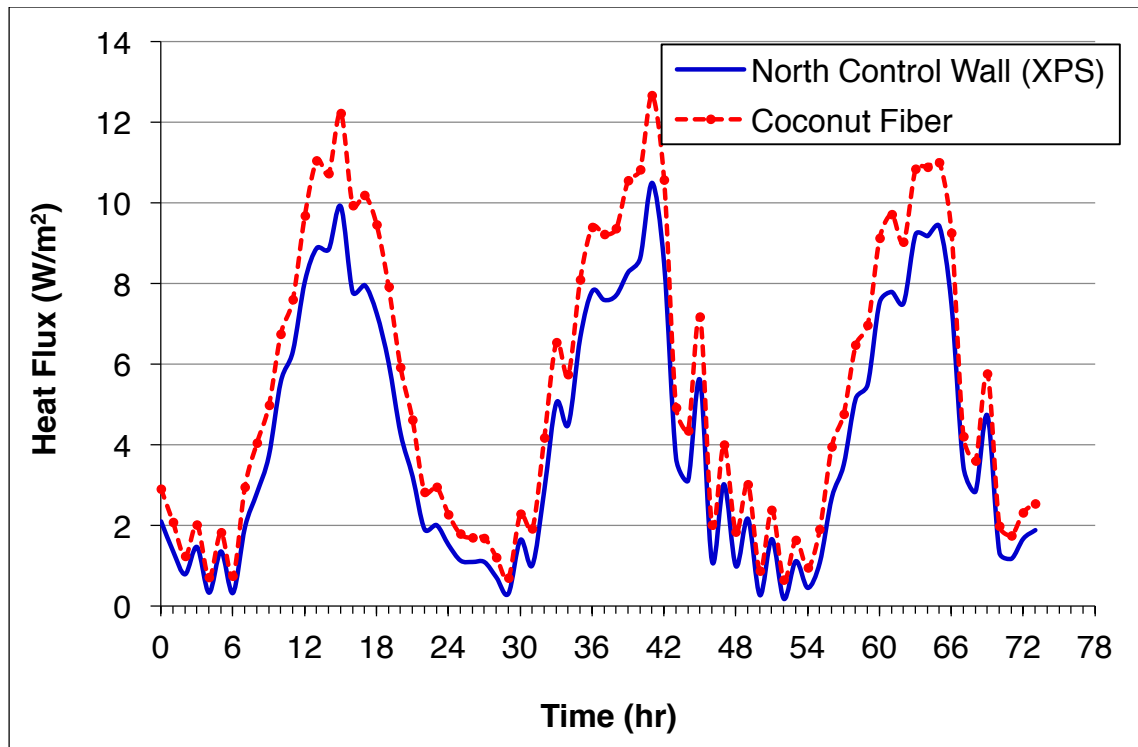


Figure 5.34 North Wall Heat Fluxes at 30 kg/m³

The heat fluxes through the wall cavity with coconut fiber were consistently higher than the heat fluxes through the wall cavity with XPS insulation throughout the testing cycle but were lower when compared to the wall cavity with Timothy grass. The differences in heat fluxes were highest during the peak temperatures of the day. The highest peak heat flux through coconut fiber was about 12.6 W/m² and the highest peak heat flux through XPS insulation was about 10.5 W/m². This translates to a difference of 20% in peak heat flux values. The average heat flux through coconut fiber per m²-day was 132 Wh/m²-day and the average heat flux per m²-day through XPS sheets was 102.4 W/m²-day, which was around 29% less than the coconut fiber. Therefore, it was proven that the XPS sheets outperformed the coconut fiber as a building insulation material when used in a density of 30 kg/m³.

Case 2

For Case 2, the density of all of the indigenous insulation was 45 kg/m^3 and similar to Case 1, the actual external surface conditions were simulated to assess the heat flux and temperature values. Each experiment lasted 72 hours. The heat sources were adjusted to work exactly as they did during the calibration. The data logger collected the data every 10 seconds, which were then converted, into average values for every hour. Then the values of the control and retrofits were compared using graphs.

Exterior Surface Temperatures

The exterior surface temperature profiles of the retrofit (Timothy grass) and control (XPS sheets) were compared and are shown in Figure 5.35.

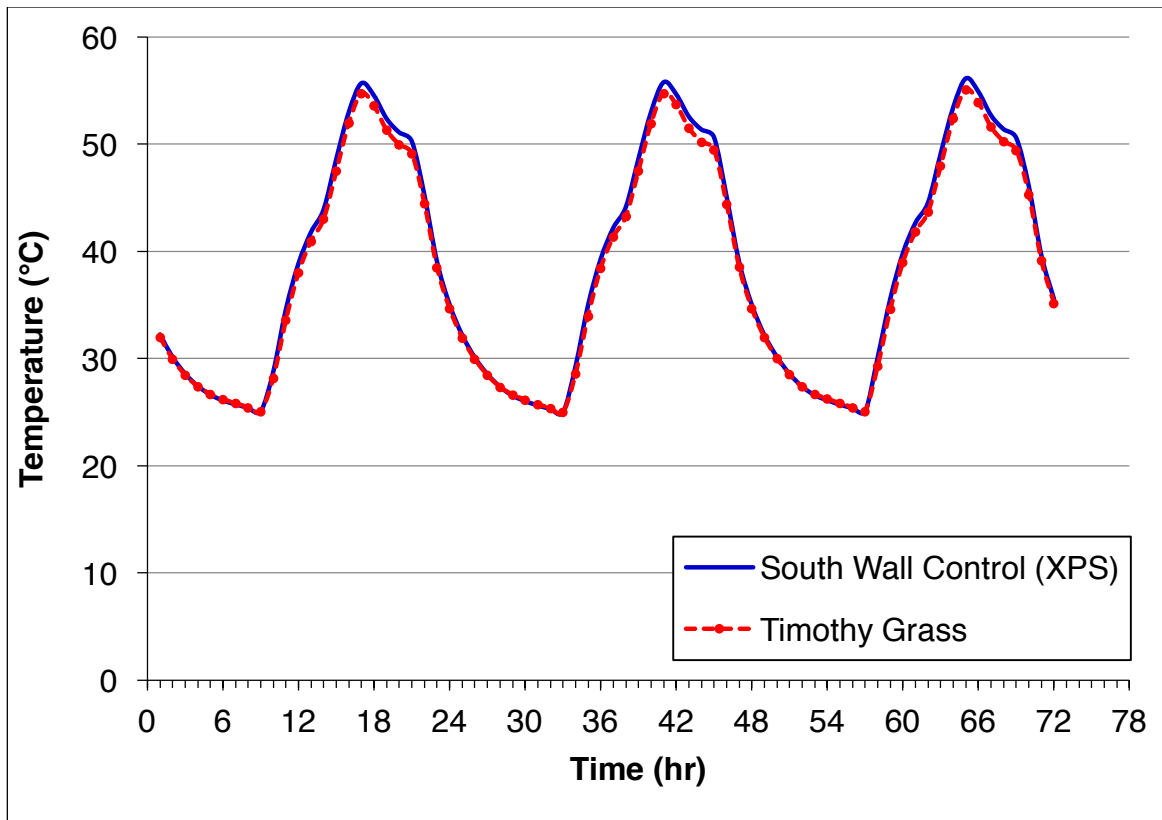


Figure 5.35 South Wall Exterior Surface Temperatures at 45 kg/m³

The temperature profiles show a maximum temperature difference of about 1°C at peak temperature. The temperature of the exterior wall surface with Timothy grass reached a peak temperature of 55.1°C and the exterior wall surface with XPS sheets reached a peak temperature of 56.1°C. As the temperature values decreased, the curves gradually merged and reached the same temperatures. From this observation, it was assumed that the Timothy grass slightly facilitated more heat transfer than the XPS sheets, increasing the conduction heat transfer and hence making the surface slightly cooler by the faster dissipation of heat. From this, it was assumed that the Timothy grass at 45 kg/m³ had a lower resistance to heat transfer when compared to the XPS sheets in this configuration.

The exterior surface temperature comparison between the wheat straw and XPS sheets is given in Figure 5.36.

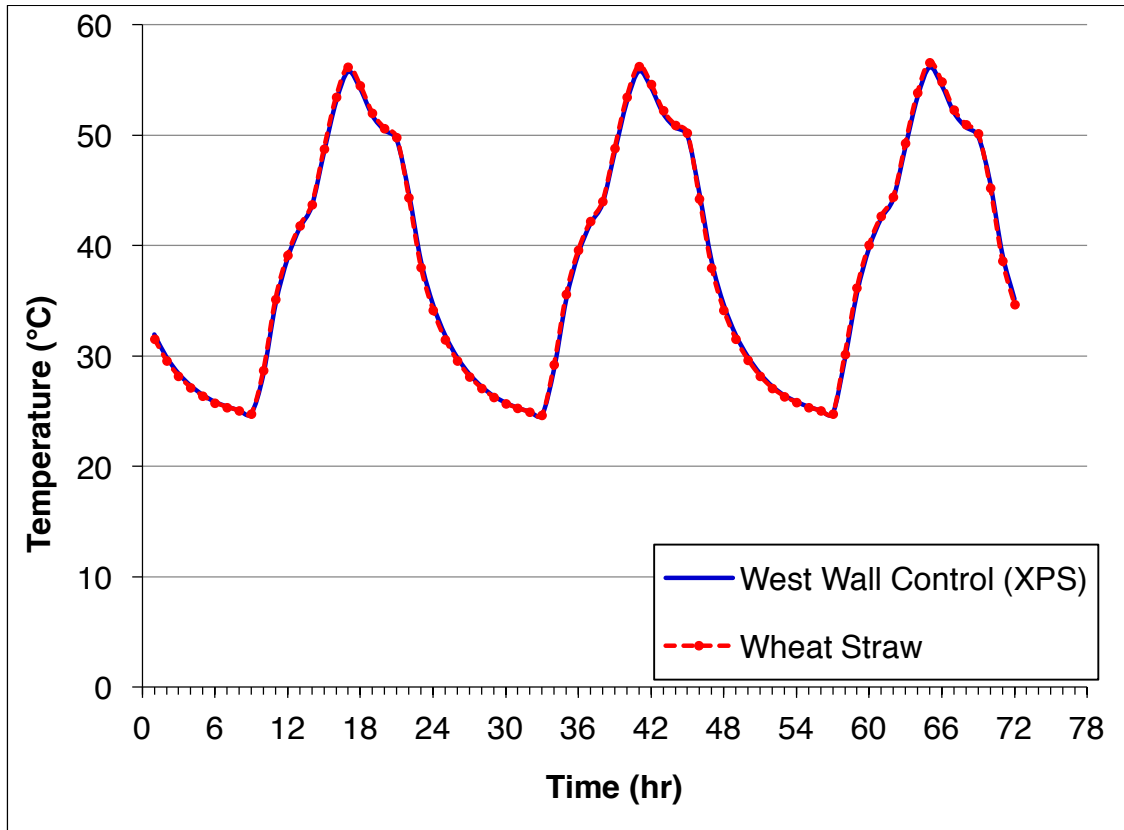


Figure 5.36 West Wall Exterior Surface Temperatures at 45 kg/m³

The exterior surface temperature profiles of both the wall cavities containing the XPS sheets and wheat straw were comparatively similar. The maximum temperature in both wall cavity surfaces reached a value of about 56.2°C during the hottest time of the day. From this observation, it was assumed that the wheat straw at 45 kg/m³ and the XPS sheets in this configuration had similar resistance to heat transfer.

The exterior surface temperature comparison between coconut fiber and XPS sheets is given in Figure 5.37.

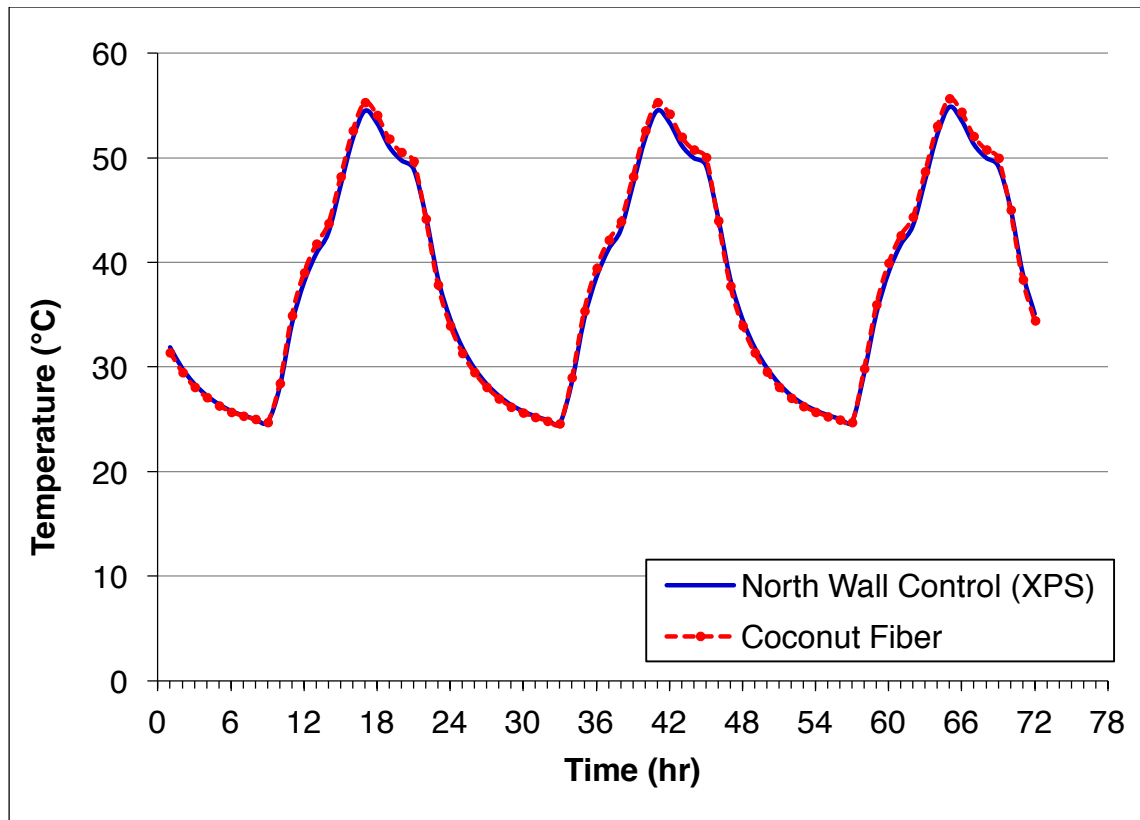


Figure 5.37 North Wall Exterior Surface Temperatures at 45 kg/m³

The temperature profiles show a maximum temperature difference of about 0.8°C at peak temperature. The temperature of the exterior wall surface with coconut fiber reached a peak temperature of 55.2°C and the exterior wall surface with XPS sheets reached a peak temperature of 54.4°C. As the temperatures of the walls were reduced during the cooling mode, the temperature profiles gradually merged and reached the same temperatures. From this observation, it was assumed that the coconut fiber slightly facilitated more heat transfer than the XPS sheets, increasing the conduction heat transfer and hence making the surface cooler by faster dissipation of heat. From this, it was assumed that the coconut fiber at 45 kg/m³ had a lower resistance to heat transfer when compared to the XPS sheets in this configuration.

Interior Surface Temperatures

The interior surface temperature profiles of the retrofit (Timothy grass) and control (XPS sheets) were compared and are shown in Figure 5.38.

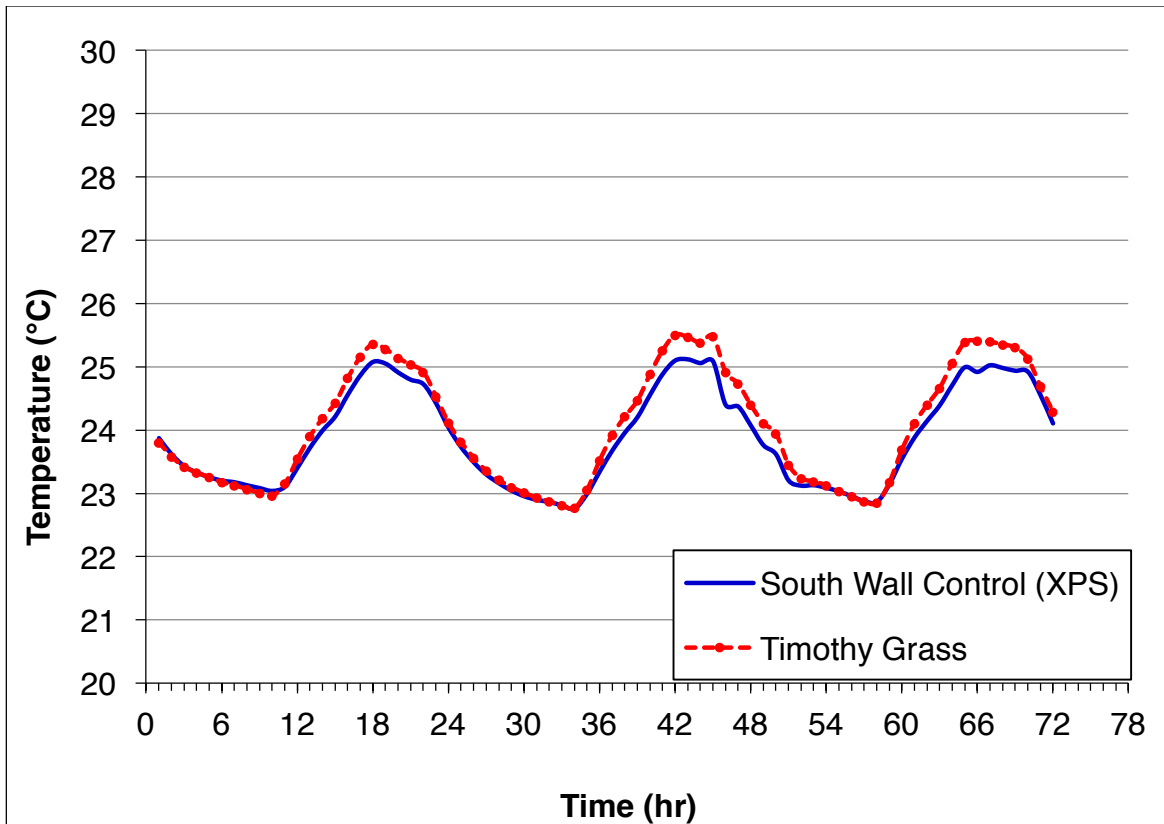


Figure 5.38 South Wall Interior Surface Temperatures at 45 kg/m³

The interior air temperature of the room was conditioned using an HVAC system as mentioned earlier. The temperature profiles of the wall cavities that had Timothy grass and XPS sheets show that during the peak temperature of the day, the temperature difference between the interior surface with the Timothy grass and XPS sheets was about 0.5°C. The peak temperature of the interior wall surface with Timothy

grass reached 25.4°C whereas the peak interior surface temperature of the wall with XPS sheets reached a maximum of 24.9°C which was 0.5°C lower than the former. The average temperature of the interior wall surface with Timothy grass reached 24.1°C whereas the average interior surface temperature of the wall with XPS sheets reached 23.9°C which was 0.2°C lower than the former. This shows that the Timothy grass slightly facilitated more heat transfer when compared to the XPS sheets.

The interior surface temperature comparison between the wheat straw and XPS sheets is given in Figure 5.39.

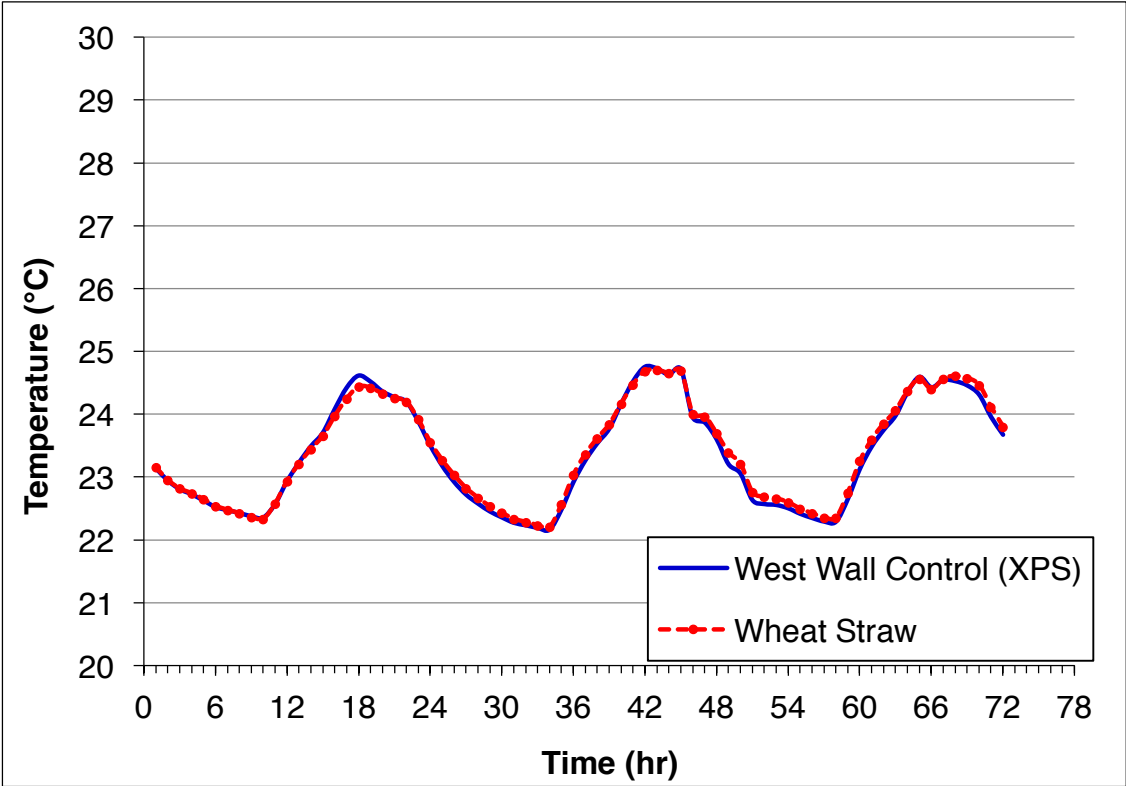


Figure 5.39 West Wall Interior Surface Temperatures at 45 kg/m³

The temperature difference between the wheat straw and XPS sheets during the peak time of the day in this case was about 0.1°C which could be considered negligible. The peak temperature of the interior wall surface with the wheat straw reached 24.6°C whereas the peak interior surface temperature of the wall with the XPS sheets reached a maximum of 24.7°C which was 0.1°C higher than the former. The average temperature of the interior wall surfaces with wheat straw and XPS sheets were about 23.4°C . This shows that the heat transfer through wheat straw and the XPS sheets were almost similar in this case.

The interior surface temperature comparison between the coconut fiber and XPS sheets is given in Figure 5.40.

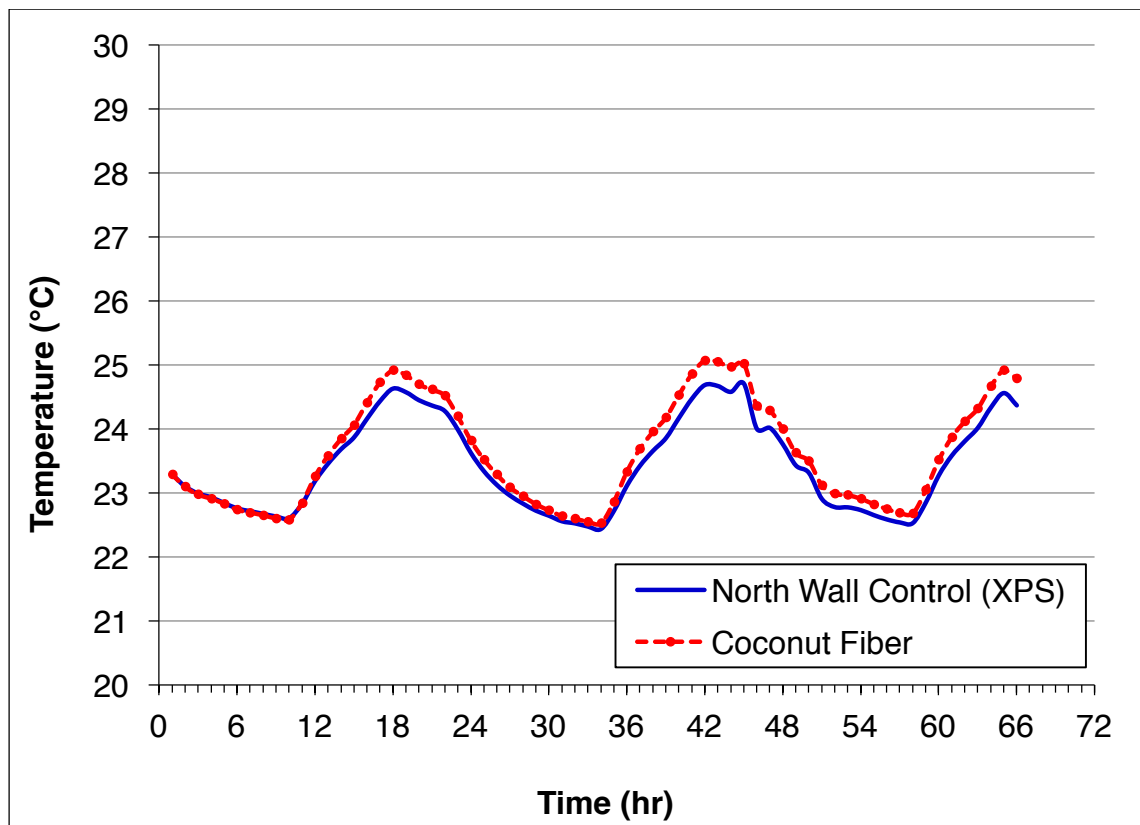


Figure 5.40 North Wall Interior Surface Temperatures at 45 kg/m^3

The temperature profiles of the wall cavities that had XPS sheets and coconut fiber show that during the peak temperature of the day, the temperature difference between the interior surface with the coconut fiber XPS sheets was about 0.4°C. The peak temperature of the interior wall surface with coconut fiber reached 24.9°C whereas the peak interior surface temperature of the wall with XPS sheets reached a maximum of 24.5°C which was 0.4°C. The average temperature of the interior wall surface with coconut fiber reached 23.7°C whereas the average interior surface temperature of the wall with XPS sheets reached 23.5°C which was 0.2°C lower than the former.

Layer Temperatures

The layer temperature profiles of the retrofit (Timothy grass) and control (XPS sheets) were compared and are shown in Figure 5.41.

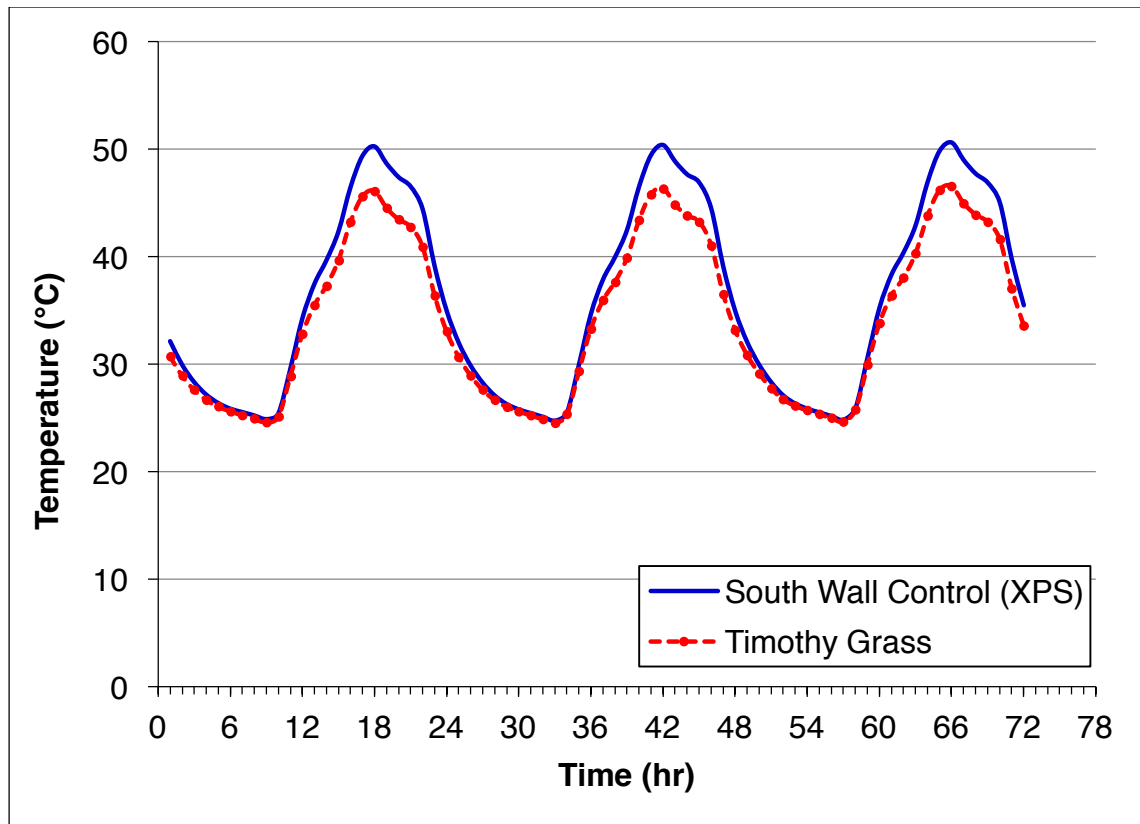


Figure 5.41 South Wall Layer Temperatures at 45 kg/m³

The temperature profiles show a maximum temperature difference of about 3.6°C at peak temperature. The temperature of the layer with Timothy grass reached a peak temperature of 46.6°C and the layer with XPS sheets reached a peak temperature of 50.2°C. When the temperatures were reduced during the cooling mode, the temperature profiles gradually merged and reached the same temperatures. The layer temperature profiles of the control (XPS sheets) and retrofit (wheat straw) were compared as shown in Figure 5.42.

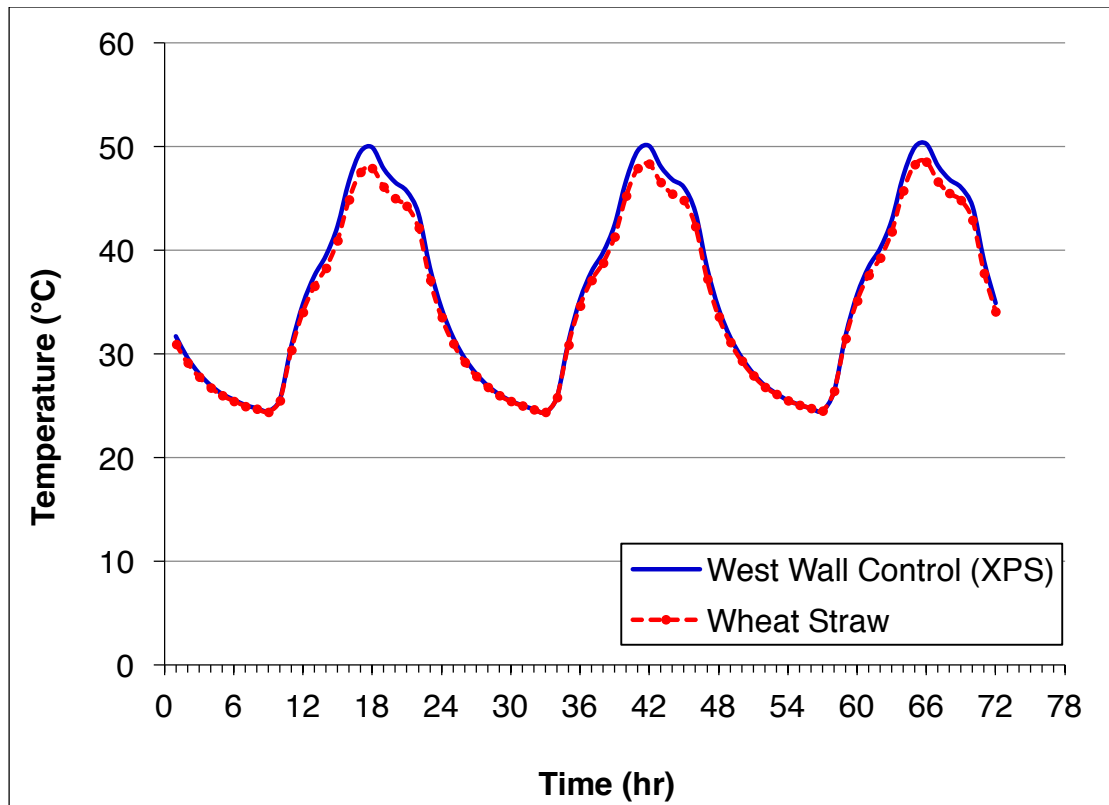


Figure 5.42 West Wall Layer Temperatures at 45 kg/m³

The temperature profiles show a maximum temperature difference of about 1.7°C at peak temperature which was 2.6°C in Case 1, which suggested a better performance. The temperature of the layer with wheat straw reached a peak temperature of 48.5°C and the layer with XPS sheets reached a peak temperature of 50.2°C. When the temperatures were reduced during the cooling mode, the temperature profiles gradually merged and reached the same temperatures. However, it was noted that the temperature difference in this case was lower when compared to the peak temperature difference between the Timothy grass and XPS sheets which was 3.6°C.

The layer temperature profiles of the retrofit (coconut fiber) and control (XPS sheets) were compared and are shown in Figure 5.43.

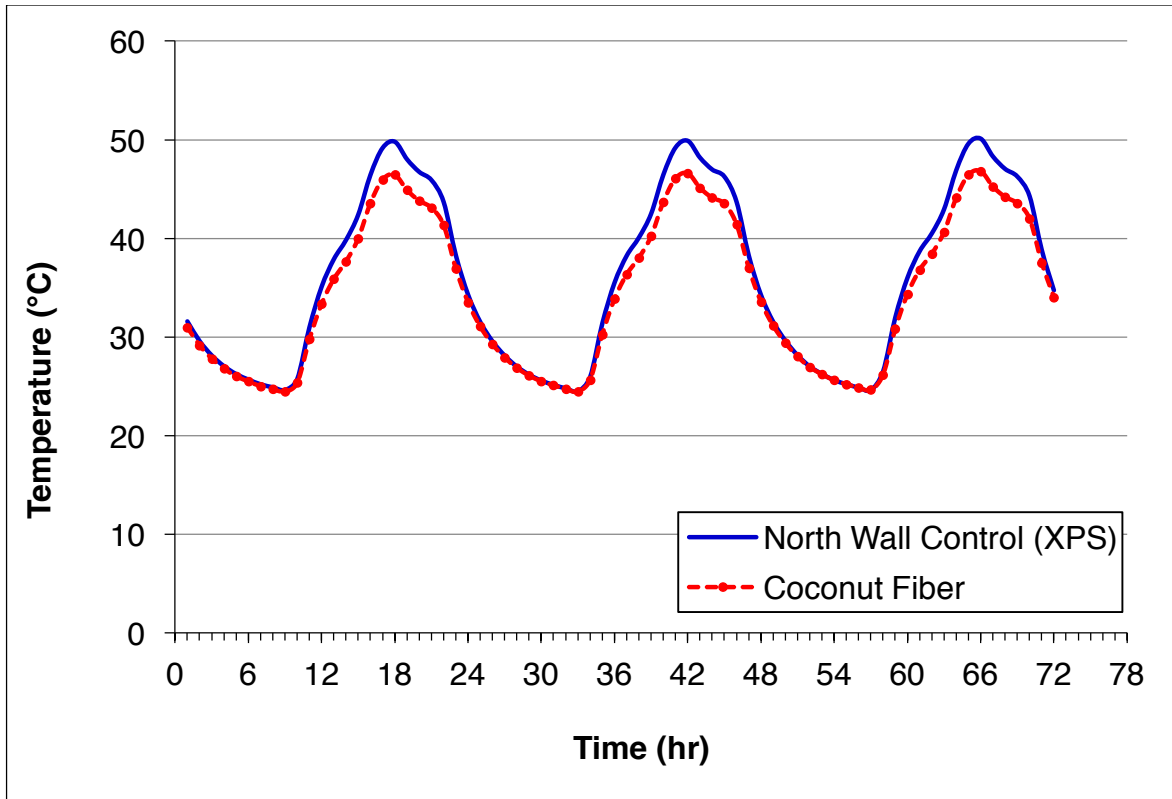


Figure 5.43 North Wall Layer Temperatures at 45 kg/m³

The temperature profiles show a maximum temperature difference of about 3.2°C at peak temperature. The temperature of the layer with coconut fiber reached a peak temperature of 46.8°C and the layer with XPS sheets reached a peak temperature of 50°C. From this observation, it was assumed that the coconut fiber slightly facilitated more heat transfer than the XPS sheets, increasing the conduction heat transfer and hence making the surface slightly cooler by faster dissipation of heat. The comparison of peak temperature values and the temperature differences are given in Table 5.2.

Table 5.2 Comparison of Peak Temperatures and Peak Temperature Differences at 45 kg/m³

Wall	Control / Retrofit	Peak Temperature (°C)	Temperature Difference (°C)
South Exterior Surface	XPS sheets	56.1	1
	Timothy grass	55.1	
West Exterior Surface	XPS sheets	56.2	0
	Wheat straw	56.2	
North Exterior Surface	XPS sheets	55.2	0.8
	Coconut fiber	54.4	
South Interior Surface	XPS sheets	24.9	-0.5
	Timothy grass	25.4	
West Interior Surface	XPS sheets	24.7	0.1
	Wheat straw	24.6	
North Interior Surface	XPS sheets	24.5	-0.4
	Coconut fiber	24.9	
South Layer	XPS sheets	50.2	3.6
	Timothy grass	46.6	
West Layer	XPS sheets	50.2	1.7
	Wheat straw	48.5	
North Layer	XPS sheets	50	3.2
	Coconut fiber	46.8	

Heat Fluxes

Heat flux values were measured using heat flux meters. Figure 5.44 shows the comparison of heat fluxes between Timothy grass and XPS insulation.

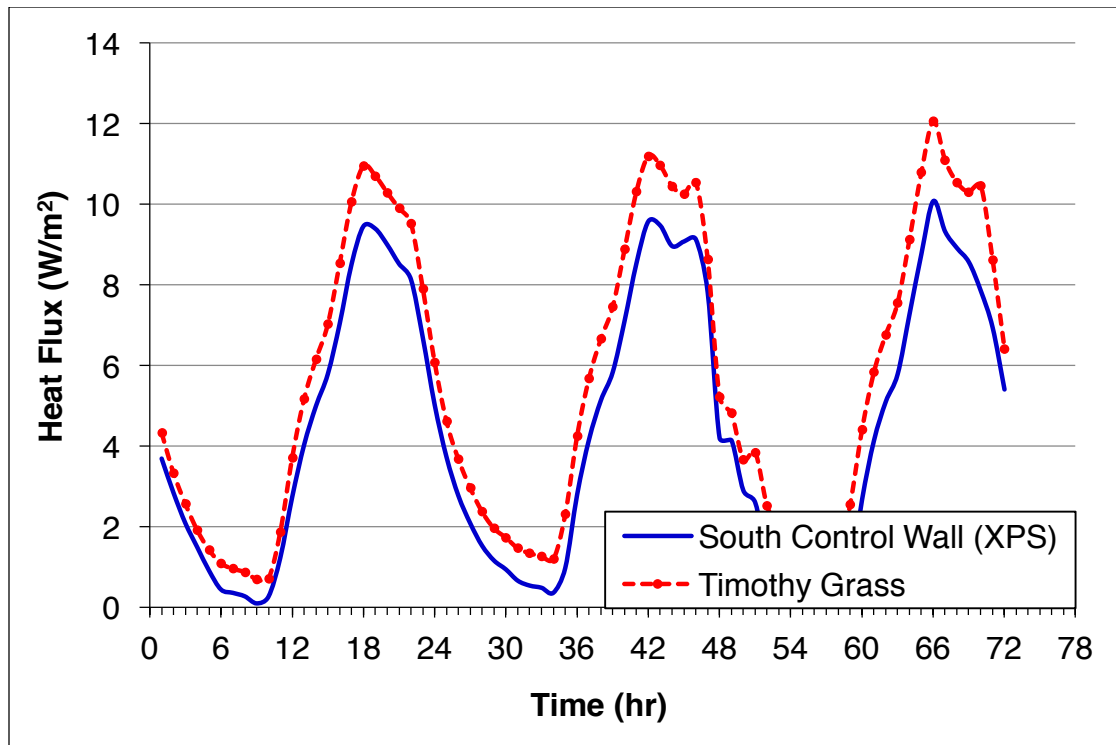


Figure 5.44 South Wall Heat Fluxes at 45 kg/m^3

The heat fluxes through the wall cavity with Timothy grass were mostly higher than the wall cavity with XPS insulation throughout the testing cycle. The differences in heat fluxes were highest during the peak temperatures of the day. The highest peak heat flux through the wall cavity with Timothy grass was about 12 W/m^2 and the highest peak heat flux through the wall cavity with XPS insulation was about 10 W/m^2 . This translated to a difference of 20% in peak heat flux values. The average heat flow through the Timothy grass per $\text{m}^2\text{-day}$ was $134 \text{ Wh/m}^2\text{-day}$ and the average heat flow per $\text{m}^2\text{-day}$ through the XPS sheets was $104.9 \text{ Wh/m}^2\text{-day}$, which was around 27% less than the Timothy grass. Therefore, it was proven that the XPS sheets outperformed the Timothy grass as a building insulation material when used in a density of 45 kg/m^3 configuration but better than 30 kg/m^3 configuration.

Figure 5.45 shows the comparison of heat fluxes between wheat straw and XPS insulation.

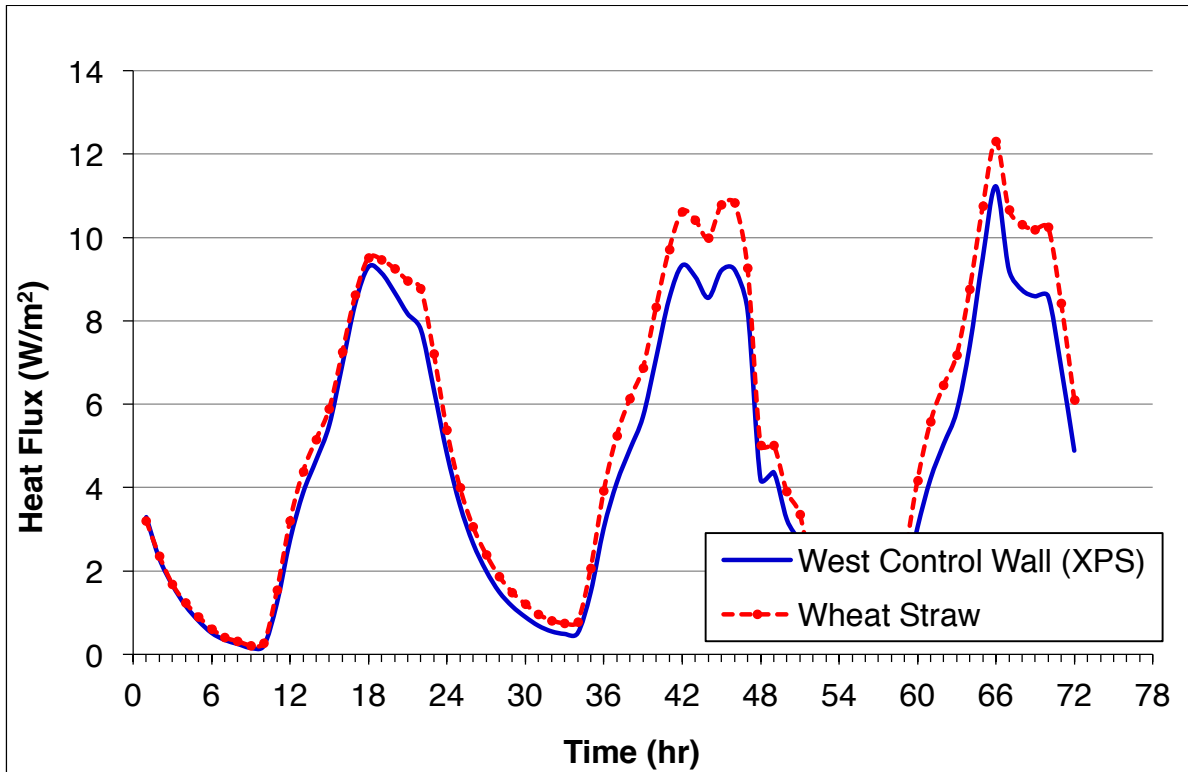


Figure 5.45 West Wall Heat Fluxes at 45 kg/m³

The heat fluxes through the wall cavity with wheat straw were marginally higher than the wall cavity with XPS insulation throughout the cycle, except during the peak temperature of the day. The differences in heat fluxes were highest during the peak temperatures of the day. The highest peak heat flux through the wheat straw was about 12.2 W/m² and the highest peak heat flux through the XPS insulation was about 11.2 W/m². This translated to a difference of 8% in peak heat flux values. The average heat flow through the wheat straw per m²-day was 122.2 Wh/m²-day and the average heat

flow per m²-day through the XPS sheets was 105.2 Wh/m²-day, which was around 16% less than the wheat straw. This was much better than the 22% when tested in 30 kg/m³ configuration.

Figure 5.46 shows the comparison of heat fluxes between coconut fiber and XPS insulation.

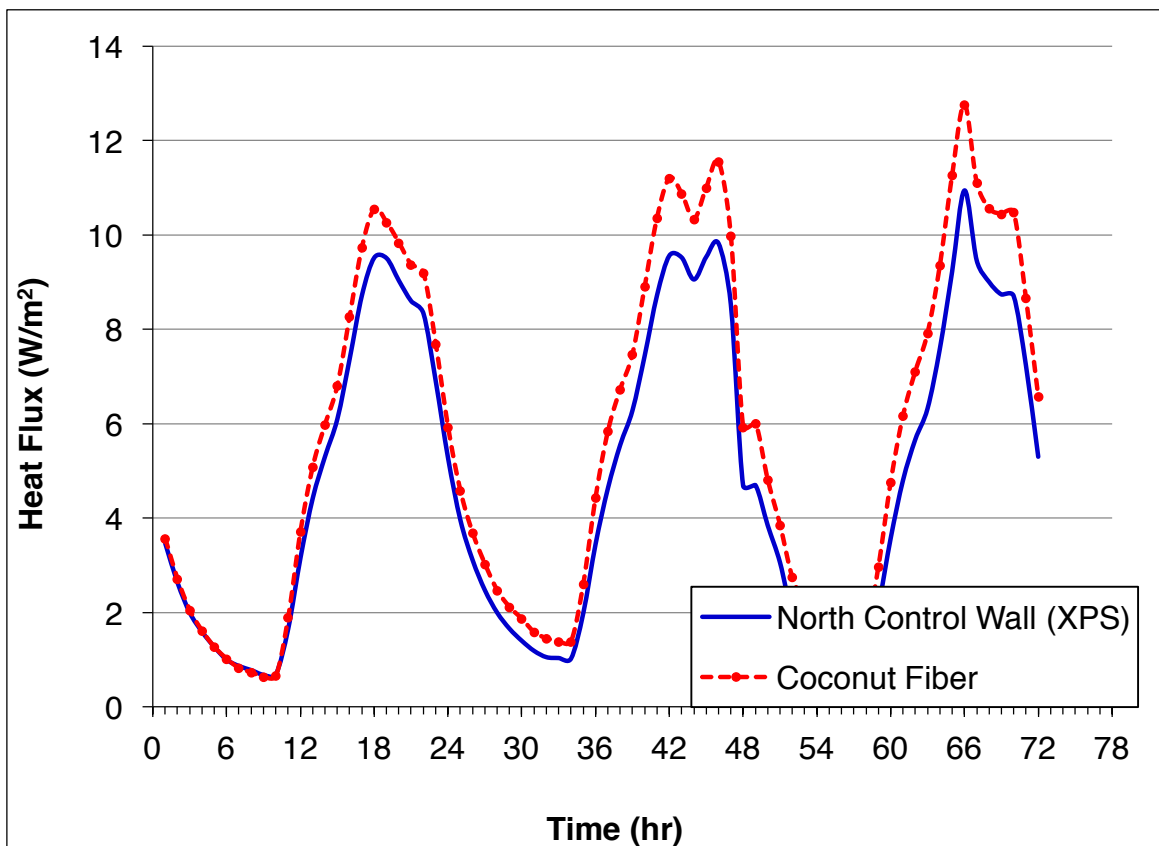


Figure 5.46 North Wall Heat Fluxes at 45 kg/m³

The heat fluxes through the wall cavity with coconut fiber were marginally higher than the wall cavity with XPS insulation throughout the cycle but were lesser when compared to the Timothy grass. The differences in heat fluxes were highest during the

peak temperatures of the day. The highest peak heat flux through the coconut fiber was about 12.7 W/m^2 and the highest peak heat flux through the XPS insulation was about 10.9 W/m^2 . This translates to a difference of 16% in peak heat flux values. The average heat flow through the wheat straw per m^2 -day was 136.2 Wh/m^2 -day and the average heat flow per m^2 -day through the XPS sheets was 115.4 Wh/m^2 -day, which was around 18% less than the coconut fiber. This was much better than the 30% when tested in 30 kg/m^3 configuration and better than the Timothy grass which was 27% in 45 kg/m^3 configuration and also performed closer to wheat straw.

Case 3

For Case 3, the density of all of the indigenous insulation was 65 kg/m^3 and similar to Case 1 and Case 2, the actual external surface conditions were simulated to assess the heat flux and temperature values. Each experiment lasted 72 hours. The heat sources were adjusted to work exactly as they did during the calibration. The data logger collected the data every 10 seconds which were then converted into average values for every hour. Then the values of the control and retrofits were compared using graphs.

Exterior Surface Temperatures

The exterior surface temperature profiles of the retrofit (Timothy grass) and control (XPS sheets) were compared and are shown in Figure 5.47.

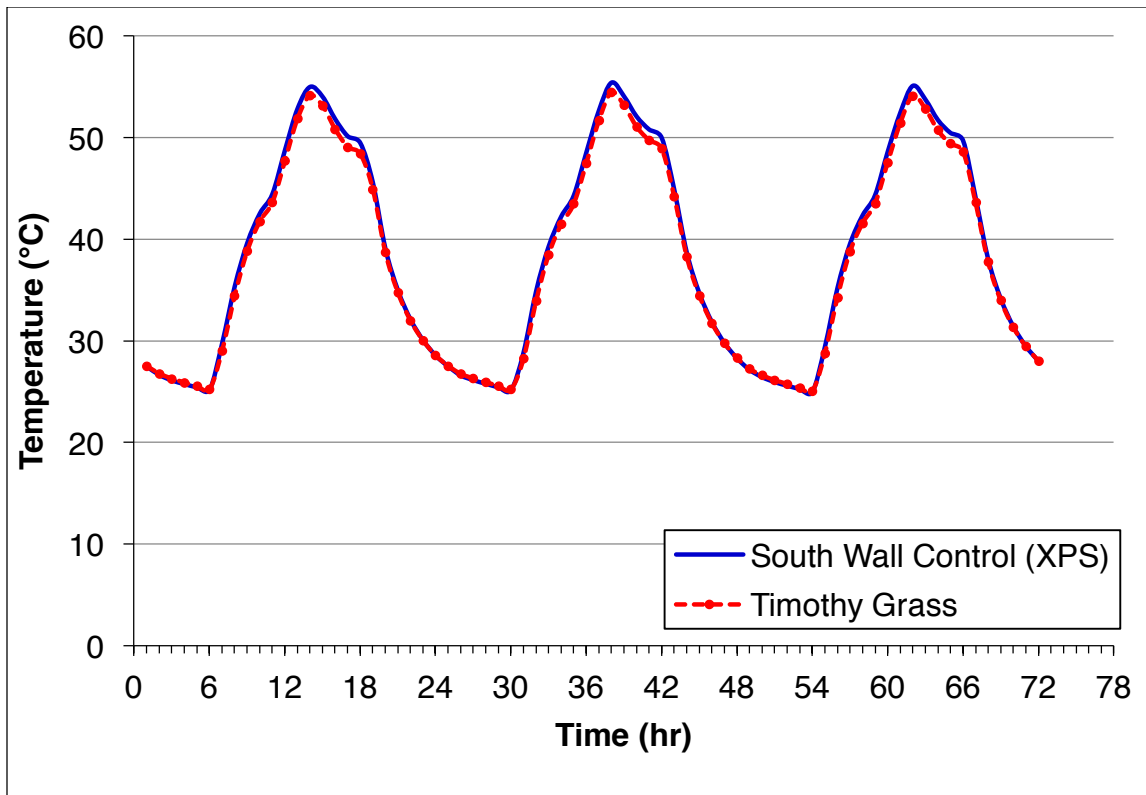


Figure 5.47 South Wall Exterior Surface Temperatures at 65 kg/m³

The temperature profiles show a maximum temperature difference of about 1°C at peak temperature. The temperature of the exterior wall surface with Timothy grass reached a peak temperature of 54.4°C and the exterior wall surface with XPS sheets reached a peak temperature of 55.4°C. As the temperature values decreased, the curves gradually merged and reached the same temperatures. From this observation, it was assumed that the Timothy grass slightly facilitated more heat transfer than the XPS sheets, increasing the conduction heat transfer and hence making the surface slightly cooler by faster dissipation of heat. From this, it was assumed that the Timothy grass at 65 kg/m³ had lower resistance to heat transfer when compared to the XPS sheets in this configuration.

The exterior surface temperature comparison between the wheat straw and XPS sheets is given in Figure 5.48.

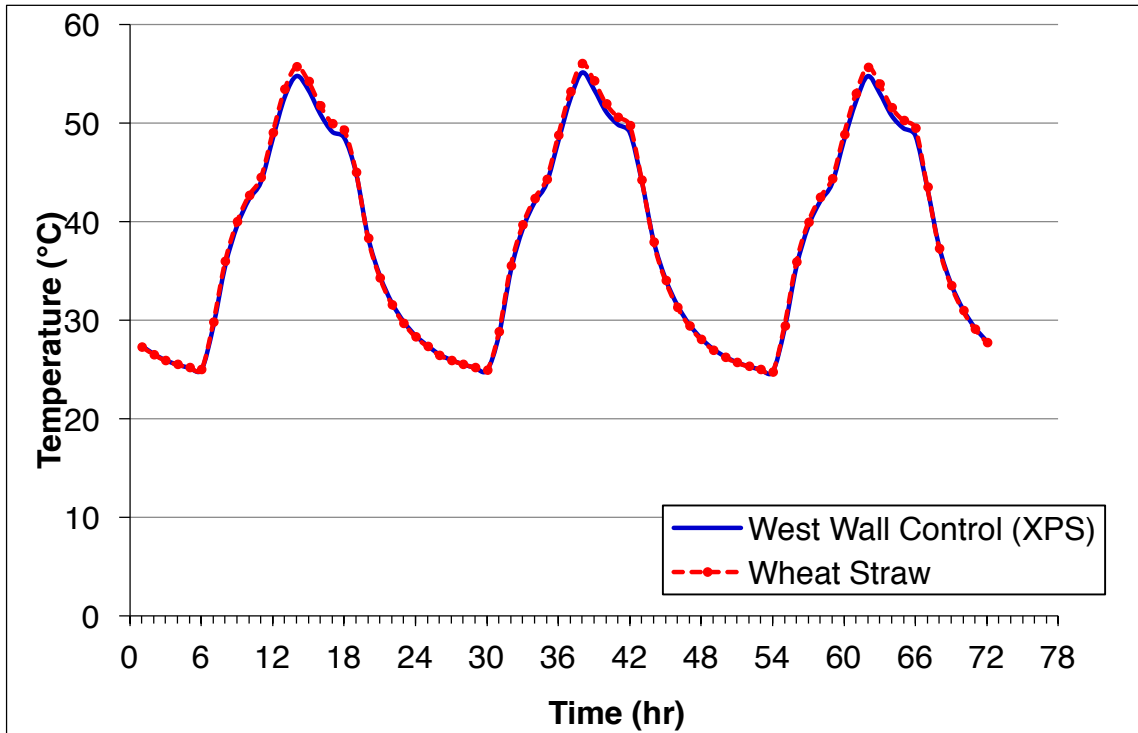


Figure 5.48 West Wall Exterior Surface Temperatures at 65 kg/m³

The temperature profiles show a maximum temperature difference of about 0.8°C at peak temperature. The temperature of the exterior wall surface with wheat straw reached a peak of 55.9°C and the exterior wall surface with XPS sheets reached a peak temperature of 55.1°C. As the temperature values decreased, the curves gradually merged and reached the same temperatures. From this observation, it was assumed that the wheat grass facilitated slightly less heat transfer than the XPS sheets, decreasing the conduction heat transfer and hence making the surface slightly hotter by dissipating heat slower. From this, it was assumed that the wheat straw at 65 kg/m³ had

higher resistance to heat transfer when compared to the XPS sheets in this configuration.

The exterior surface temperature comparison between coconut fiber and XPS sheets is given in Figure 5.49.

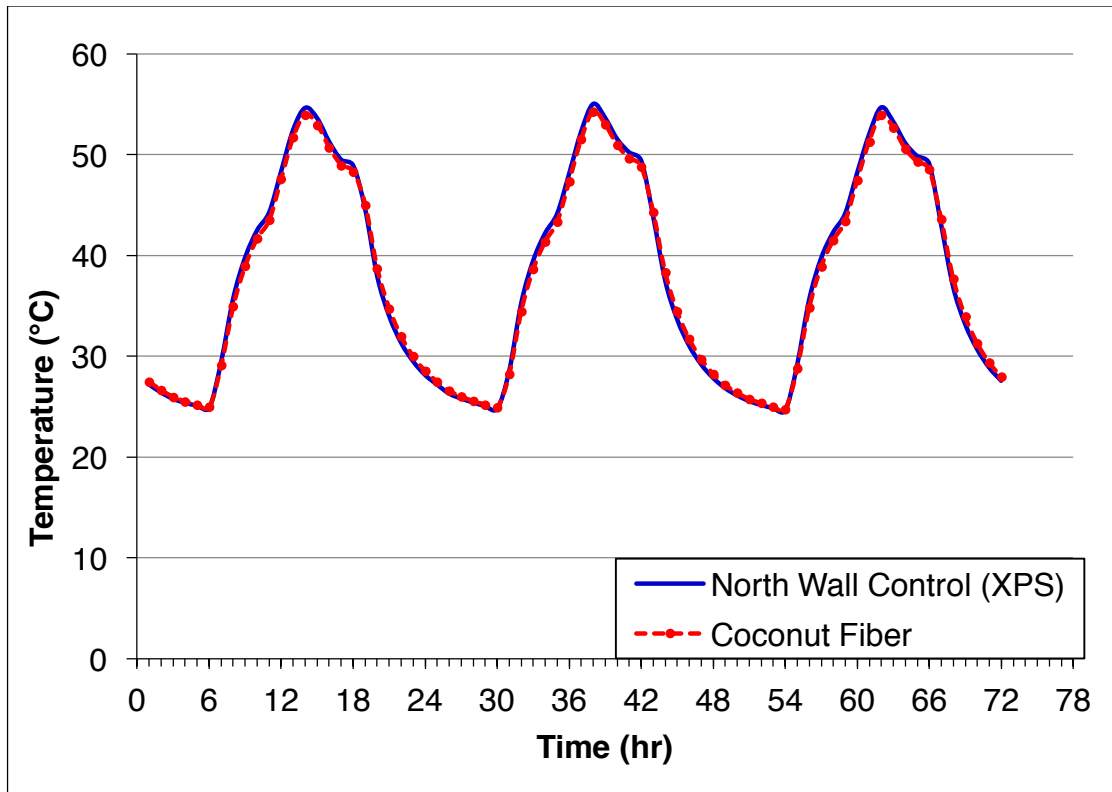


Figure 5.49 North Wall Exterior Surface Temperatures at 65 kg/m³

The temperature profiles show a maximum temperature difference of about 0.7°C at peak temperature. The temperature of the exterior wall surface with coconut fiber reached a highest peak temperature of 54.2°C and the exterior wall surface with XPS sheets reached a highest peak temperature of 54.9°C. When the temperatures were reduced during the cooling mode, the temperature profiles gradually merged and

reached the same temperatures. From this observation, it was assumed that the coconut fiber slightly facilitated more heat transfer than the XPS sheets, increasing the conduction heat transfer and hence making the surface slightly cooler by faster dissipation of heat. From this, it was assumed that the coconut fiber at 65 kg/m^3 had lower resistance to heat transfer when compared to the XPS sheets in this configuration.

Interior Surface Temperatures

The interior surface temperature profiles of the retrofit (Timothy grass) and control (XPS sheets) were compared and are shown in Figure 5.50.

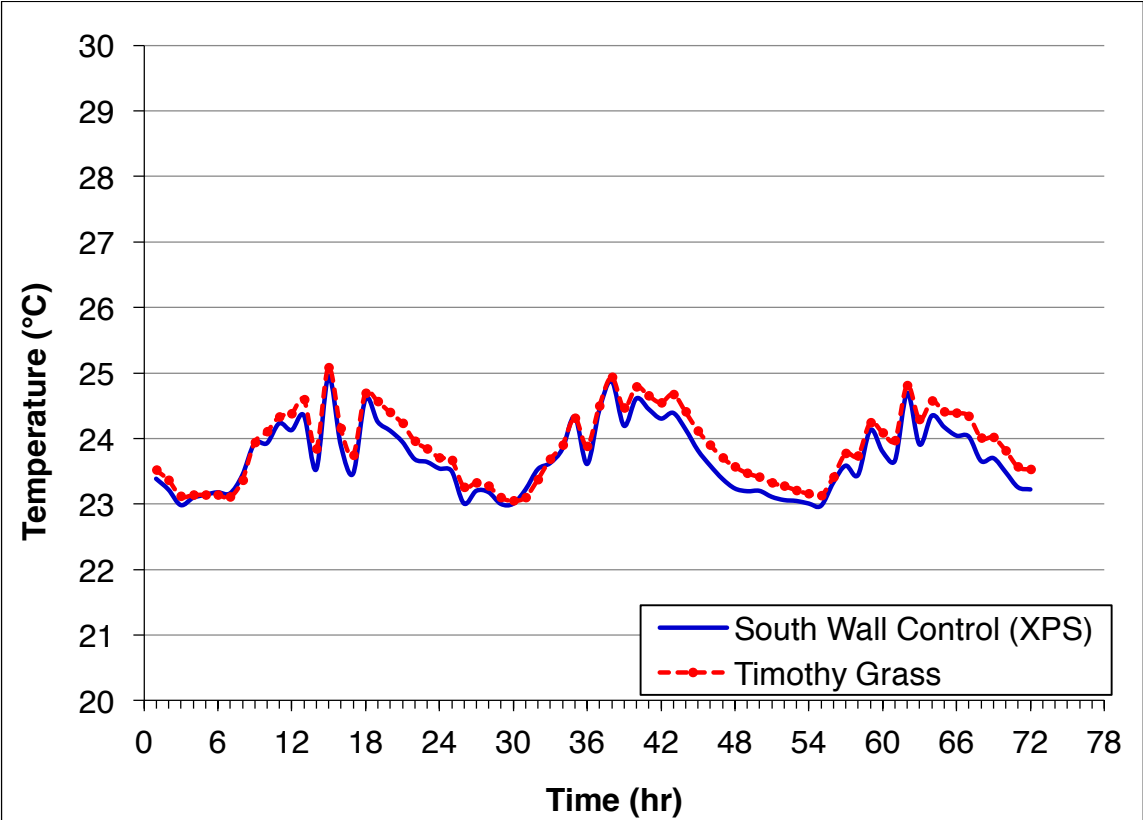


Figure 5.50 South Wall Interior Surface Temperatures at 65 kg/m^3

The temperature profiles of the wall cavities that had Timothy grass and XPS sheets show that the temperature profiles were almost similar, but the maximum temperature difference between the interior surface with Timothy grass and XPS sheets was about 0.3°C during the cooling phase. The average temperature of the interior wall surface with Timothy grass reached 23.9°C whereas the average interior surface temperature of the wall with XPS sheets reached 23.7°C which was 0.2°C lower. This shows that the Timothy grass performed better than in Case 1 and Case 2.

The interior surface temperature comparison between the wheat straw and XPS sheets is given in Figure 5.51.

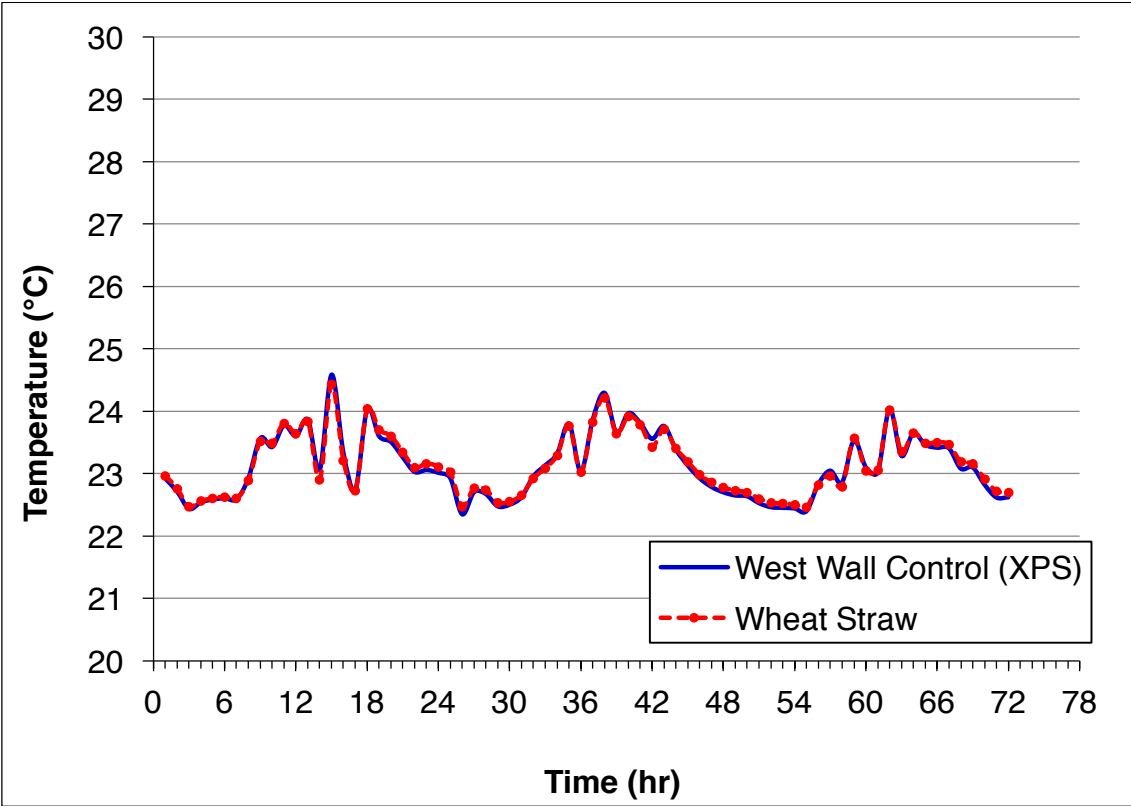


Figure 5.51 West Wall Interior Surface Temperatures at 65 kg/m³

The temperature profiles of the wheat straw and the XPS sheets were nearly identical. The average temperature of the interior wall surfaces with wheat straw and XPS sheets reached 23.1°C. This shows that the heat transfer through wheat straw and the XPS sheets were nearly identical in this case and that wheat straw performed better at a density of 65 kg/m³ than the previous two cases.

The interior surface temperature comparison between the coconut fiber and XPS sheets is given in Figure 5.52.

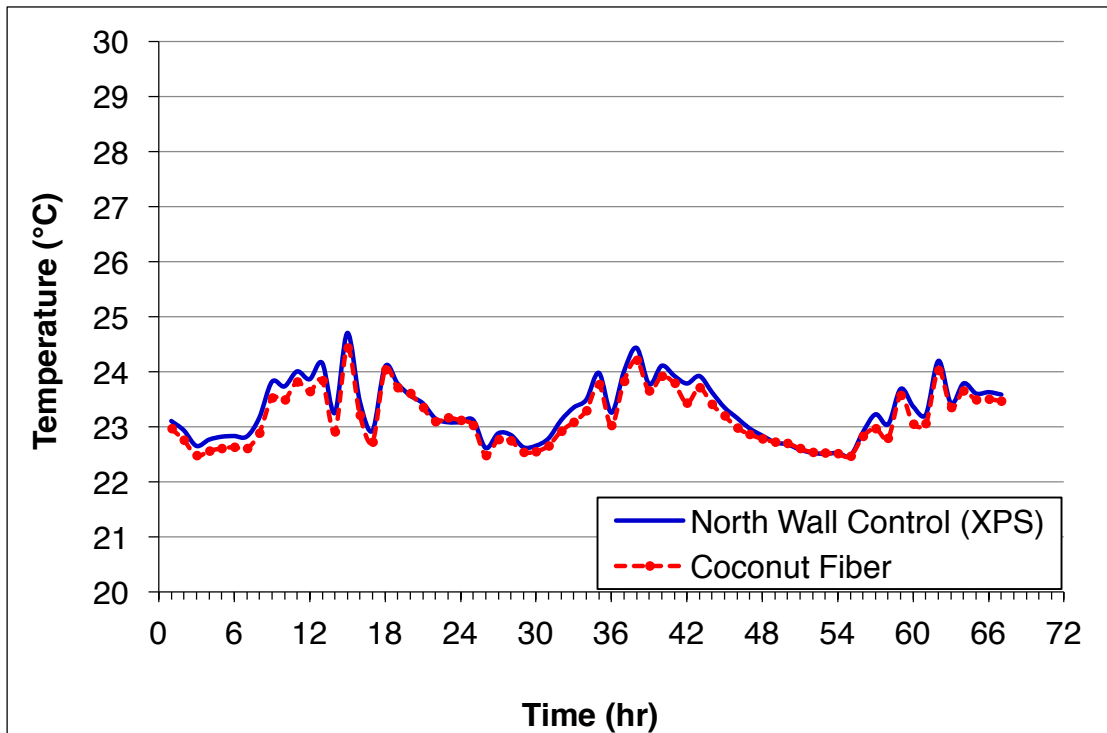


Figure 5.52 North Wall Interior Surface Temperatures at 65 kg/m³

The temperature profiles of the wall cavities that had coconut fiber and XPS sheets show that the temperature profiles were very similar, but the maximum temperature difference between the interior surface with the coconut fiber and XPS

sheets was about 0.3°C during the heating and cooling phases. The average temperature of the interior wall surface with coconut fiber reached 23.1°C whereas the average interior surface temperature of the wall with XPS sheets reached 23.2°C which was 0.1°C higher. The interesting fact here was that the surface temperature of the cavity with coconut fiber was consistently lower than the surface temperature of the cavity with the XPS sheets during the cooling phase. This shows that the coconut fiber could have performed better than XPS sheets in this case.

Layer Temperatures

The layer temperature profiles of the retrofit (Timothy grass) and control (XPS sheets) were compared and are shown in Figure 5.53.

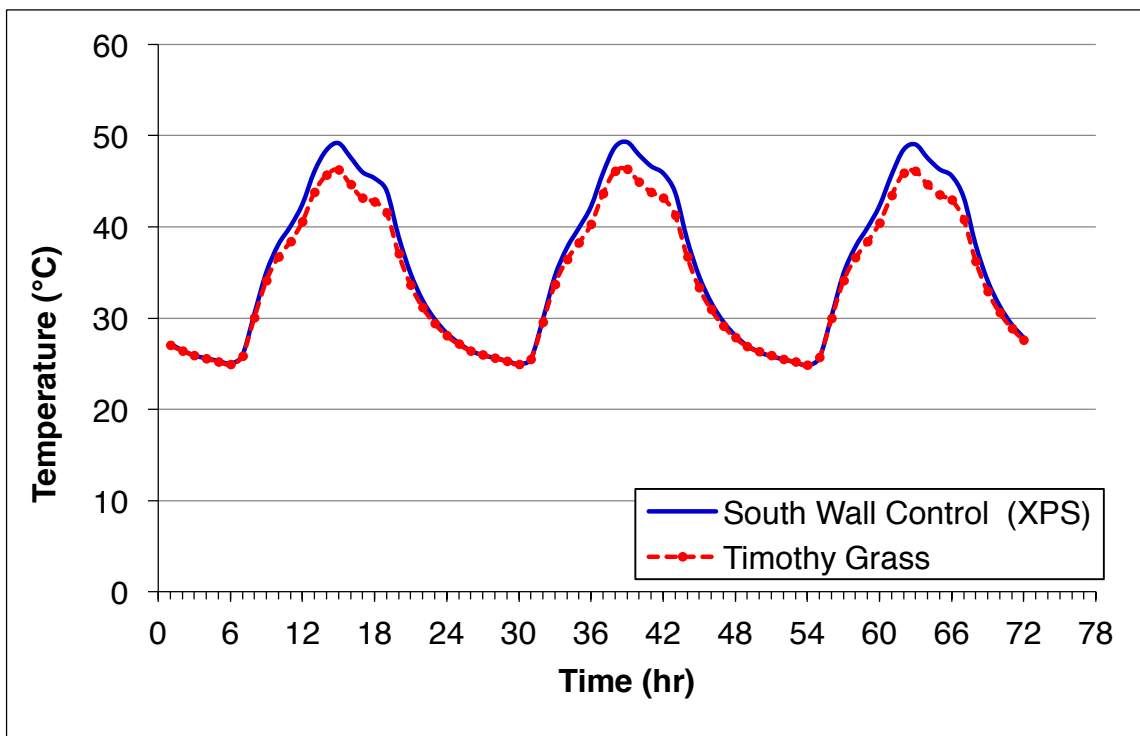


Figure 5.53 South Wall Layer Temperatures at 65 kg/m³

The temperature profiles show a maximum temperature difference of about 2.9°C at peak temperature, which was 0.7°C lower than Case 2, which suggested a better performance. The temperature of the layer with Timothy grass reached a highest peak temperature of 46.2°C and the layer with XPS sheets reached a highest peak temperature of 49.1°C. When the temperatures were reduced during the cooling mode, the temperature profiles gradually merged and reached the same temperatures.

The layer temperature profiles of the retrofit (wheat straw) and control (XPS sheets) were compared and are shown in Figure 5.54.

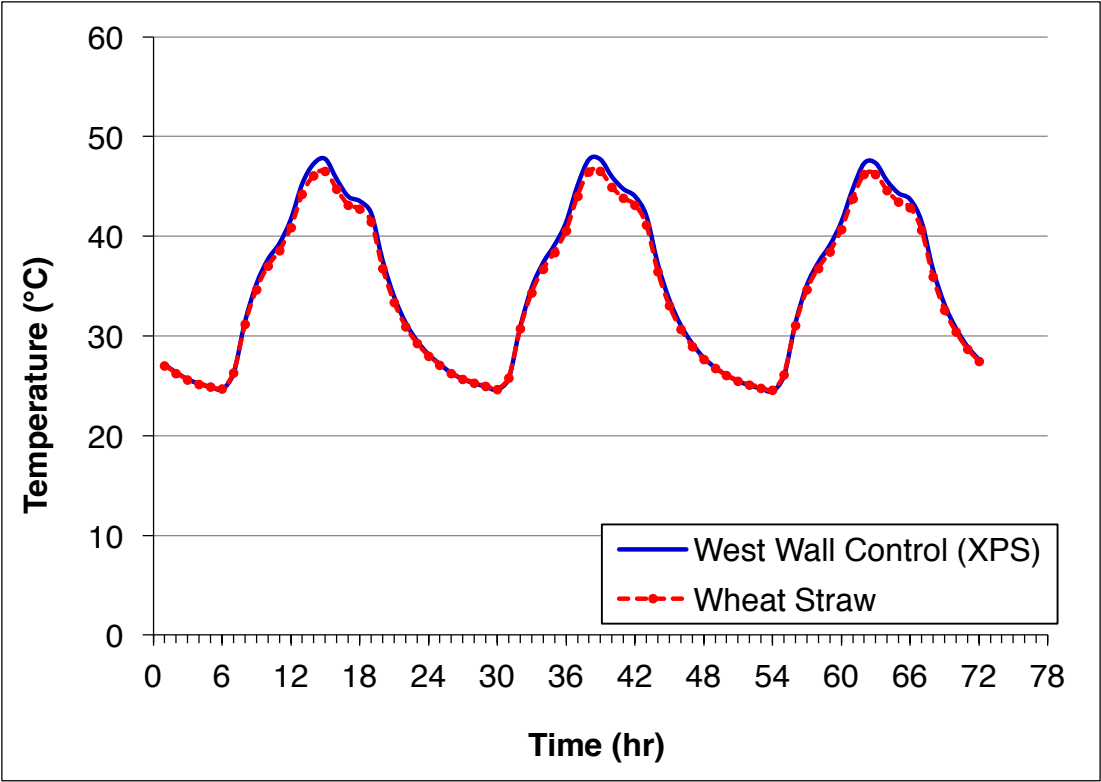


Figure 5.54 West Wall Layer Temperatures at 65 kg/m³

The temperature profiles show a maximum temperature difference of about 1.2°C at peak temperature which was 0.5°C lower than Case 2, which suggested a better performance. The temperature of the layer with wheat straw reached a highest peak temperature of 46.5°C and the layer with XPS sheets reached a highest peak temperature of 47.7°C. When the temperatures were reduced during the cooling mode, the temperature profiles gradually merged and reached the same temperatures. However, it was noted that the temperature difference in this case was lower when compared to the peak temperature difference between the XPS sheets and the Timothy grass which was 2.9°C.

The layer temperature profiles of the retrofit (coconut fiber) and control (XPS sheets) were compared and are shown in Figure 5.55.

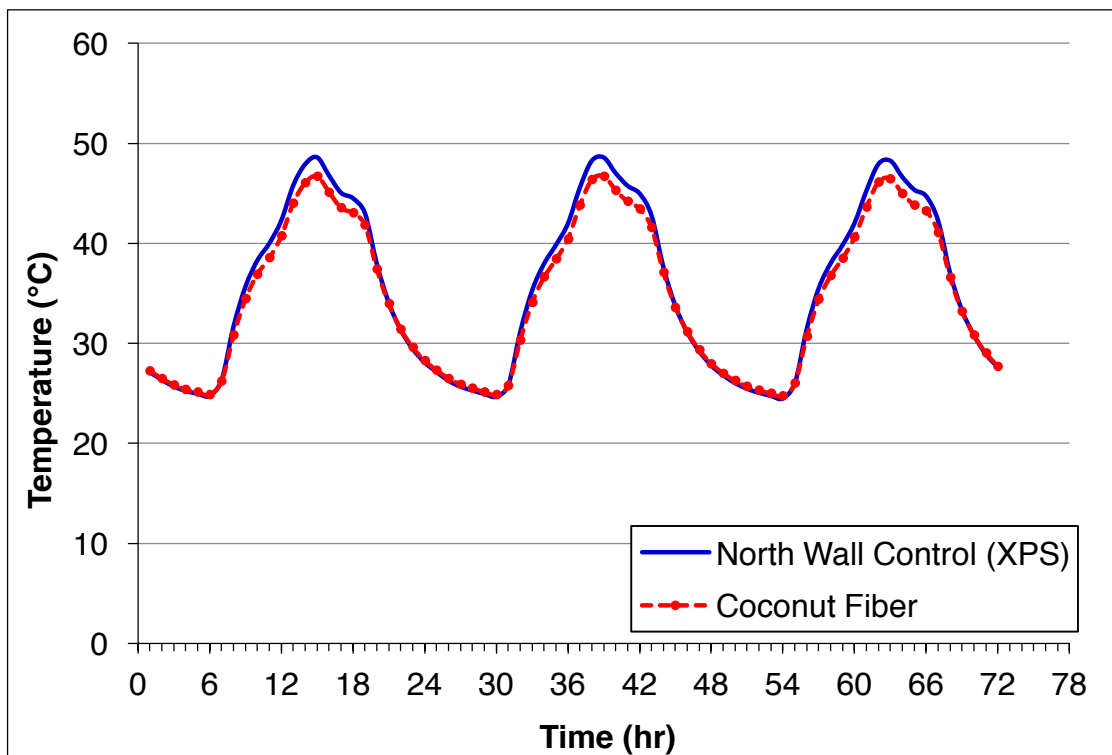


Figure 5.55 North Wall Layer Temperatures at 65 kg/m³

The temperature profiles show a maximum temperature difference of about 1.8°C at peak temperature which was 1.4°C lower than Case 2, which suggested a better performance. The temperature of the layer with coconut fiber reached a highest peak temperature of 46.7°C and the layer with XPS sheets reached a highest peak temperature of 48.5°C. The comparison of peak temperature values and the temperature differences are given in Table 5.3.

Table 5.3 Comparison of Peak Temperatures and Peak Temperature Differences at 65 kg/m³

Wall	Control / Retrofit	Peak Temperature (°C)	Temperature Difference (°C)
South Exterior Surface	XPS sheets	55.4	1
	Timothy grass	54.4	
West Exterior Surface	XPS sheets	55.1	-0.8
	Wheat straw	55.9	
North Exterior Surface	XPS sheets	54.9	0.7
	Coconut fiber	54.2	
South Interior Surface	XPS sheets	25.1	0
	Timothy grass	25.1	
West Interior Surface	XPS sheets	24.4	0
	Wheat straw	24.4	
North Interior Surface	XPS sheets	24.7	0.3
	Coconut fiber	24.4	
South Layer	XPS sheets	49.1	2.9
	Timothy grass	46.2	
West Layer	XPS sheets	47.7	1.2
	Wheat straw	46.5	
North Layer	XPS sheets	48.5	1.8
	Coconut fiber	46.7	

Heat Fluxes

Heat flux values were measured using heat flux meters. Figure 5.56 shows the comparison of heat fluxes between Timothy grass and XPS insulation.

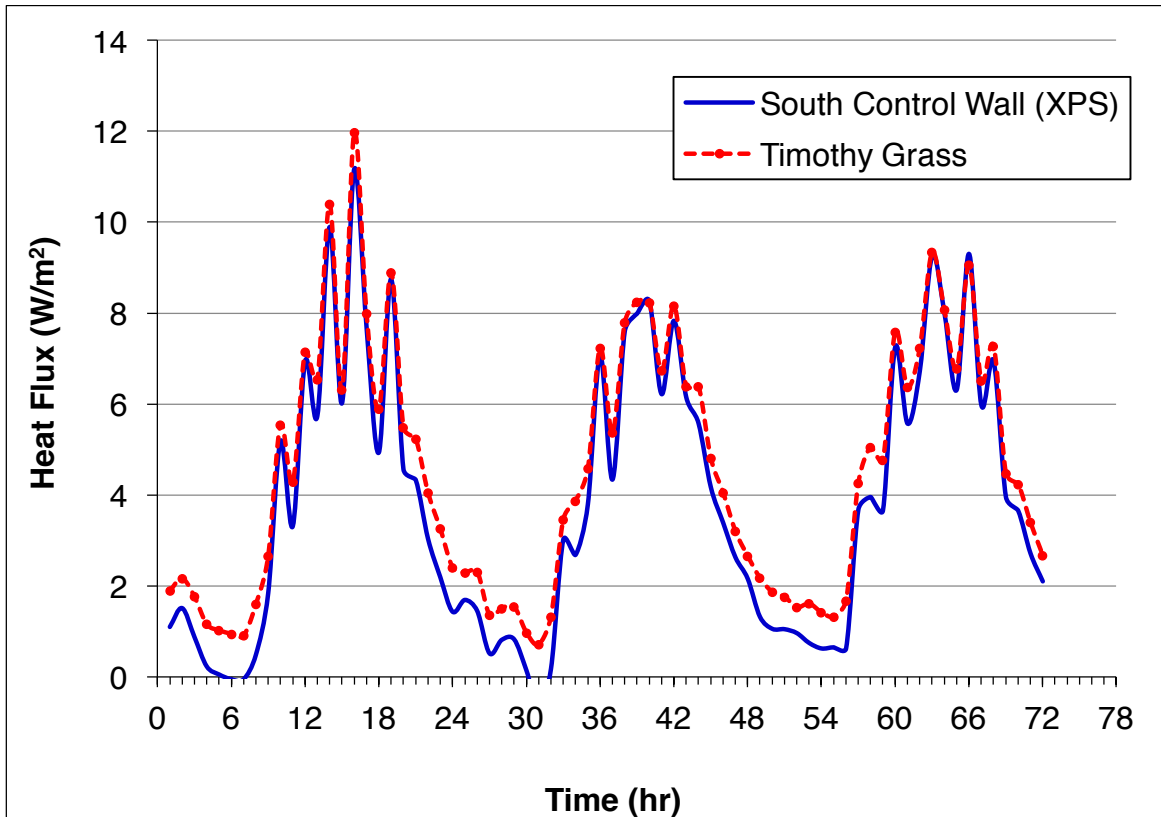


Figure 5.56 South Wall Heat Fluxes at 65 kg/m³

The heat fluxes through the wall cavity with Timothy grass were almost similar to the wall cavity with XPS insulation throughout the cycle except during cooling and heating cycles. This observation suggested that the Timothy grass may have higher thermal mass which stored heat for a longer time than the XPS sheets. The highest peak heat flux through wall cavity with Timothy grass was about 12 W/m² and the highest peak heat flux through the wall cavity with XPS insulation was about 11.5 W/m².

This translated to a difference of 4% in peak heat flux values. The average heat flow through Timothy grass per $\text{m}^2\text{-day}$ was $107.7 \text{ Wh/m}^2\text{-day}$ and the average heat flow per $\text{m}^2\text{-day}$ through XPS sheets was $91.8 \text{ Wh/m}^2\text{-day}$, which was around 17% less than the Timothy grass. Therefore, it was proven that the XPS sheets outperformed the Timothy grass as a building insulation material when used in a density of 65 kg/m^3 configuration but better than the 30 and 45 kg/m^3 configurations.

Figure 5.57 shows the comparison of heat fluxes between wheat straw and XPS insulation.

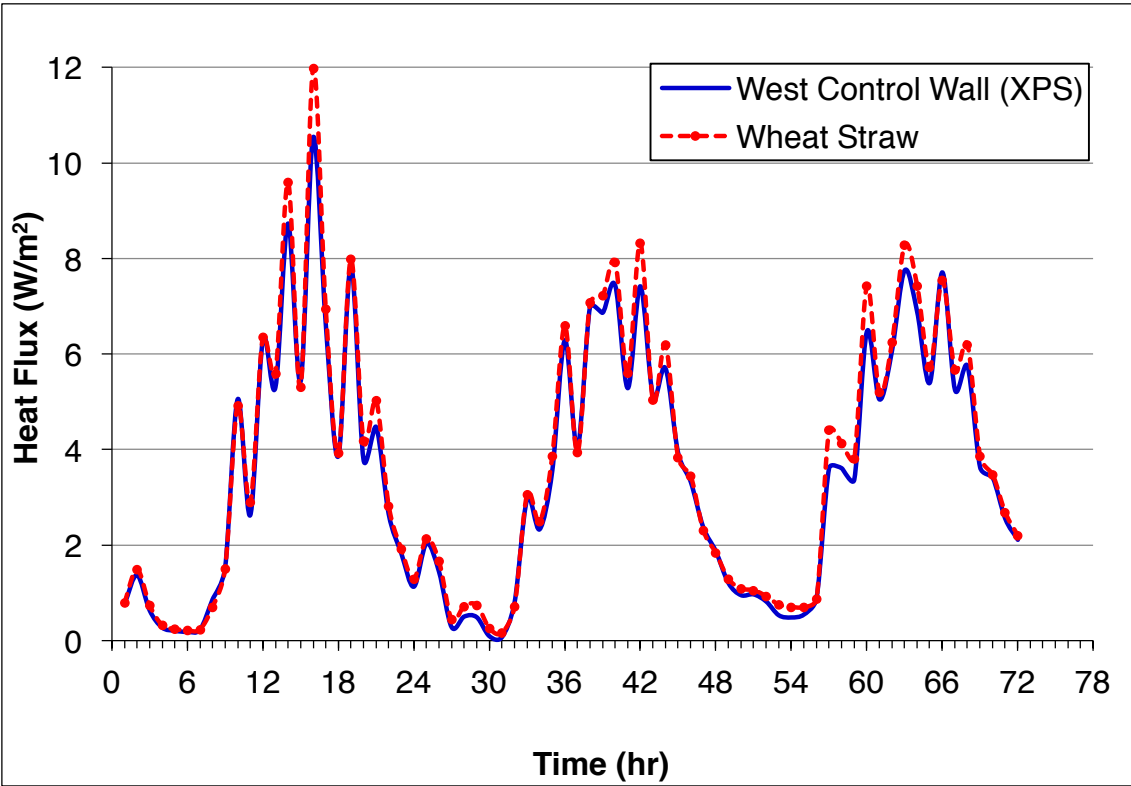


Figure 5.57 West Wall Heat Fluxes at 65 kg/m^3

The heat fluxes through the wall cavity with wheat straw were almost similar to the wall cavity with XPS insulation throughout the cycle, except during the peak temperature of the day. The differences in heat fluxes were highest during the peak temperatures of the day. The highest peak heat flux through the wall cavity with wheat straw was about 12 W/m^2 and the highest peak heat flux through the wall cavity with XPS insulation was about 10.8 W/m^2 . This translated to a difference of 11% in peak heat flux values. The average heat flow through wheat straw per m^2 -day was 88 Wh/m^2 -day and the average heat flow per m^2 -day through XPS sheets was 82.9 Wh/m^2 -day, which was around 6% less than the wheat straw which was marginal. This was much better than the Case 1 and Case 2.

Figure 5.58 shows the comparison of heat fluxes between coconut fiber and XPS insulation.

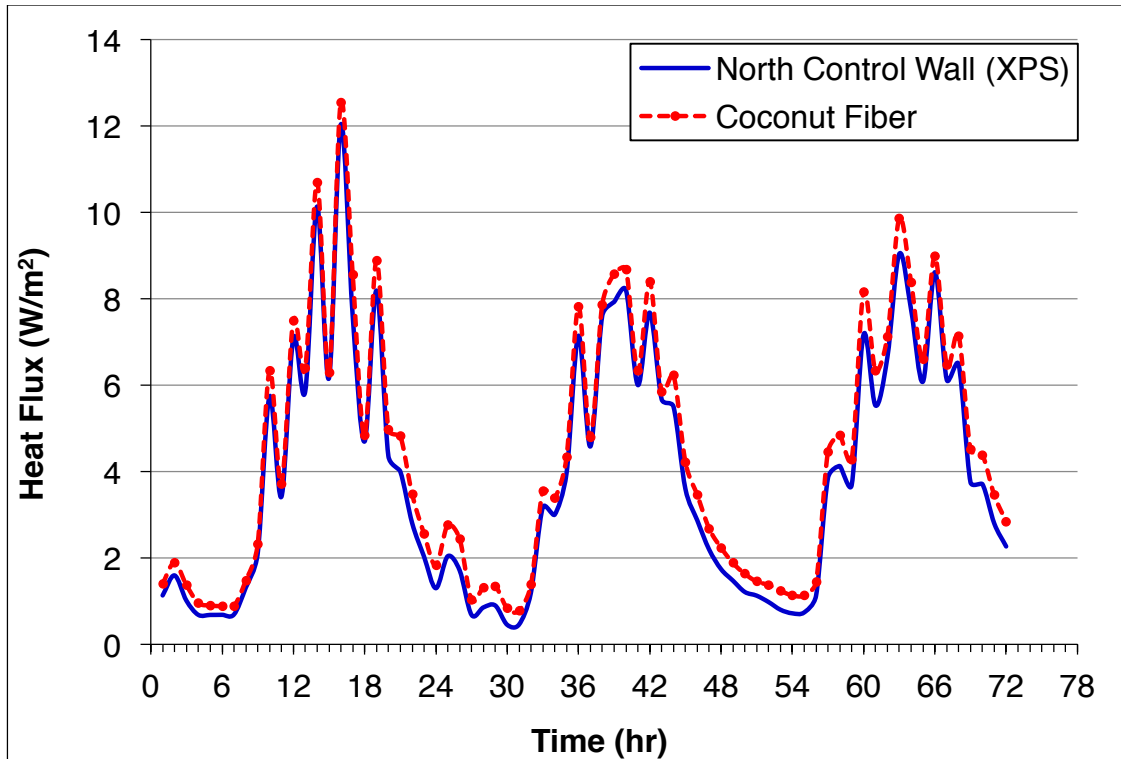


Figure 5.58 North Wall Heat Fluxes at 65 kg/m³

The heat fluxes through the wall cavity with coconut fiber were marginally higher than the wall cavity with XPS insulation during the peaks and during cooling cycles. The differences in heat fluxes were highest during the peak temperatures of the day. The highest peak heat flux through coconut fiber was about 12.6 W/m² and the highest peak heat flux through XPS insulation was about 12.1 W/m². This translated to a difference of 4% in peak heat flux values. The average heat flow through the wheat straw per m²-day was 105.2 Wh/m²-day and the average heat flow per m²-day through the XPS sheets was 93.4 Wh/m²-day, which was around 12% less than the coconut fiber. Table 5.4 shows the percentage difference, in average heat flow per m²-day, of the indigenous materials with respect to the XPS insulation sheets.

Table 5.4 Comparison of Average Heat Flow Values

Cases	Materials	% Difference in Total Heat Flow per m²-day
Case 1	Timothy Grass	30%
	Wheat Straw	20%
	Coconut Fiber	29%
Case 2	Timothy Grass	27%
	Wheat Straw	16%
	Coconut Fiber	27%
Case 3	Timothy Grass	17%
	Wheat Straw	6%
	Coconut Fiber	12%

Figure 5.59 shows the comparison of percentage difference, in average heat flow per m²-day, of the indigenous materials with respect to the XPS insulation sheets.

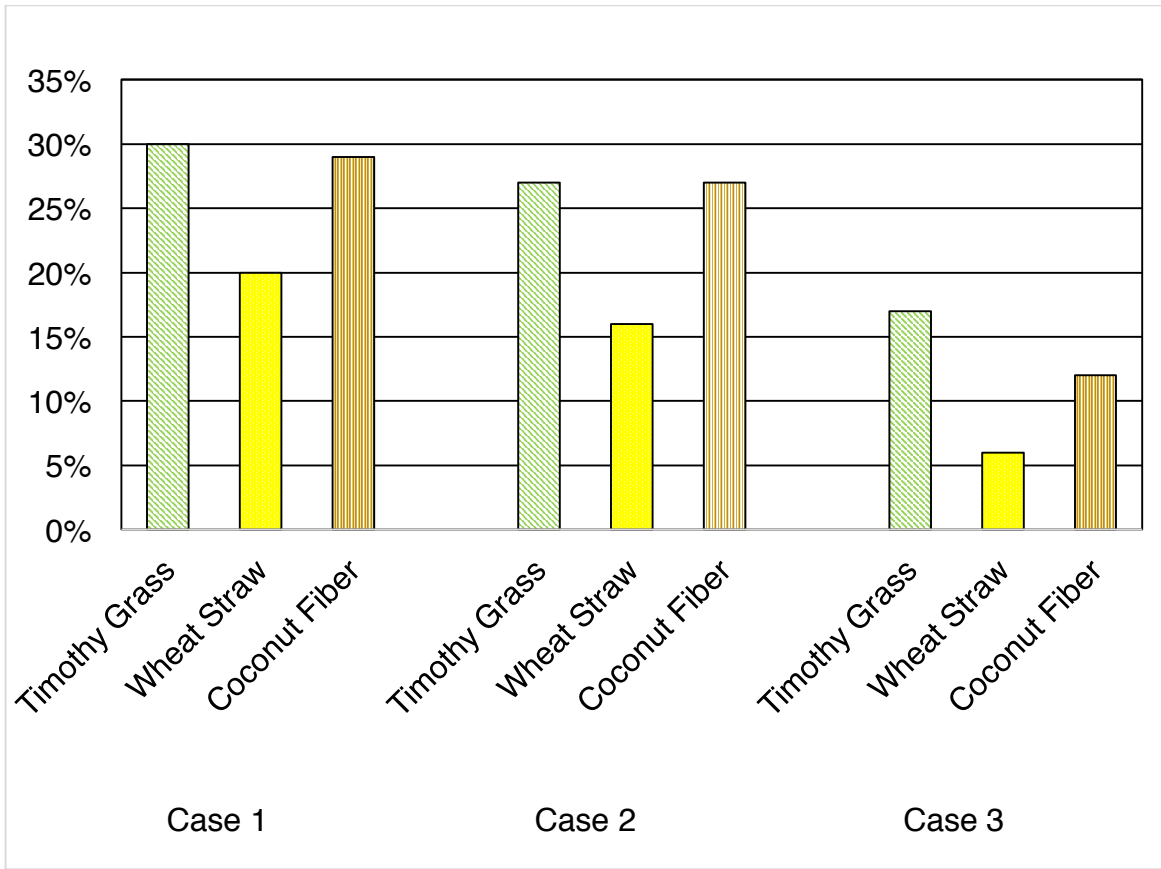


Figure 5.59 Comparison of Percentage Difference in Average Heat Flow

Steady State Heat Transfer Conditions

The indigenous materials were tested under steady state heat transfer conditions for three densities as explained before. In this setting, the exterior and interior layer temperatures were maintained at around 55°C and 25°C, respectively. Each experiment lasted 72 hours. These experiments were performed under these settings to calculate the R-values of the indigenous materials at various densities using Fourier’s law of heat conduction equation, which was explained in the previous chapter.

Case 1

The indigenous materials were tested at a density of 30 kg/m^3 .

Timothy Grass

The average exterior surface temperature, T_o , of the wall cavity with Timothy grass was 52.8°C , the average interior surface temperature, T_i , was 25.9°C , and the average layer temperature was 45.9°C . The average steady state heat flux through the wall cavity, q , with Timothy grass was 9.4 W/m^2 . R-values of drywall, air gap, XPS sheet and the wooden siding were 0.079 , 0.16 , 0.528 and $0.23 \text{ m}^2\cdot^\circ\text{C/W}$, respectively.

The section of the wall panel with Timothy grass is shown in Figure 5.60.

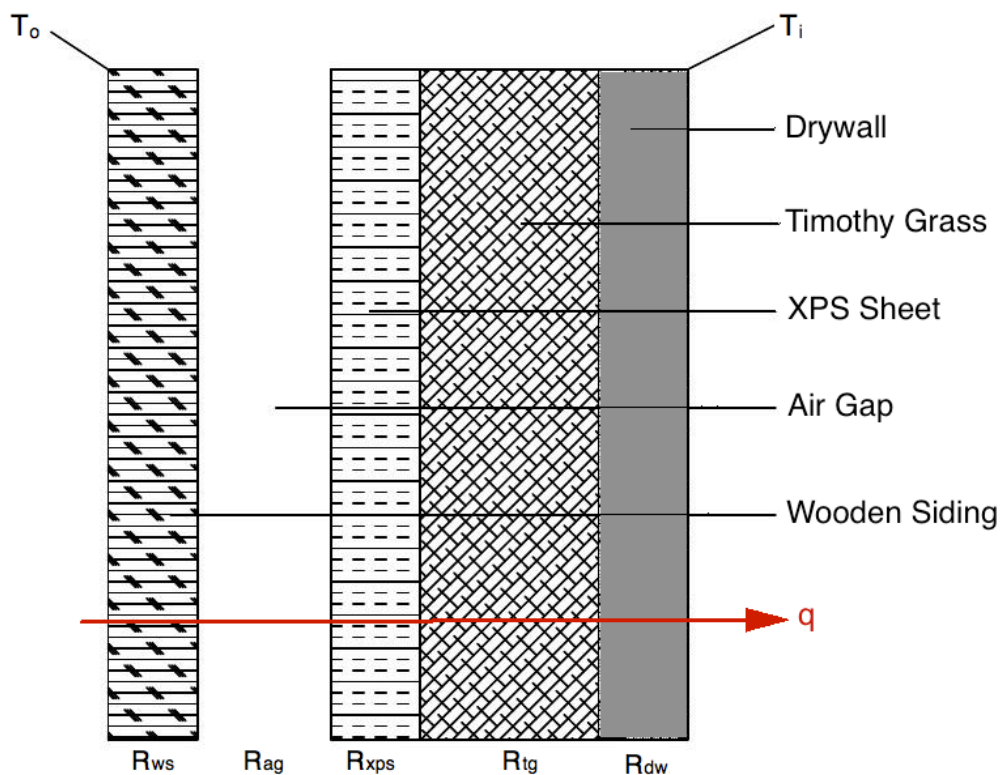


Figure 5.60 Section of Wall Panel

For this case, Fourier's law of heat conduction can be represented by,

$$q = \frac{(T_o - T_i)}{(R_{dw} + R_{ag} + R_{xps} + R_{tg} + R_{ws})} \quad \text{--- Eq. (5.1)}$$

where,

T_o and T_i are the exterior and interior surface temperatures, respectively,

R_{dw} , R_{ag} , R_{xps} , R_{tg} , and R_{ws} are the resistances of drywall, air gap, XPS sheet,

Timothy grass and wooden siding, respectively.

Substituting the known values, the equivalent R-value of Timothy grass at 30 kg/m³ density was found to be 1.86 m².°C/W.

Wheat Straw

The average exterior surface temperature of the wall cavity with wheat straw was 53.5°C, the average interior surface temperature was 25.1°C, and the average layer temperature was 46.5°C. The average heat flux through the wall cavity with wheat straw was 8.1 W/m². R-values of drywall, air gap, XPS sheet and the wooden siding are 0.079, 0.16, 0.528 and 0.23 m².°C/W, respectively. Using Fourier's law of heat conduction equation and substituting the known values, the equivalent R-value of wheat straw at 30 kg/m³ density was found to be 2.51 m².°C/W.

Coconut Fiber

The average exterior surface temperature of the wall cavity with coconut fiber was 52.7°C, the average interior surface temperature was 25.5°C, and the average layer temperature was 46.6°C. The average heat flux through the wall cavity with

coconut fiber was 9.8 W/m^2 . R-values of drywall, air gap, XPS sheet and the wooden siding are 0.079 , 0.16 , 0.528 and $0.23 \text{ m}^2 \cdot ^\circ\text{C/W}$, respectively. Using Fourier's law of heat conduction equation and substituting the known values, the equivalent R-value of coconut fiber at 30 kg/m^3 density was found to be $1.78 \text{ m}^2 \cdot ^\circ\text{C/W}$.

Case 2

The indigenous materials were tested at a density of 45 kg/m^3 .

Timothy Grass

The average exterior surface temperature of the wall cavity with Timothy grass was 52.6°C , the average interior surface temperature was 25.6°C , and the average layer temperature was 44.8°C . The average heat flux through the wall cavity with Timothy grass was 8.9 W/m^2 . R-values of drywall, air gap, XPS sheet and the wooden siding are 0.079 , 0.16 , 0.528 and $0.23 \text{ m}^2 \cdot ^\circ\text{C/W}$, respectively. Using Fourier's law of heat conduction equation and substituting the known values, the equivalent R-value of Timothy grass at 45 kg/m^3 density was found to be $2.04 \text{ m}^2 \cdot ^\circ\text{C/W}$.

Wheat Straw

The average exterior surface temperature of the wall cavity with wheat straw was 53.5°C , the average interior surface temperature was 24.7°C , and the average layer temperature was 47.1°C . The average heat flux through the wall cavity with wheat straw was around 7 W/m^2 . R-values of drywall, air gap, XPS sheet and the wooden siding are

0.079, 0.16, 0.528 and 0.23 m².°C/W, respectively. Using Fourier's law of heat conduction equation and substituting the known values, the equivalent R-value of wheat straw at 45 kg/m³ density was found to be 3.11 m².°C/W.

Coconut Fiber

The average exterior surface temperature of the wall cavity with coconut fiber was 52.5°C, the average interior surface temperature was 25.3°C, and the average layer temperature was 47.6°C. The average heat flux through the wall cavity with coconut fiber was 9.3 W/m². R-values of drywall, air gap, XPS sheet and the wooden siding are 0.079, 0.16, 0.528 and 0.23 m².°C/W, respectively. Using Fourier's law of heat conduction equation and substituting the known values, the equivalent R-value of coconut fiber at 45 kg/m³ density was found to be 1.93 m².°C/W.

Case 3

The indigenous materials were tested at a density of 65 kg/m³.

Timothy Grass

The average exterior surface temperature of the wall cavity with Timothy grass was 50.1°C, the average interior surface temperature was 25°C, and the average layer temperature was 41.9°C. The average heat flux through the wall cavity with Timothy grass was around 6 W/m². R-values of drywall, air gap, XPS sheet and the wooden siding are 0.079, 0.16, 0.528 and 0.23 m².°C/W, respectively. Fourier's law of heat

conduction equation and substituting the known values, the equivalent R-value of Timothy grass at 65 kg/m^3 density was found to be $3.19 \text{ m}^2 \cdot \text{°C/W}$.

Wheat Straw

The average exterior surface temperature of the wall cavity with wheat straw was 51.8°C , the average interior surface temperature was 24.5°C and the average layer temperature was 46.3°C . The average heat flux through the wall cavity with wheat straw was around 6 W/m^2 . R-values of drywall, air gap, XPS sheet and the wooden siding are 0.079 , 0.16 , 0.528 and $0.23 \text{ m}^2 \cdot \text{°C/W}$ respectively. Using Fourier's law of heat conduction equation and substituting the known values, the equivalent R-value of wheat straw at 65 kg/m^3 density was found to be $3.55 \text{ m}^2 \cdot \text{°C/W}$.

Coconut Fiber

The average exterior surface temperature of the wall cavity with coconut fiber was 50.9°C , the average interior surface temperature was 24.9°C and the average layer temperature was 46°C . The average heat flux through the wall cavity with coconut fiber was 7.4 W/m^2 . R-values of drywall, air gap, XPS sheet and the wooden siding are 0.079 , 0.16 , 0.528 and $0.23 \text{ m}^2 \cdot \text{°C/W}$, respectively. Using Fourier's law of heat conduction equation and substituting the known values, the equivalent R-value of coconut fiber at 65 kg/m^3 density was found to be $2.52 \text{ m}^2 \cdot \text{°C/W}$.

Economic Analysis

The R-values of the indigenous materials at different densities were compared to the R-values of XPS insulation during each steady state heat conduction experiment. When XPS sheets were used as control and Timothy grass as retrofit, the average equivalent R-value of XPS insulation was found to be $3.48 \text{ m}^2 \cdot ^\circ\text{C}/\text{W}$.

Figure 5.61 shows the comparison of R-values of Timothy grass at different densities.

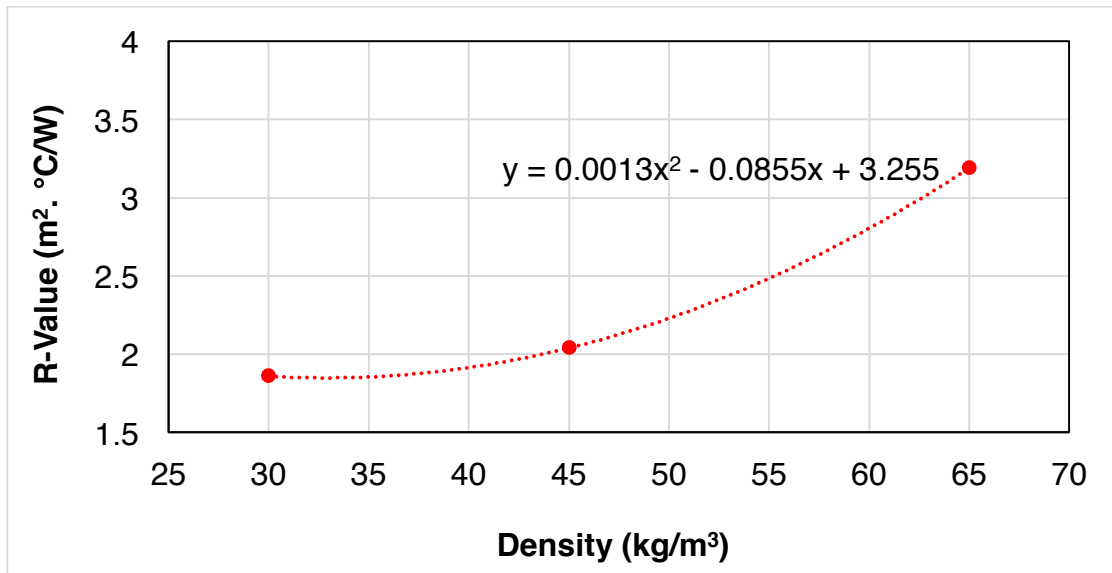


Figure 5.61 R-Value Curve of Timothy Grass

A graph was plotted between R-value and density of Timothy grass and a polynomial equation was generated using MS Excel. By solving the polynomial equation for $y = 3.48$, the density at which the Timothy grass matches the performance of XPS insulation was found to be 68.3 kg/m^3 . The quantity of Timothy grass that has to be used to achieve this density is 1.3 kg. Premium quality Timothy grass costs around

\$200 per ton (USDA). Therefore, the cost of the insulation material in this case was around \$0.26. The cost of 12.7 mm thick XPS sheet of size 1.2 m x 2.4 m costs around \$14.25 in commercial stores (Home Depot). Therefore, the cost of XPS insulation used (four sheets of size 1.12 m x 0.37 m) was around \$8.3. Therefore, Timothy grass costs 32 times cheaper than XPS insulation.

When XPS sheets were used as control and wheat straw as retrofit, the average equivalent R-value of XPS insulation was found to be $4.12 \text{ m}^2 \cdot \text{C/W}$.

Figure 5.62 shows the comparison of R-values of wheat straw at different densities.

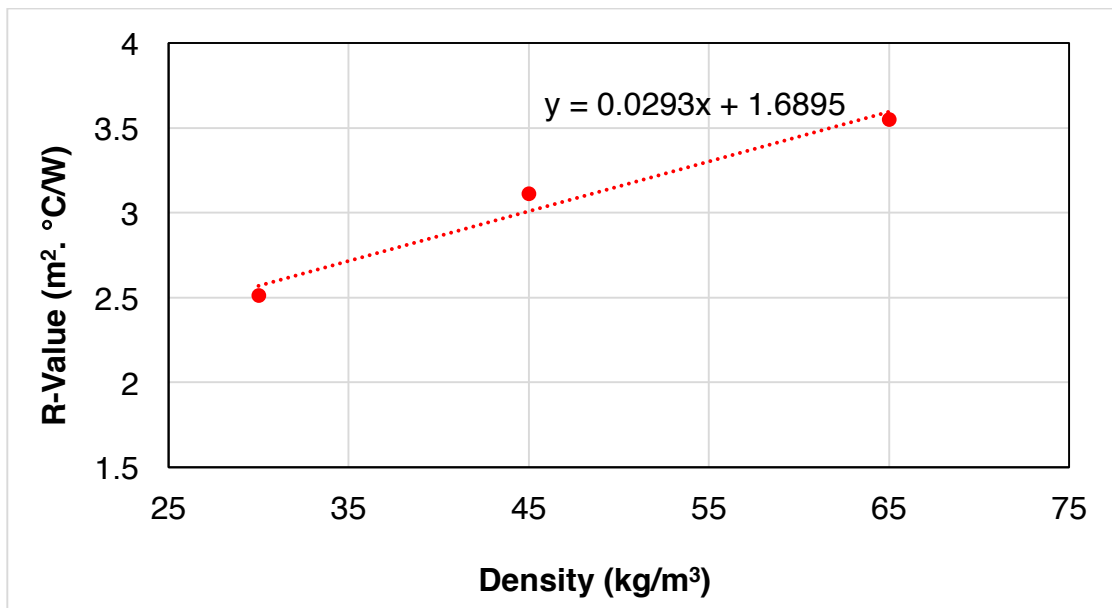


Figure 5.62 R-value Curve of Wheat Straw

A graph was plotted between R-value and density of wheat straw and a linear equation was generated using MS Excel. By solving the linear equation for $y = 4.12$, the density at which the wheat straw matches the performance of XPS insulation was found

to be 80.18 kg/m^3 . The amount of wheat straw that has to be used to achieve this density is 1.52 kg. Good quality wheat straw costs around \$150 per ton (OCJ). Therefore, the cost of the insulation material in this case was around \$0.23 which is around 36 times cheaper than the XPS insulation.

When XPS sheets were used as control and coconut fiber as retrofit, the average equivalent R-value of XPS insulation was found to be $3.54 \text{ m}^2 \cdot \text{°C/W}$. Figure 5.63 shows the comparison of R-values of coconut fiber at different densities.

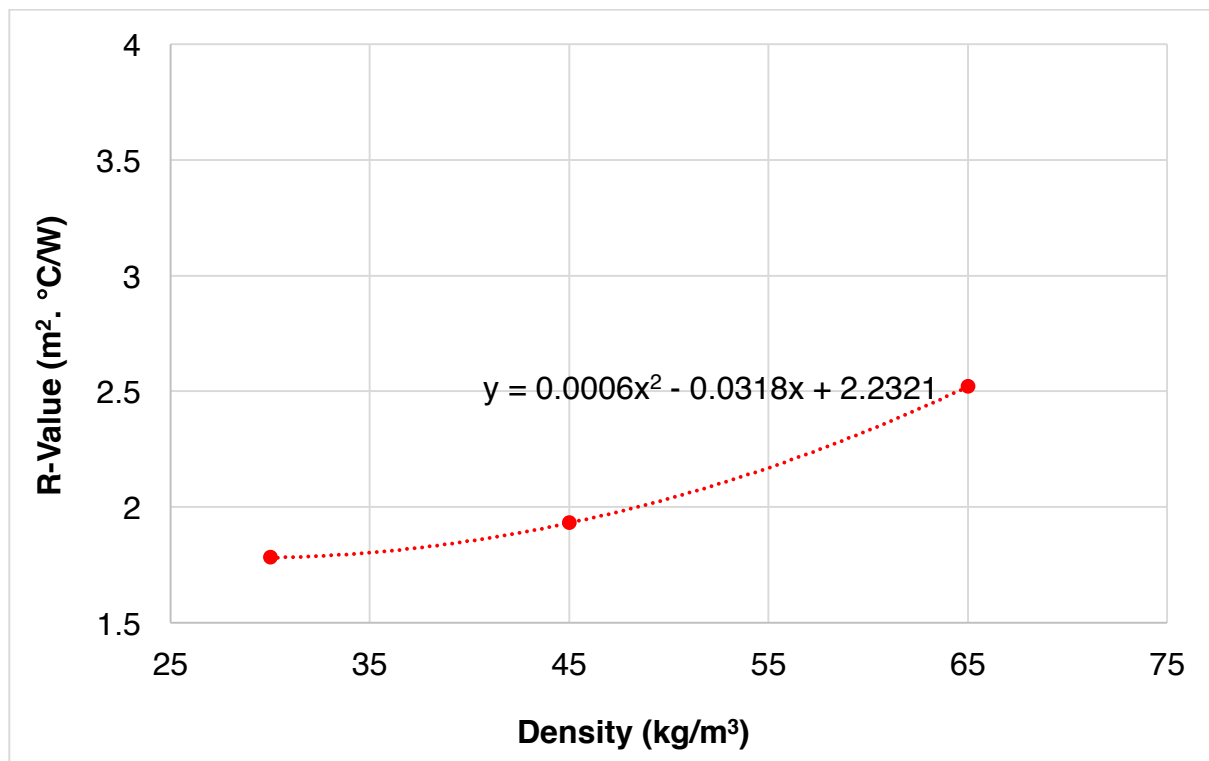


Figure 5.63 R-value Curve of Coconut Fiber

A graph was plotted between R-value and density of coconut fiber and a polynomial equation was generated using MS Excel. By solving the polynomial equation for $y = 3.54$, the density at which the coconut fiber matches the performance of XPS

insulation was found to be 80.2 kg/m^3 . The amount of coconut fiber that has to be used to achieve this density is 1.52 kg. Coconut fiber costs around \$0.25 per kg at the production facility (FAO). Therefore, the cost of the insulation material in this case was around \$0.38 which is around 22 times cheaper than the XPS insulation.

CHAPTER VI

CONCLUSIONS AND RECOMMENDATIONS

The purpose of this research was to test the thermal performance of the indigenous natural fibrous materials when used as insulation in building walls. A dynamic wall simulator with six sides was used in this research. Each side of the simulator had a wall panel with a hollow cavity that was split into two equal halves longitudinally. Thermocouples and heat flux meters were fitted to the simulator and connected to a data logger, which was fed into a computer. The dynamic wall simulator was calibrated with XPS sheets in all the wall cavities as insulation. Calibration was performed multiple times to ensure accuracy of data. Then the experiments were conducted with Timothy grass, wheat straw and coconut fiber as insulations in half wall cavity and the other halves of each wall panel cavity were filled with XPS insulation to compare the thermal performance of each indigenous material against the XPS sheets. Since the indigenous fibrous materials were difficult to hold in place inside the wall panel cavity, a replaceable panel was created by using wooden frames and chicken mesh, where the indigenous materials were spread evenly and placed inside the wall panel cavity.

The experiments were conducted with materials at 30, 45 and 65 kg/m³ densities and each experiment lasted 72 hours. Actual external wall conditions were simulated by heating the simulator for 12 hours (6 AM to 6 PM) and cooling it for another 12 hours (6

PM to 6 AM), which was considered one complete cycle. Therefore, each experiment had three cycles.

Based on the data collected, graphs were plotted, comparing the temperatures and heat fluxes of the indigenous materials and XPS sheet insulation. The peak and average temperature and heat flux values were compared. Based on the comparison results, the thermal performance of indigenous materials as insulators and the percentage difference in thermal performance with XPS insulation, were ranked from highest to lowest as follows:

- Wheat straw at 65 kg/m^3 - 6% lower than XPS sheets
- Coconut fiber at 65 kg/m^3 - 12% lower than XPS sheets
- Wheat straw at 45 kg/m^3 - 16% lower than XPS sheets
- Timothy grass at 65 kg/m^3 - 17% lower than XPS sheets
- Wheat straw at 30 kg/m^3 - 20% lower than XPS sheets
- Coconut fiber at 45 kg/m^3 - 27% lower than XPS sheets
- Timothy grass at 45 kg/m^3 - 27% lower than XPS sheets
- Coconut fiber at 30 kg/m^3 - 29% lower than XPS sheets
- Timothy grass at 30 kg/m^3 - 30% lower than XPS sheets

The insulation performances of the Timothy grass, wheat straw and coconut fiber were equal to the insulation performances of the respective XPS insulations at 68.3, 81.3, and 80.2 kg/m^3 respectively. Based on the cost of insulation, which was calculated from the steady state heat conduction experiments, the indigenous materials were ranked from highest to lowest, with the least cost being the first, as follows:

- Wheat straw at 80.18 kg/m³ - 36 times cheaper than XPS insulation
- Timothy grass at 68.3 kg/m³ - 32 times cheaper than XPS insulation
- Coconut fiber at 80.2 kg/m³ - 22 times cheaper than XPS insulation

In summary, the experiments led to the following discoveries:

When the densities were increased, the insulation performance of the indigenous materials increased. At higher densities, the insulation performances of the indigenous materials were very close to the insulation performance of the XPS sheets. The cost of insulation using the indigenous materials are much lower when compared to the cost of insulation using the XPS sheets. Since the indigenous natural fibrous materials are biodegradable, the disposal of these materials would not pose any environmental hazard. When the indigenous materials were used locally in buildings as an insulation material, the cost of insulation would be very economical, increase the energy efficiency of the building and decrease the environmental impact.

Recommendations

Determination of the effect of water vapor on these materials inside the walls is recommended. The coconut fiber used in this research was separated from the spongy pith, which was naturally present along with the coconut fiber. Experimentation on the thermal performance of coconut fiber along with the pith is recommended. Combined thermal performance of these materials can be determined by mixing the materials in different ratios. Thermal mass of these materials can be calculated to determine if these materials can provide better thermal comfort than conventional insulations.

REFERENCES

U.S. Department of Energy (DOE), 2016, "Insulation Materials," retrieved from:
<http://energy.gov/energysaver/insulation-materials>

M. G. Jackson., 1977, "Rice Straw as Livestock Feed," *FAO Corporate Document Repository*, retrieved from: <http://www.fao.org/docrep/004/x6512e/X6512E07.htm>

U.S. Department of Agriculture, 2016, "Crop Yield and Production – United States: 2013-2014," pp. 81, retrieved from:
<http://www.usda.gov/nass/PUBS/TODAYRPT/cropan15.pdf>

Kew Royal Botanic Gardens (KRBG), 2016, "Triticum aestivum – Description," retrieved from: <http://www.kew.org/science-conservation/plants-fungi/triticum-aestivum-bread-wheat>

Timothy K. Broschat., and Jonathan H. Crane., 2014, "The Coconut Palm in Florida," retrieved from: <http://edis.ifas.ufl.edu/mg043>

Thomas Shoepke., 2006, "Cocos nucifera L.," retrieved from: <http://www.plant-pictures.de/allgemei/koehler/koeh-186.jpg>

The Food and Agriculture Organization of the United Nations (FAO), 2016, "Coir Fibre Processing," retrieved from: <http://www.fao.org/docrep/005/y3612e/y3612e04.htm>

The Food and Agriculture Organization of the United Nations (FAO), 2016, "Coir – Geotextiles," retrieved from: <http://www.fao.org/economic/futurefibres/fibres/coir/en/>

Johnson, D. Emil, Charles M. Krutchen, and G. Vincent Sharps Jr. "Polymer foam extrusion system." U.S. Patent 4,344,710, issued August 17, 1982.

Východoslovenská Energetika., 2012, "Thermal Insulation of Buildings," retrieved from: http://www.vse.sk/wps/portal/zb/domov/setrenie-energie/podnikatelia/zateplenie-objektov/!ut/p/b0/04_Sj9CPykssy0xPLMnMz0vMAfGjzOLd_Q2dLZ0MHQ38vd0MDTydAtxM_V0cjU2czfWDU_P0C7ldFQGRd2Rx/

Ross S. Cann., 2013, "A Brief History of Insulation," retrieved from: <http://a4arch.com/blog/a-brief-history-of-insulation/>

Paul Fiset., 2005, "Cellulose Insulation – A Smart Choice," retrieved from: <https://bct.eco.umass.edu/publications/by-title/cellulose-insulation-a-smart-choice/>

Silvia Banfi., Mehdi Farsi., Massimo Filippini., and Martin Jakob., 2008, "Willingness to pay for energy-saving measures in residential buildings." *Energy economics* 30, no. 2 pp: 503-516.

Shine, Keith P., Jan S. Fuglestvedt, Kinfe Hailemariam, and Nicola Stuber. "Alternatives to the global warming potential for comparing climate impacts of emissions of greenhouse gases." *Climatic Change* 68, no. 3 (2005): 281-302.

Lim, Hyun Sul, Yun Chul Hong, Jung Ran Kim, Hae Kwan Cheong, Ji Yong Kim, Nam Won Paik, Hoe Kyeong Cheong, and Chong Han Lem. "An epidemiologic study on the health hazards of inhabitants chronically exposed to glass fiber." *Korean Journal of Epidemiology* 17, no. 1 (1995): 76-93.

Qureshi, Nasib, Badal C. Saha, Ronald E. Hector, Stephen R. Hughes, and Michael A. Cotta. "Butanol production from wheat straw by simultaneous saccharification and fermentation using *Clostridium beijerinckii*: Part I—Batch fermentation." *Biomass and Bioenergy* 32, no. 2 (2008): 168-175.

Nikolopoulos, N., P. Grammelis, K. Atsonios, M. Agraniotis, R. Isemin, S. Kuzmin, O. Milovanov, And A. Mikhalev. "Straw torrefaction: a new modeling approach and new two-stage reactor."

Brady, Nyle C. "Alternatives to slash-and-burn: a global imperative." *Agriculture, Ecosystems & Environment* 58, no. 1 (1996): 3-11.

Qureshi, Nasib, Badal C. Saha, and Michael A. Cotta. "Butanol production from wheat straw hydrolysate using *Clostridium beijerinckii*." *Bioprocess and biosystems engineering* 30, no. 6 (2007): 419-427.

Zeng, Xianyang, Yitai Ma, and Lirong Ma. "Utilization of straw in biomass energy in China." *Renewable and Sustainable Energy Reviews* 11, no. 5 (2007): 976-987.

Van der Stelt, M. J. C., H. Gerhauser, J. H. A. Kiel, and K. J. Ptasinski. "Biomass upgrading by torrefaction for the production of biofuels: A review." *Biomass and bioenergy* 35, no. 9 (2011): 3748-3762.

Salem, H. Ben, and T. Smith. "Feeding strategies to increase small ruminant production in dry environments." *Small Ruminant Research* 77, no. 2 (2008): 174-194.

Nelson, Richard G. "Resource assessment and removal analysis for corn stover and wheat straw in the Eastern and Midwestern United States—rainfall and wind-induced soil erosion methodology." *Biomass and Bioenergy* 22, no. 5 (2002): 349-363.

United States Department of Agriculture, Nature Resources Conservation Service, 2016, "Plants Guide," retrieved from: <http://plants.usda.gov/java/>

Neill, Sean P., and David R. Lee. "Explaining the adoption and disadoption of sustainable agriculture: the case of cover crops in Northern Honduras." *Economic development and cultural change* 49, no. 4 (2001): 793-820.

DebMandal, Manisha, and Shyamapada Mandal. "Coconut (*Cocos nucifera* L.: Arecaceae): in health promotion and disease prevention." *Asian Pacific journal of tropical medicine* 4, no. 3 (2011): 241-247.

Log, T., and S. E. Gustafsson. "Transient plane source (TPS) technique for measuring thermal transport properties of building materials." *Fire and materials* 19, no. 1 (1995): 43-49.

Yıldız, Nilüfer. "A novel technique to determine pressure in pressure garments for hypertrophic burn scars and comfort properties." *Burns* 33, no. 1 (2007): 59-64.

Ma, Jie, Yao Wang, and Yong Jin. "Energy-Saving and CO₂-Emission-Reducing Features of Straw-Based Building Insulation Material." *Journal of Ecology and Rural Environment* 5 (2010): 006.

Ashour, Taha, Hansjörg Wieland, Heiko Georg, Franz-Josef Bockisch, and Wei Wu. "The influence of natural reinforcement fibres on insulation values of earth plaster for straw bale buildings." *Materials & Design* 31, no. 10 (2010): 4676-4685.

Goodhew, Steven, and Richard Griffiths. "Sustainable earth walls to meet the building regulations." *Energy and Buildings* 37, no. 5 (2005): 451-459.

Toguyeni, David YK, Ousmane Coulibaly, Abdoulaye Ouedraogo, Jean Koulidiati, Yvan Dutil, and Daniel Rousse. "Study of the influence of roof insulation involving local materials on cooling loads of houses built of clay and straw." *Energy and Buildings* 50 (2012): 74-80.

Garas, G., M. Allam, and R. El Dessuky. "Straw bale construction as an economic environmental building alternative-a case study." *ARPJ Journal of Engineering and Applied Sciences* 4, no. 9 (2009): 54-59.

Khedari, Joseph, Noppanun Nankongnab, Jongjit Hirunlabh, and Sombat Teekasap. "New low-cost insulation particleboards from mixture of durian peel and coconut coir." *Building and environment* 39, no. 1 (2004): 59-65.

Manohar, Krishpersad, Dale Ramlakhan, Gurmohan Kochhar, and Subhas Haldar. "Biodegradable fibrous thermal insulation." *Journal of the Brazilian Society of Mechanical Sciences and Engineering* 28, no. 1 (2006): 45-47.

Andoh, H. Y., P. Gbaha, B. K. Koua, P. M. E. Koffi, and S. Touré. "Thermal performance study of a solar collector using a natural vegetable fiber, coconut coir, as heat insulation." *Energy for Sustainable Development* 14, no. 4 (2010): 297-301.

Yaakob, Mohd Yuhazri, Haeryip Sihombing IP, Jeefferie AR, and Balamurugan AG. "Optimization of coconut fibers toward heat insulator applications." *Global Engineers & Technologists Review* 1, no. 1 (2011): 35-40.

Rodríguez, N. J., M. Yáñez-Limón, F. A. Gutiérrez-Miceli, O. Gomez-Guzman, T. P. Matadamas-Ortiz, Luicita Lagunez-Rivera, and JA Vazquez Feijoo. "Assessment of coconut fibre insulation characteristics and its use to modulate temperatures in concrete slabs with the aid of a finite element methodology." *Energy and buildings* 43, no. 6 (2011): 1264-1272.

Abdou, Adel A., and Ismail M. Budaiwi. "Comparison of thermal conductivity measurements of building insulation materials under various operating temperatures." *Journal of Building Physics* 29, no. 2 (2005): 171-184.

Ucar, Aynur, and Figen Balo. "Determination of the energy savings and the optimum insulation thickness in the four different insulated exterior walls." *Renewable Energy* 35, no. 1 (2010): 88-94.

Vo, Chau V., and Andrew N. Paquet. "An evaluation of the thermal conductivity of extruded polystyrene foam blown with HFC-134a or HCFC-142b." *Journal of Cellular Plastics* 40, no. 3 (2004): 205-228.

Saleh A. Al-Ajlan, "Measurements of thermal properties of insulation materials by using transient plane source technique." *Applied Thermal Engineering journal* 26, no. 17-18 (2006): 2184-2191.

Frydrych, Iwona, Gabriela Dziworska, and Joanna Bilska. "Comparative analysis of the thermal insulation properties of fabrics made of natural and man-made cellulose fibres." *Fibres and Textiles in Eastern Europe* 10, no. 4 (2002): 40-44.

Kymäläinen, Hanna-Riitta, and Anna-Maija Sjöberg. "Flax and hemp fibres as raw materials for thermal insulations." *Building and environment* 43, no. 7 (2008): 1261-1269.

Korjenic, Azra, Vít Petránek, Jiří Zach, and Jitka Hroudová. "Development and performance evaluation of natural thermal-insulation materials composed of renewable resources." *Energy and Buildings* 43, no. 9 (2011): 2518-2523.